Conasense

12th CONASENSE

Symposium - Proceedings

Rute C. Sofia
Ramjee Prasad
Paulo Rufino

River Publishers

Introduction to the CONASENSE 2022 Symposium

Rute C. Sofia, Ramjee Prasad, Paulo Rufino

Rute C. Sofia, fortiss GmbH, Munich, Germany. sofia@fortiss.org

Ramjee Prasad, CGC, Aarhus University, Denmark

Paulo Rufino, CGC, Aarhus University, Denmark

Abstract

This report provides an overview on CONASENSE 2022 international symposium, heald in Munich on 27th and 28th June 2022, having been jointly organised by fortiss and CGC, Aarhus University. CONASENSE 2022 counted with 25 international speakers, presentations of papers, presentations of of next generation projects, and also with a co-located Hackathon focused on next generation mobile IoT applications across multiple domains. The event counted with an international audience of 90 participants, where 40 were in Munich. The overall event, including the peer-reviewed papers, and abstracts of talks are summarised in this report, which corresponds to the proceedings of CONASENSE 2022.

Contents

1. INTRODUCTION

6G is currently under definition, being often addressed from a plain telecommunications perspective, as an evolutionary paradigm that represents an extension of 5G. Having as horizon 2030, 6G initiatives are being deployed across the globe, to further ignite the development of 6G services. In its philosophy core, 6G embodies the "human in the loop" principle. The research effort being developed towards 6G requires an interdisciplinary approach that ignites discussion across different key technological sectors, ranging from communications until services and business cases.

In the context of 6G, the CONASENSE2022 provided an interdisciplinary view on latest trends in 6G communications, sensing, services and sustainability aspects based on the *CONASENSE (Communications, Navigation, Sensing, Services)* community vision.

The event corresponds to a 12th edition of former CONASENSE workshops, and has been based on a symposium format, including invited talks from industry; sessions for the presentation of peer-reviewed papers in selected topics; invited talks focusing on the presentation of next generation Internet of Things (IoT) projects; a Hackathon, with focus on the development of mobile, sustainable IoT applications.

The 2022 CONASENSE International Symposium has been jointly organised in hybrid mode by fortiss and CGC, Aarhus University within the context of a research partnership established between the two institutions in 2021. In total, per day, the symposium counted with 90 participants, of which 40 attended in person in Munich.

1.1. Symposium Objectives

The key objectives established for the 2022 symposium were:

- To further expand the CONASENSE community, integrating peer-reviewed research work from younger researchers.
- To ignite discussion focused on the development of the 6G paradigm based on an interdisciplinary methodology.
- To provide a balanced overview on today´s advancements in relevant 6G areas, e.g., IoT, AI, telecommunications, by bringing together experts developing scientific work, research and development projects, and developers and students more focused on the application of open-source solutions.

1.2. Format and Expected Outcome

As part of the symposium organization, the CONASENSE community Website[1] has been updated with the proposed agenda and with the talks provided by the speakers, upon prior consent. Moreover, partners CGC and fortiss have developed also specific Webpages for the event and announced the event broadly via their channels.

The organizing committee has decided to, due to COVID-19, organize a hybrid event, but motivating speakers speakers and main authors of papers to attend in Munich.

The event had an attendance of 90 participants (25 speakers), where 40 participants (including speakers) were in Munich. The remote participation has been supported by fortiss via Web conferencing.

In Munich, the event has been organised by fortiss in the Munich Highlight Towers, having the support of IBM, C4AI joint cooperation between fortiss and IBM.

The overall expertise of the participants related with research, innovation. A few participants concerned technology management, standardisation.

The event started on June 27th 2022 with a welcoming round provided by the organizers and has then proceeded to the keynote session , where experts from IBM, Infineon, Eclipse Foundation, and UnternhemerTUM gave input to relevant products and services.

The next sessions related with the presentation of full peer-reviewed technical papers, followed by invited talks with focus on 6G wireless changes, and a session on next generation IoT projects.

The event proceeded with additional invited talks focusing on 6G business models and use-cases.

For the second day, the event started with sessions focusing on the presentations of both full and short papers, followed by a session focusing on cooperation opportunities towards 6G IoT in Brazil, and then by a session of invited talks on advanced visions towards 6G.

---

[1] https://www.conasense.org

The Hackathon was developed in parallel. The Hackathon started in the afternoon of the first day of CONASENSE 2022. Several meetups with mentors have been set, given that the participants were in hybrid mode.

The event closed with a final session, where awards to the best paper, best presentation and Hackathon awards have been provided.

The symposium derived the following outcome:

- These proceedings.
- A book based on selected invited talks, edited by River Publishers, under the "CONASENSE series"[2].
- A Future MDPI special issue based on selected papers[3].
- A River Journal of Mobile Multimedia (JMM) special issue, based on selected papers.

1.3. Symposium Topics

The theme of the symposium concerned "6G communications, services, and sustainability". The main topics of the symposium concerned the following areas:

- **Communications**: Unified architectural communications involving ground to spaceborne infrastructures; quantum communications and their role and challenges in 6G; Machine-to-machine and device-to-device communication aspects; security aspects in 6G, including mitigation of attacks and architectural challenges; network architectures and protocols for 6G;
- **Navigation and Satellite Integration**: AR/VR advanced navigation approaches, considering both indoor and outdoor scenarios; new navigation

---

2 https://www.riverpublishers.com/series_search.php?val=+conasense+&search=Search

3 https://www.mdpi.com/journal/futureinternet/special_issues/_CONASENSE

applications, e.g., navigation systems for visually impaired people; navigation based on wireless systems; the role of satellite systems and space communications in supporting future IoT systems; geolocalization services and challenges; Data verification, data curation aspects, data privacy aspects.

- **Sensing**: Internet of Things and its integration in different vertical markets; Internet of Everything and AIoT; Interfacing to the real world, in particular tactile interfacing, user-centric, context-aware man-machine interfacing.
- **Services**: The role of the Metaverse, AR/VR development towards 6G; Semantic technologies and their role in the development of a 6G unified architectural communications vision; ML application, in particular federated learning and decentralised learning approaches (e.g., swarm, hybrid federated learning approaches) required to support 6G services; new services and use-cases, e.g., emergency services, remote surgery, smart manufacturing, space exploration, underwater communications; New Edge-based services and the role of Edge computing
- **Sustainability and Greenness**: methodological analysis and research focused on automated evaluation of sustainable solutions towards 6G; analysis of 6G business advantages, proposal of business models and green business frameworks, etc.

2. COMMITTEES

2.1. General Chairs

Rute C. Sofia, fortiss GmbH, Munich, Germany

Ramjee Prasad, CGC, Aarhus University, Denmark

2.2. Publicity Chair and Treasurer:

Paulo Rufino, CGC, Aarhus University, Denmark

2.3. Student Forum Chairs:

Ernestina Cianca, University of Rome, Italy

Manel Khelifi, fortiss GmbH, Munich, Germany

2.4. EU-IoT/EFPF Hackathon Chairs

Mitula Donga, fortiss GmbH, Munich, Germany

Rute C. Sofia, fortiss GmbH, Munich, Germany

2.5. Technical Programme Commitee

- Albena Mihovksa, CGC, Aarhus University, Denmark (Chair)

- Ernestina Cianca, University of Rome, Italy
- Tomaso de Cola, DLR, Germany
- Eduardo Cerqueira, UFPA, Brazil
- Augusto Casaca, INESC-ID, Portugal
- Elefteris Mamathas, Democritus University, Greece
- Henning Schulzrinne, Columbia University, USA
- Anand Prasad, Deloitte, Japan
- Valeria Loscri, INRIA, France
- Eirini Eleni Tsiropoulo, University of New Mexico, USA
- Diego Lopez, Telefonica, Spain
- Jonathan Fürst, NEC, Germany
- Simone Morosi, University of Florence, Italy
- Pedro Sebastião, ISCTE-IUL, Portugal
- Xiaoming Fu, University of Göttingen, Germany
- Maria Papadopouli, FORTH, Greece
- John Soldatos, Intrasoft, Luxembourg
- Jorge Sá Silva, University of Coimbra, Portugal
- Vassilis Tsaoussidis, Democritus University, Greece
- Artur Hecker, Huawei, Germany
- Marica Amadeo, University Mediterranea of Reggio Calabria, Italy
- Laura Feeney, Uppsala University, Sweden
- Ignacio Lacalle, Universitat Politecnica de Valencia, Spain
- Dianne Medeiros, Universidade Federal Fluminense, Brazil
- Evsen Yanmaz, Ozyegin University, Turkey
- Huiling Zhu, University of Kent, United Kingdom
- Jose Sallent, Universitat Politecnica de Madrid
- Anna Triantafyllou, University of Western Macedonia, Greece
- David Jimenez, Universidad Politecnica de Madrid, Spain
- Carlos Raniery Paula Dos Santos, Federal University of Santa Maria, Brazil
- Arne Bröring, Siemens AG, Germany

3. SYMPOSIUM AGENDA

The symposium has been organized in June 27th-June 28th 2022, with a co-located Hackathon. The agenda is presented in Tables Table 1 and Table 2.

Table 1: CONASENSE 2022 Symposium, Agenda Day 1, 27th June 2022.

Time (CET)	Sessions	
8:30-9:30	Registration period – Highlight towers, groundfloor	
9:00-09:30	**Welcoming Session** *CONASENSE welcome*, Rute Sofia, Ramjee Prasad *IBM Welcome*, Felizitas Müller, IBM *fortiss Welcome*, Harald Rueß, fortiss	
09:30-10:30	**Keynote Session – 21st floor, room Yorktown South** Chair: Paulo Rufino , Aarhus University *IBM Innovation Studio Munich*, Felizitas Müller, IBM UnternehmerTUM - We turn visions into value , Florian Küster, Unternehmer TUM Makerspace *The EU platform for IoT and Edge must be open source!* ,Gael Blondelle, Eclipse (remote) *AI based sensing for IoT Building Applications*, Avik Santra, Infineon	
10:30-11:00	**Coffee-break** - 21st floor, Yorktown South	
11:00-12:00	**Hackathon session 1** 20th floor, Large Board room	**11:00-12:00 Technical session - Full paper session 1 (20m plus 10m)** Chair: Manel Khelifi, fortiss *GDOP Optimised LEO Constellation for Positioning,* Harshal More, Mauro de Sanctis, Ernestina Cianca, Cosimo Stallo Achievable Bandwidth of Reconfigurable Intelligent Surfaces (RIS) Concepts Towards 6G Communications*, Werner Mohr*
12:00-12:30	Hackathon session 1 (cont)	Invited Talks Track: 6G Wireless Challenges part I (15m plus 5m) Chair: Paulo Rufino, Aarhus University *Cybersecurity in the Era of Next Generation Wireless Networks,* Milica Pejanović-Djurišić, University of Montenegro
13:00-14:30	**Lunch Break** – 21st floor, Yorktown South	
14:30-16.15	Hackathon Session 2 14:30-15:30 – mentor get	**Project Presentation Session: Next Generation IoT Projects- Yorktown South** Chair: Victor Banos, fortiss

Time (CET)	**Sessions**	
	together	ASSIST-IoT, Ignacio Lacalle Ubela, Universidad Politecnica di Valencia (remote) IntellIoT, Arne Bröring, Siemens AG (remote) iNGENIOUS, Giacomo Bernini and Erin Seder, Nextworks (remote) 'TERMINET: nexT gEneRation sMart INterconnectEd ioT', Panagiotis Sariagiannidis, University Western Macedonia (remote) VEDL-IoT, Jens Hagemeyer, University of Bielefeld IOT-NGIN, Jonathan Klimt, RWTH, Aachen EFPF, Usman Wajid, Information Catalyst
16:15-16:30	Coffee-break	
16:30-18:00	Hackathon Session 3	16:30-18:00 Invited Talks Track (15m plus 5 for questions): Business Models and Use-cases for 6G *Chair: Rute C. Sofia, fortiss* *Challenges in the design of a holographic telepresence system – the current outcomes from the implementation of a use case scenario*, Vladimir Poulkov,Technical University of Sofia, Bulgaria *6G - An Ecosystem for Technology and Market Opportunities*, Martjin Kuipers,University Lusiada/ INESC-INOV, Portugal *Green Business Model 6G Services: A new perspective with Internet of Things connected Green Business Models empowered with Artificial Intelligence*, Per Valter, Aarhus University *Green Business Models and Use-cases for 6G***,** Peter Lindgren, vice-president CGC, Aarhus University, Denmark
18:00-18:30	Hackathon Mentors´ get-together	

Table 2: CONASENSE Symposium Agenda, Day 2, 28th June 2022.

Time (CET)	Tracks	
09:30-10:30	Hackathon session 4	**Technical session - Full paper session 2 ((20m plus 10m) *Chair: Manel Khelifi, fortiss*** Catarinha Castanheira, Rita Almeida, Duarte Marques, Guilherme Firmino, Luis Elvas, Joao C. Ferreira, *How tourists move in a city.* *Susmita Paul, Intrusion Detection System in IoT to Prevent Cyber-Attacks in Organization*
10:30-11:00	Coffee-break	
11:00-12:00	Hackathon Session 5	**Short paper session (20m plus 10m)** Chair: Albena Mihovska, Aarhus University Savita Sthawarmarth, Eric Renault, *Stateless Paradigm for Resiliency in Beyond 5G Networks* Nidhi, Bahram Khan, Albena Mihovska, Ramjee Prasad, Vladimir Poulkov, Fernando J Velez. *Dynamic Resource Block Allocation in Network Slicing*
12:00-12:20		Invited Talks Track: 6G Wireless Challenges part II (15m plus 5m) Chair: Paulo Rufino, Aarhus University *Green OFDM Transmission: An optimal Signal Design Approach*, Hoomayoun Nikookar, Defence Academy, Netherlands
12:30-14:30	Lunch Break	
14:30-15:30		Invited Talks Track 2: IoT Cooperation Opportunities towards Brazil (15m plus 5m) Chair: Paulo Rufino, Aarhus University *Information Technology courses in large scale to supply national demands*, Rodolfo Azevedo,

	President of UNIVESP, Brazil Sergio Paulo Gaulindo, President of Brasscom, Brazil *IoT in Brazil understanding challenges and opportunities*, Paulo José Spaccaquerche, President of ABINC (Brazilian Association of IoT)	
15:30-16:00	Coffee-break	
16:00-17:00	Hackathon pitching	Invited Talks Track 3: Advanced Visions Towards 6G Chair: Rute C. Sofia, fortiss *Machine Learning Enables Radio Resource Utilization of uRLLC*, Kwan-Cheng Chen, University of Florida *Reaching out to billions of client devices: Challenges and opportunities in very dense wireless networks*, Jean-Paul Linnarzt, Signify, Philips Lightiing, Netherlands *Polyphase Channelizers in Modern Communication Systems*, Fred Harris, University of San Diego
17:00-17:30	Hackathon Juri meeting	Break
17:30-18:00	Awards Session, Closure and announcement of next event	

4. AWARDS

The Symposium has provided the following awards:

- Best paper award has been provided by the general chairs to the paper entitled "Achievable Bandwidth of Reconfigurable Intelligent Surfaces (RIS) Concepts Towards 6G Communications", *by Werner Mohr.*
- Best presentation award, sponsored by Future Internet MDPI in 200CH, has

been provided to the talk "*Machine Learning Enables Radio Resource Utilization of uRLLC"***,** by Kwan-Cheng Chen, University of Florida

Hackathon awards, sponsored by several Hackathon sponsors: Infineon, H2020 EU-IoT and H2020 EFPF projects (rf. To Part VIII) were provided by the Hackathon juri to the following Hackathon teams:

1. First Place, Sustainable Irrigation, skills training project by Team 4, Cassio Dias, Felipe da Silva Braz, Gabriel Negri, Jose Angelo de Oliveira, UNIVESP, Brazil.

- Second place, Anomaly Detection, by Team 2: Sudhir Kshirsagar, University of Illinois at Urbana-Champaign, USA
- Third place, Green Backup, by Team 3: Bruno Lowczy, UNIVESP, Brazil

5. SYMPOSIUM HIGHLIGHTS

Figure 1: CONASENSE2022 Closure Session.

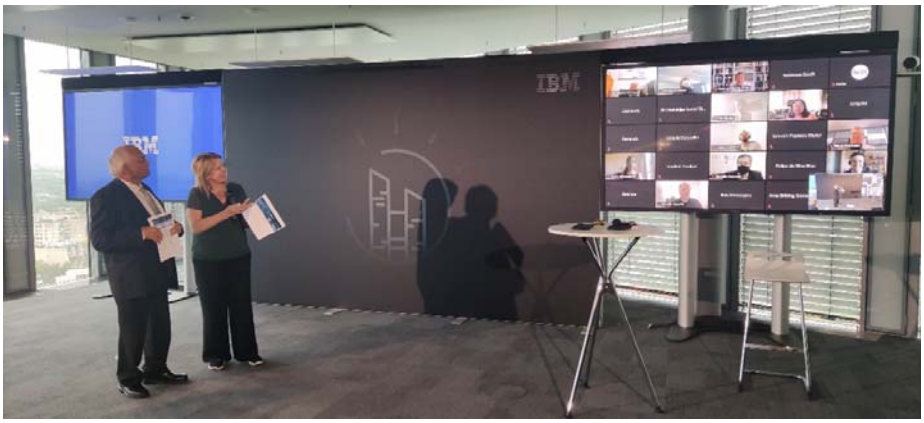

Figure 2: Closure session, Best Presentation Award.

Figure 3: Awards' ceremony.

6. PROCEEDINGS STRUCTURE

The proceedings count with 10 parts, that have been organized as follows:

- **Part I – Introduction.**
- **Part II - Scientific papers**. This part covers the peer-reviewed scientific papers accepted in the symposium. The papers have been reviewed by the TPC members. Each paper had a minimum of three individual reviews. The conference management and peer-reviewing process has been developed via EDAS[4].
- **Part III – Keynote Speeches.** This part provides an overview (title, abstract, bio and photo) for the keynote speeches.
- **Part IV – Invited Talks, Advanced 6G Visions.** This part provides an overview (title, abstract, bio and photo) for the invited talks concerning the symposium session "advanced 6G visions".
- **Part V – Invited Talks, 6G Business Models, Use-cases towards Sustainability.** This part provides an overview (title, abstract, bio and photo) for the invited talks concerning the symposium session "6G technical and business challenges".
- **Part VI – Invited Talks, 6G IoT Cooperation Opportunities towards Brazil**. This part provides an overview (title, abstract, bio and photo) for the invited talks concerning the symposium session "6G IoT cooperation opportunities towards Brazil".
- **Part VII, Next Generation IoT Project Talks.** Covers next generation IoT project presentations, providing an overview towards innovative and active projects in the field, under development in Europe, with focus on IoT and Edge computing.
- **Part VIII, EU-IoT/EFPF Hackathon Summary**. Covers the event main goals, development, and outcome.
- **Part IX – Acknowledgements to the Symposium Sponsors, Promoters and Committees.**

Author Biographies

Rute C. Sofia (PhD 2004) is the Industrial IoT Head at fortiss - research institute of the Free State of Bavaria for software intensive services and systems in Munich, Germany. She is also an Invited Associate Professor of University Lusófona de Humanidades e

[4] https://edas.info

Tecnologias, and an Associate Researcher at ISTAR, Instituto Universitário de Lisboa. Rute's research background has been developed on industrial and on academic context, and she has co-founded COPELABS (2012-2019, Lisbon, Portugal), research unit which she also steered between 2013-2017. and where she was a Senior Researcher until 2019. She has co-founded Senception Lda (2013), a start-up focused on personal communication platforms. Her current research interests are: network architectures and protocols; IoT; edge computing; in-network computation; network mining. Rute holds over 60 peer-reviewed publications in her fields of expertise, and 9 patents.

She is an ACM Senior member and an IEEE Senior Member, and an ACM Europe Councillor. She is also an N2Women Awards Co-chair. Before COPELABS/ULHT, she was a senior researcher at INESC TEC (07-10, Porto, Portugal), where she steered the "Internet Architectures and Networking" area of UTM, team dedicated to wireless/cellular networking architectures and to user-centric networking paradigms. She was (04-07, Munich, Germany) a senior research scientist in Siemens AG and Nokia-Siemens Networks GmbH, focusing on aspects such as: fixed-mobile convergence; carrier-grade Ethernet; QoS; IPv6 interoperability. Rute holds a BEng in Informatics Engineering by Universidade de Coimbra (1995); M.Sc. (1999) and Ph.D. (2004) in Informatics by Universidade de Lisboa. During her PhD studies, she was a visiting scholar (2000-2003) at Northwestern University (ICAIR) and at University of Pennsylvania

Ramjee Prasad, Fellow IEEE, IET, IETE, and WWRF, is a Professor of Future Technologies for Business Ecosystem Innovation (FT4BI) in the Department of Business Development and Technology Aarhus University, Herning, Denmark. He is the Founder President of the CTIF Global Capsule (CGC). He is also the Founder Chairman of the Global ICT Standardization Forum for India, established in 2009. He has been honoured by the University of Rome "Tor Vergata", Italy as a Distinguished Professor of the Department of Clinical Sciences and Translational Medicine on March 15, 2016. He is an Honorary Professor of the University of Cape Town, South Africa, and the University of KwaZulu-Natal, South Africa. He has received the Ridderkorset of Dannebrogordenen (Knight of the Dannebrog) in 2010 from the Danish Queen for the internationalization of top-class telecommunication research and education. He has received several international awards such as IEEE Communications Society Wireless Communications Technical Committee Recognition Award in 2003 for making a contribution in the field of "Personal, Wireless and Mobile Systems and Networks", Telenor's Research Award in 2005 for impressive merits, both academic and organizational within the field of wireless and personal communication, 2014 IEEE AESS Outstanding Organizational Leadership Award

for: "Organizational Leadership in developing and globalizing the CTIF (Center for TeleInFrastruktur) Research Network", and so on. He has been the Project Coordinator of several EC projects, namely, MAGNET, MAGNET Beyond, eWALL. He has published more than 50 books, 1000 plus journal and conference publications, more than 15 patents, over 140 Ph.D. Graduates and a larger number of Masters (over 250). Several of his students are today worldwide telecommunication leaders themselves.

Paulo S. Rufino Henrique holds more than 20 years of experience working in telecommunications. His career began as a field engineer at UNISYS in Brazil, where he was born. There, Paulo worked for almost nine years in the Service Operations, repairing and installing corporative servers and networks before joining British Telecom (BT) Brazil. Paulo worked five years at BT Brazil managing MPLS networks, satellites (V-SAT), IP-Telephony for Tier 1 network operations. He became the Global Service Operations Manager during that period overseeing BT operations in EMEA, Americas, India, South Korea, South African, and China. After a successful career in Brazil, Paulo got transferred to the BT headquarters in London, where he worked for six and a half years as a service manager for Consumers Broadband in the UK and IPTV Ops manager for BT TV Sports channel. Additionally, during his tenure as IPTV Ops manager for BT, Paulo also participated in the BT project of launching the first UHD (4K) TV channel in the UK. He then joined Vodafone UK as a Quality Manager for Consumers Broadband Services and OTT platforms, and he worked in that capacity for almost two years. During his stay in London, Paulo completed a Post-graduation Degree at Brunel London University. His thesis was entitled 'TV Everywhere and the Streaming of UHD TV over 5G Networks & Performance Analysis'. Presently, Paulo Henrique holds the Head of Delivery and Operations position at Spideo, Paris, France. He is also a Ph.D. candidate under Professor Ramjee Prasad's supervision at Global CTIF Capsule, Department of Business, Aarhus University, Denmark. His research field is 6G Networks - Performance Analysis for Mobile Multimedia Services for the Future Wireless Technologies.

Achievable bandwidth of Reconfigurable Intelligent Surfaces (RIS) concepts towards 6G communications

Werner Mohr
Consultant
Munich, Germany
mohr_werner@t-online.de

***Abstract*—In the research community the concept of Reconfigurable Intelligent Surfaces (RIS) is currently discussed in the context of post-Shannon activities. It is the objective of RIS to improve the radio channel environment by specific adjustable reflecting surfaces to maximize the received power and thereby the radio channel capacity. This paper is investigating the achievable bandwidth of the RIS approach from a system and signal theoretical perspective and under realistic propagation conditions as well as the sensitivity with respect to displacements of the mobile station. In addition, the overall achievable channel capacity is compared with a wideband system for the same transmit power. Based on these investigations, the achievable bandwidth can be increased by RIS arrays, where different RIS elements are adjusted to different center frequencies as a spatial filter bank to support wideband systems like LTE, 5G and 6G.**

Keywords—multipath propagation, reconfigurable intelligent surfaces, channel bandwidth, channel capacity

I. INTRODUCTION

The radio propagation channel is characterized by different effects [1] to [12]: distant-dependent pathloss, multipath propagation which results in fading (Rayleigh or Rice), shadowing, atmospheric, rain and foliage attenuation.

The distant-dependent pathloss, shadowing, atmospheric, rain and foliage attenuation are given by the environment and weather conditions, which can be mitigated to a certain extend by the deployment of base station antennas, micro and macro diversity, repeaters and antenna concepts such as high gain antennas, antenna arrays, MIMO antenna concepts and increased transmit power within legal radiation limits.

Multipath propagation is determined by the radio environment and the antenna diagrams at transmitter and receiver. The vectorial superposition of different multipath components at the receiver results in fading of the received signal. In the case of narrowband transmission with respect to the radio channel coherence bandwidth the fading statistics require significant additional transmit power margins to ensure low outage probability. The statistical expectation value of the available channel capacity especially for narrowband transmission is significantly reduced. In the case of wideband transmission with respect to the radio channel coherence bandwidth frequency selective fading occurs within the transmission bandwidth, which results in inter-symbol interference. This impact can be mitigated by signal processing (channel estimation, equalization). For cases with a strong direct component a Rice amplitude distribution and in the case without a direct component a Rayleigh amplitude distribution provide a good model for the fading statistics.

There are new approaches discussed in literature by directly influencing the radio propagation environment. The concept of Reconfigurable Intelligent Surfaces (RIS) or IRS (Intelligent Reflecting Surfaces) is trying to mitigate the impact of multipath propagation by a constructive superposition of the different multipath components at the receiver location. This concept is basically described in [13] to [22]. The RIS approach intends to influence the radio propagation environment by appropriate reflecting areas to increase the received signal amplitude compared to a standard fading channel. However, in the literature often flat fading is assumed, which means that the transmission bandwidth B is much smaller than the radio channel coherence bandwidth B_c. In this paper the achievable RIS bandwidth compared to wideband channels with $B >> B_c$ and the impact of displacements of the mobile station is investigated to understand the applicability of RIS concepts for wideband systems like 5G/6G, which is not yet described in literature.

Section II is describing the basic RIS approach. The characterization of multipath propagation in Section III shows, which path delays may occur under practical conditions. Section IV provides the conditions for an ideal – but not feasible – frequency-independent RIS system and Section V the occurring phased shifts of the different multipath components. This results in the optimum RIS settings in Section VI but also in a narrowband transfer function around center frequency f. The sensitivity of the transfer function with respect to displacements of the mobile station is described in Section VII. Finally, Section VIII provides an approach to increase the achievable bandwidth of the transfer function followed by conclusions in Section IX.

II. BASIC RIS APPROACH

In the case of multipath propagation with a direct path the channel impulse response $h_{mp}(t)$ of the radio channel is described with the path amplitudes h and path delays τ_i by

$$h_{mp}(t) = h_d \cdot \delta(t) + \sum_{i=1}^{I} h_{r,i} \cdot \delta(t - \tau_i) \qquad (1)$$

$$\tau_i = \tau_{sr,i} + \tau_{rd,i} \quad . \qquad (2)$$

The path amplitudes h_d and $h_{r,i}$ implicitly include the pathloss along the distances d_d (direct path), $d_{sr,i}$ (transmitter to reflecting area) and $d_{rd,i}$ (reflecting area to receiver) and the reflection coefficient ϱ_i at the reflecting surface of path i. For simplicity a reflection coefficient of $\varrho = -1$ at metallic surfaces with infinite conductivity is assumed.

The pathloss depends on the reflecting area [15]:

- If the RIS reflector is much bigger than the wavelength λ of the carrier frequency f, an incoming plane wave is reflected again as a plane wave. Here the pathloss depends on the sum of the distances $d_{sr,i}$ and $d_{rd,i}$ with the pathloss exponent n:

$$PL_{reflected} \propto \frac{1}{(d_{sr}+d_{rd})^n} \quad . \qquad (3)$$

- For a RIS reflecting area comprising adjustable parts, which are smaller than the wavelength λ, reflection

corresponds to a scattering process of electromagnetic waves at small objects. At a scatterer a spherical wave is generated with the scattering coefficient σ. This corresponds to the equation of a bistatic Radar [1], p. S1, where the pathloss depends on the product of the distances $d_{sr,i}$ and $d_{rd,i}$ with the pathloss exponent n:

$$PL_{reflected} \propto \frac{1}{(d_{sr} \cdot d_{rd})^n} \quad . \tag{4}$$

Due to the product of distances and the small reflection area the path loss in (4) will be bigger than in (3).

For **standard SISO transmission** without specific reflecting areas or materials the actual received power $P_{r,SISO}$ follows for multipath propagation as the sum of the power of each multipath component with the antenna gains at transmitter G_t and receiver G_r. In this case the different multipath components are super imposed randomly. For narrowband transmission with flat fading the fading can be described by a Rayleigh or Rice distribution. Under these conditions the received power $P_{r,SISO}$ and the actual channel capacity C_{SISO} with the noise power N follow as [23], pp. 568:

$$P_{r,SISO} = P_t \cdot G_t(\varphi,\theta) \cdot G_r(\varphi,\theta) \cdot \left(|h_d|^2 + \sum_{i=1}^{I} |h_{r,i}|^2\right) \tag{5}$$

$$C_{SISO} = B_{SISO} \cdot \log_2\left(1 + \frac{P_{r,SISO}}{N}\right) =$$

$$= B_{SISO} \cdot \log_2\left(1 + \frac{P_t \cdot G_t(\varphi,\theta) \cdot G_r(\varphi,\theta) \cdot \left(|h_d|^2 + \sum_{i=1}^{I} |h_{r,i}|^2\right)}{N}\right) . \tag{6}$$

In the **RIS approach** the radio channel should be influenced by appropriate reflecting surfaces to increase the overall actual received power $P_{r,RIS}$ compared to $P_{r,SISO}$. This can be achieved by adjusting the delay τ_i or phase ϑ_i of each path that all paths have at least the same modulo 2π phase at the receiver and thereby are super imposed constructively. Then $P_{r,RIS}$ and the actual channel capacity C_{RIS} follow:

$$P_{r,RIS} = P_t \cdot G_t(\varphi,\theta) \cdot G_r(\varphi,\theta) \cdot \left(|h_{sd}| + \sum_{i=1}^{I} |h_{r,i}|\right)^2 \tag{7}$$

$$C_{RIS} = B_{RIS} \cdot \log_2\left(1 + \frac{P_{r,RIS}}{N}\right) =$$

$$= B_{RIS} \cdot \log_2\left(1 + \frac{P_t \cdot G_t(\varphi,\theta) \cdot G_r(\varphi,\theta) \cdot \left(|h_{sd}| + \sum_{i=1}^{I} |h_{r,i}|\right)^2}{N}\right) . \tag{8}$$

The intended increased received power is basically increasing the channel capacity. The gain in received power and channel capacity follows from (5) to (8). Then the following inequality holds in all cases, if the reflection coefficients are the same for SISO and RIS transmission:

$$|h_{sd}|^2 + \sum_{i=1}^{I} |h_{r,i}|^2 \le \left(|h_{sd}| + \sum_{i=1}^{I} |h_{r,i}|\right)^2 \quad , \tag{9}$$

because all terms are ≥ 0 and in addition to the terms $|h_d|^2$ and $|h_{r,i}|^2$ on the left side also all mixed terms appear on the right side and contribute to the received power. Both sides are equal only for $I = 0$, i.e., only a direct path is present. The gain is increasing with the number of considered paths, where the gain by RIS compared to standard SISO transmission will be higher for Rayleigh fading channels than for Rice fading channels with a dominating direct component.

III. MULTIPATH PROPAGATION

A. *Path lengths and path delays versus transmitter and receiver antenna pattern*

For the evaluation of the RIS approach it is necessary to investigate, which maximum path length differences Δd_{max} or delay differences $\Delta\tau_{max}$ occur under practical conditions. In the following it is assumed that only single reflections provide a significant contribution to the received signal. Therefore, according to Fig. 1 the curves of constant path length or path delay are ellipses. In the case of mobility, a wide range of path lengths Δd or excess delays $\Delta\tau$ is possible, which depends on the distance d between transmitter and receiver and their antenna patterns. With Fig. 1 the maximum possible path difference Δd_{max} or maximum delay $\Delta\tau_{max}$ is calculated.

In the case

$$\theta_{MS} < 360° - \theta_{BS} \tag{10}$$

Δd_{max} or $\Delta\tau_{max}$ follow from the intersection of the straight lines parallel to r_1 and parallel to r_2 and the 3 dB beamwidth θ_{BS} of the base station antenna and θ_{MS} of the mobile station antenna normalized to the distance d:

$$\frac{\Delta d_{max}}{d} = \frac{\tan\left(\frac{\theta_{MS}}{2}\right)}{\cos\left(\frac{\theta_{BS}}{2}\right) \cdot \left[\tan\left(\frac{\theta_{BS}}{2}\right) + \tan\left(\frac{\theta_{MS}}{2}\right)\right]} + \\ + \frac{\tan\left(\frac{\theta_{BS}}{2}\right)}{\cos\left(\frac{\theta_{MS}}{2}\right) \cdot \left[\tan\left(\frac{\theta_{BS}}{2}\right) + \tan\left(\frac{\theta_{MS}}{2}\right)\right]} - 1 \tag{11}$$

$$\frac{\Delta\tau_{max}}{d} = \frac{1}{c_0} \cdot \left\{ \frac{\tan\left(\frac{\theta_{MS}}{2}\right)}{\cos\left(\frac{\theta_{BS}}{2}\right) \cdot \left[\tan\left(\frac{\theta_{BS}}{2}\right) + \tan\left(\frac{\theta_{MS}}{2}\right)\right]} + \right. \\ \left. + \frac{\tan\left(\frac{\theta_{BS}}{2}\right)}{\cos\left(\frac{\theta_{MS}}{2}\right) \cdot \left[\tan\left(\frac{\theta_{BS}}{2}\right) + \tan\left(\frac{\theta_{MS}}{2}\right)\right]} - 1 \right\} \quad . \tag{12}$$

With (11) and (12) it is shown that both values only depend on the 3 dB beamwidth θ_{BS} of the base station antenna, θ_{MS} of the mobile station and are linearly dependent on the distance d between transmitter and receiver.

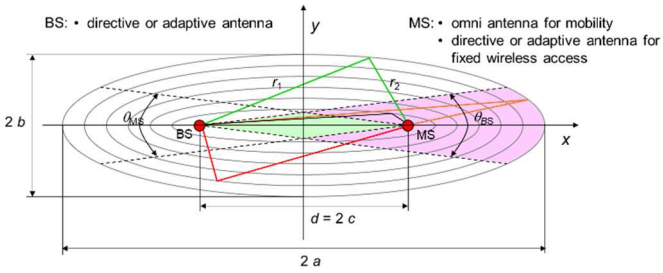

Fig. 1. Propagation scenario for single reflection between transmitter and receiver including 3 dB beamwidth of transmitter and receiver antennas

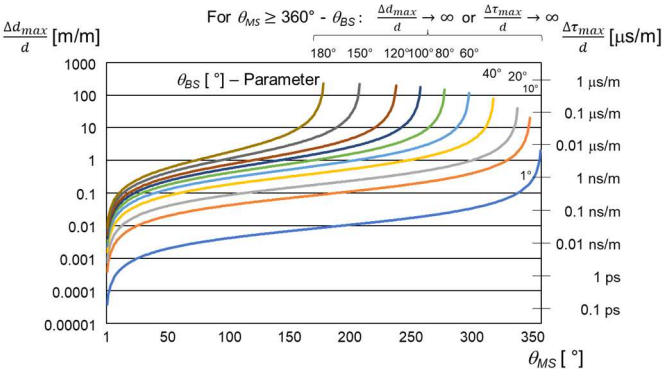

Fig. 2. Maximum normalized path length $\Delta d_{max}/d$ and path delay $\Delta\tau_{max}/d$ versus 3 dB beamwidth θ_{MS} (receiver) with 3 dB beamwidth θ_{BS} (transmitter) as parameter

In the case

$$\theta_{MS} \geq 360° - \theta_{BS} \tag{13}$$

the maximum normalized path length and path delay may tend theoretically to $\Delta d_{max}/d \to \infty$ and $\Delta\tau_{max}/d \to \infty$, because reflections are coming from the back of the receiver antenna, if the 3 dB beamwidth θ_{MS} is rather big.

Fig. 2 is showing the evaluation of (11) and (12). The maximum path length and delay can significantly be reduced, if at the transmitter and receiver directive antennas are applied to avoid reflections from the back of the receiver. With increasing 3 dB beamwidth of the transmitter antenna higher delays are possible even for smaller 3 dB beamwidth of the receiver antenna. The absolute value of the maximum possible path length Δd_{max} and excess delay $\Delta\tau_{\max}$ is achieved by multiplying the values in Fig. 2 by the distance d between transmitter and receiver. Especially in bigger halds and outdoor scenarios big Δd_{max} and $\Delta\tau_{\max} > 1$ µs is very realistic.

B. Distribution functions of Rayleigh and Rice fading

The amplitude and power distribution functions of the received signal for Rayleigh and Rice fading are the basis to estimate the standard SISO radio channel capacity.

- Rayleigh distribution

The Rayleigh distribution for amplitude r_0 and phase θ is describing multipath propagation without a LOS (Line-of-Sight) component, [10], pp. 64:

$$p_{r_0,\theta}(r_0,\theta) = \frac{r_0}{2\cdot\pi\cdot\sigma^2}\cdot e^{-\frac{{r_0}^2}{2\cdot\sigma^2}} \tag{14}$$

$$p_{r_0}(r_0) = \frac{r_0}{\sigma^2}\cdot e^{-\frac{{r_0}^2}{2\cdot\sigma^2}} \quad r_0 \geq 0 \tag{15}$$

$$p_\theta(\theta) = \begin{cases} \frac{1}{2\cdot\pi} & 0 \leq \theta \leq 2\cdot\pi \\ 0 & \text{otherwise} \end{cases} . \tag{16}$$

By means of the Jacobi determinant [24], pp. 37 the distribution function of the received power P_r at the receiver input impedance R follows as

$$P_r = \frac{{r_0}^2}{2\cdot R} \tag{17}$$

$$p_{P_r}(P_r) = \frac{\sqrt{2\cdot P_r\cdot R}}{\sigma^2}\cdot e^{-\frac{2\cdot P_r\cdot R}{2\cdot\sigma^2}}\cdot\sqrt{\frac{R}{2\cdot P_r}} = \frac{R}{\sigma^2}\cdot e^{-P_r\cdot\frac{R}{\sigma^2}} \quad P_r \geq 0 \tag{18}$$

with the mean received power

$$\overline{P_r} = E\{P_r\} = \frac{\sigma^2}{R} \quad . \tag{19}$$

For narrowband systems with a system bandwidth $B < B_c$ channel coherence bandwidth the received power is following the exponential power probability distribution function in (18). The available channel capacity depends on the actual fading value and received power.

In the case of wideband systems with $B >> B_c$ the fading process can be assumed to be ergodic [10], pp. 54 and [25], pp. 55, where the time average is equal to the ensemble average versus frequency f within B. Then the Rayleigh fading results in frequency selective fading, where always the average received power $\overline{P_r}$ applies.

- Rice distribution

The Rice distribution is describing multipath propagation with a LOS component or dominant component r_s. According to [1], p. H3; [3], pp. 134, [11], pp. 26 and [26], pp. 34 the joint distribution function of amplitude r_0 and phase θ of the fading signal and the distribution functions of the envelope r_0 and the phase θ is given as follows [3], pp. 134 with $I_0(\ldots)$ modified Bessel function of first kind and zero order.

$$p_{r_0,\theta}(r_0,\theta) = \frac{r_0}{2\cdot\pi\cdot\sigma^2}\cdot e^{-\frac{{r_0}^2+{r_S}^2-2\cdot r_0\cdot r_S\cdot\cos\theta}{2\cdot\sigma^2}} \tag{20}$$

$$p_{r_0}(r_0) = \frac{r_0}{\sigma^2}\cdot e^{-\frac{{r_0}^2+{r_S}^2}{2\cdot\sigma^2}}\cdot I_0\left(\frac{r_0\cdot r_S}{\sigma^2}\right) \quad r_0 \geq 0 \tag{21}$$

$$p_\theta(\theta) = \tag{22}$$

$$= \begin{cases} \frac{1}{2\cdot\pi}\cdot e^{-\frac{{r_S}^2}{2\cdot\sigma^2}}\cdot\left[1+\sqrt{\frac{\pi}{2}}\cdot\frac{r_S\cdot\cos\theta}{\sigma}\cdot e^{\frac{{r_0}^2\cdot\cos^2\theta}{2\cdot\sigma^2}}\right]\cdot & 0 \leq \theta \leq 2\cdot\pi \\ \quad\cdot\left[1+\operatorname{erf}\frac{r_S\cdot\cos\theta}{\sigma\cdot\sqrt{2}}\right] & \\ 0 & \text{otherwise} \end{cases}$$

In the case of $r_s = 0$ with no dominant component (21) results in the Rayleigh distribution. According to [3], pp. 134 the measure of the dominant component compared to the statistical fading process is the Rice-factor K.

$$K = 10\cdot\log\frac{{r_S}^2}{2\cdot\sigma^2} = 10\cdot\log K' \tag{23}$$

For $K' >> 1$ the modified Bessel function $I_0(\ldots)$ can be approximated by series expansion [27], p. 377 and the distribution function of the envelope in (21) is approaching a Gaussian distribution [11], p. 27 and [28], p. 1063.

$$p_{r_0}(r_0) \approx \frac{1}{\sigma}\cdot\frac{1}{\sqrt{2\cdot\pi}}\cdot e^{-\frac{(r_0-r_S)^2}{2\cdot\sigma^2}} \quad -\infty \leq r_0 \leq \infty \tag{24}$$

The worst case with the deepest fades occurs for $K' = 0$ for the Rayleigh distribution, where the probability for deep fades is decreasing with increasing K'.

The distribution function of the received power P_r at the receiver input impedance R follows from the transformation of (24) by means of the Jacobi determinant [24], pp. 37 as

$$P_r = \frac{{r_0}^2}{2\cdot R} \tag{25}$$

$$p_{P_r}(P_r) \approx \frac{1}{\sigma}\cdot\frac{1}{\sqrt{2\cdot\pi}}\cdot\sqrt{\frac{R}{2\cdot P_r}}\cdot e^{-\frac{\left(\sqrt{2\cdot P_r\cdot R}-r_S\right)^2}{2\cdot\sigma^2}} \quad P_r \geq 0 \quad . \tag{26}$$

with the mean received power

$$\overline{P_r} = E\{P_r\} = \frac{\sigma^2+{r_S}^2}{2\cdot R} \quad . \tag{27}$$

For narrowband systems with a system bandwidth $B < B_c$ channel coherence bandwidth the received power is following the power probability distribution function in (21) or approximately (26). The available channel capacity depends on the actual fading value and received power.

In the case of wideband systems with $B >> B_c$ the fading process can be assumed to be ergodic [10], pp. 54 and [25], pp. 55, where the time average is equal to the ensemble average versus frequency f within B. Then the Rice fading results in frequency selective fading, where always the average received power $\overline{P_r}$ applies.

C. Distribution functions of the channel capacity for Rayleigh and Rice fading

The channel capacity depends on the system bandwidth B, the received power P_r and the noise power N as in (6). The effective received power is following the fading statistic in Section III.B.

$$C_{Rayleigh\ or\ Rice} = B \cdot \log_2\left(1 + \frac{P_r}{N}\right) \quad (28)$$

- Channel capacity for Rayleigh distribution

The probability distribution function $p_{c_{Rayleigh}}$ of the normalized channel capacity $c_{Rayleigh} = C_{Rayleigh}/B$ is calculated with (18) and (28) and the Jacobian determinant J [24] pp. 37.

$$P_r = \left(e^{c_{Rayleigh}\cdot \ln 2} - 1\right) \cdot N \quad (29)$$

$$J = \left|\frac{\partial P_r}{\partial c_{Rayleigh}}\right| = N \cdot \ln 2 \cdot e^{c_{Rayleigh}\cdot \ln 2} \quad (30)$$

$$p_{c_{Rayleigh}}\left(c_{Rayleigh}\right) = \quad (31)$$

$$= \frac{R}{\sigma^2} \cdot N \cdot \ln 2 \cdot e^{N\cdot\frac{R}{\sigma^2}} \cdot e^{-N\cdot\frac{R}{\sigma^2}e^{c_{Rayleigh}\cdot \ln 2}} \cdot e^{c_{Rayleigh}\cdot \ln 2}$$

This is related with (19) to the average signal/noise-ratio

$$SNR = \frac{\sigma^2}{R\cdot N} = \frac{\overline{P_r}}{N} \quad (32)$$

$$p_{c_{Rayleigh}}\left(c_{Rayleigh}\right) = \quad (33)$$

$$= \frac{1}{SNR} \cdot \ln 2 \cdot e^{\frac{1}{SNR}} \cdot e^{-\frac{1}{SNR}e^{c_{Rayleigh}\cdot \ln 2}} \cdot e^{c_{Rayleigh}\cdot \ln 2} \quad .$$

Fig. 3 shows the probability density function $p_{c_{Rayleigh}}\left(c_{Rayleigh}\right)$ in (33) of $c_{Rayleigh}$ with the average signal/noise-ratio *SNR* as parameter. Due to Rayleigh fading there is a big variance of the channel capacity for narrowband systems with $B < B_c$. For $B >> B_c$ the Rayleigh fading results in frequency selective fading, where always the average channel capacity $\overline{c_{Rayleigh}} = E\{c_{Rayleigh}\}$ applies.

This average or expectation value of the normalized channel capacity $\overline{c_{Rayleigh}} = E\{c_{Rayleigh}\}$ is increasing with *SNR* and follows from numerical evaluation of:

$$\overline{c_{Rayleigh}} = E\{c_{Rayleigh}\} =$$

$$= \int_0^\infty c_{Rayleigh} \cdot p_{c_{Rayleigh}}\left(c_{Rayleigh}\right) dc_{Rayleigh} \quad . \quad (34)$$

As summarized in Table I $\overline{c_{Rayleigh}} = E\{c_{Rayleigh}\}$ can be approximated by a quadratic equation or by the average *SNR* with (19), (28) and (32)

$$\overline{c_{Rayleigh,quadratic}} \approx \quad (35)$$

$$\approx 0.8598 + 0{,}2125 \cdot SNR\ [dB] + 0{,}0019 \cdot SNR\ [dB]^2$$

$$\overline{C_{Rayleigh,estimate}} = B \cdot \log_2(1 + SNR) \quad . \quad (36)$$

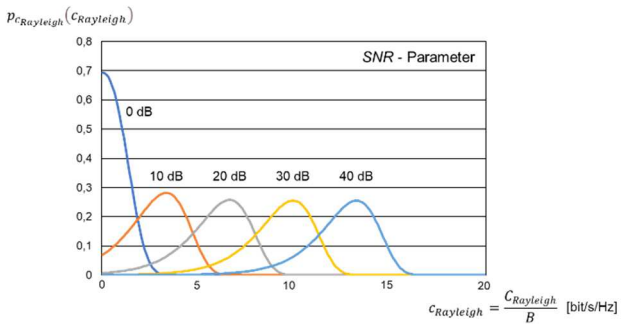

Fig. 3. Probability density function of the normalized channel capacity $c_{Rayleigh} = C_{Rayleigh}/B$ for Rayleigh fading with the average *SNR* as parameter

TABLE I. EXPECTATION VALUE OF THE NORMALIZED CHANNEL CAPACITY $\overline{c_{Rayleigh}} = E\{c_{Rayleigh}\}$ VERSUS AVERAGE *SNR* [dB] AND APPROXIMATIVE FUNCTIONS

SNR [dB]	$\overline{c_{Rayleigh}}$ (34)	Approximations	
		quadratic (35)	based and *SNR* (36)
0	0.8598	0.8598	1.0000
10	2.9065	3.1784	3.4594
20	5.8840	5.8840	6.6582
30	9.1436	8.9767	9.9672
40	12.4564	12.4564	13.2879

Wideband systems with $B >> B_c$ mitigate the impact of Rayleigh fading on channel capacity, because $\overline{c_{Rayleigh}} = E\{c_{Rayleigh}\}$ is constant for an ergodic fading process and follows with reasonable accuracy from the average *SNR*.

- Channel capacity for Rice distribution

The probability distribution function $p_{c_{Rice}}$ of the normalized channel capacity $c_{Rice} = C_{Rice}/B$ is calculated with (26) and (28) and the Jacobian determinant J [24] pp. 37.

$$P_r = \left(e^{c_{Rice}\cdot \ln 2} - 1\right) \cdot N \quad (37)$$

$$J = \left|\frac{\partial P_r}{\partial c_{Rice}}\right| = N \cdot \ln 2 \cdot e^{c_{Rice}\cdot \ln 2} \quad (38)$$

$$p_{c_{Rice}}(c_{Rice}) = \frac{\ln 2}{\sqrt{2\cdot\pi}} \cdot \sqrt{\frac{R\cdot N}{2\cdot\sigma^2\cdot\left(e^{c_{Rice}\cdot \ln 2} - 1\right)}} \cdot \quad (39)$$

$$\cdot\, e^{-\frac{\left(\sqrt{2\cdot\left(e^{c_{Rice}\cdot \ln 2}-1\right)\cdot N\cdot R} - r_s\right)^2}{2\cdot\sigma^2}} \cdot e^{c_{Rice}\cdot \ln 2} \quad .$$

This is related with (23) and (27) to the average signal/noise-ratio

$$SNR = \frac{\sigma^2 + {r_s}^2}{2\cdot R\cdot N} = \frac{\overline{P_r}}{N} \quad (40)$$

$$p_{c_{Rice}}(c_{Rice}) = \frac{\ln 2}{\sqrt{2\cdot\pi}} \cdot \sqrt{\frac{1 + 2\cdot K'}{4\cdot SNR\cdot\left(e^{c_{Rice}\cdot \ln 2} - 1\right)}} \cdot \quad (41)$$

$$\cdot\, e^{-\frac{\left(\sqrt{\left(e^{c_{Rice}\cdot \ln 2}-1\right)\cdot\left(\frac{1+2\cdot K'}{SNR}\right)} - \sqrt{2\cdot K'}\right)^2}{2}} \cdot e^{c_{Rice}\cdot \ln 2} \quad .$$

Fig. 4 shows the probability density function $p_{c_{Rice}}(c_{Rice})$ in (41) of c_{Rice} with the average signal/noise-ratio *SNR* as parameter. Due to Rice fading there is a lower variance of the channel capacity for narrowband systems with $B < B_c$ than for Rayleigh fading. For $B >> B_c$ the Rice fading results in frequency selective fading, where always the average channel capacity $\overline{c_{Rice}} = E\{c_{Rice}\}$ applies.

This average or expectation value of the normalized channel capacity $\overline{c_{Rice}} = E\{c_{Rice}\}$ is increasing with *SNR* and follows from numerical evaluation of:

$$\overline{c_{Rice}} = E\{c_{Rice}\} = \int_0^\infty c_{Rice} \cdot p_{c_{Rice}}(c_{Rice}) dc_{Rice} \quad . \quad (42)$$

As summarized in Table II. $\overline{c_{Rice}} = E\{c_{Rice}\}$ can be approximated by a quadratic equation or by the average *SNR* with (27), (28) and (40)

$$\overline{c_{Rice,quadratic}} \approx \quad (43)$$

$$\approx 0.9674 + 0{,}2503 \cdot SNR\ [dB] + 0{,}0014 \cdot SNR\ [dB]^2$$

$$\overline{C_{Rice,estimate}} = B \cdot \log_2(1 + \mathrm{SNR}) \quad , \quad (44)$$

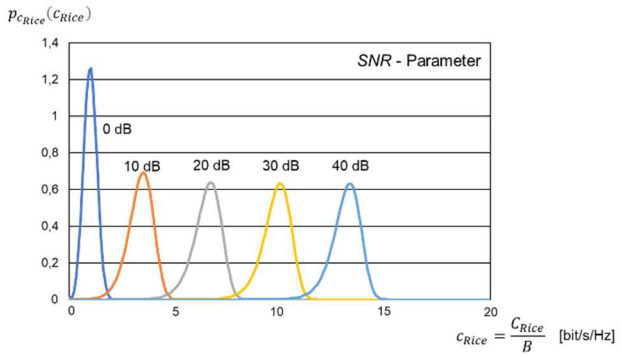

Fig. 4. Probability density function of the normalized channel capacity $c_{Rice} = C_{Rice}/B$ for Rayleigh fading with the average *SNR* as parameter for $K' = 10$

TABLE II. EXPECTATION VALUE OF THE NORMALIZED CHANNEL CAPACITY $\overline{c_{Rice}} = E\{c_{Rice}\}$ VERSUS AVERAGE *SNR* [DB] AND APPROXIMATIVE FUNCTIONS FOR RICE FACTOR $K' = 10$

SNR [dB]	$\overline{c_{Rice}}$ (42)	Approximations	
		quadratic (43)	based on *SNR* (44)
0	0.9674	0.9674	1.0000
10	3.3417	3.6051	3.4594
20	6.5129	6.5129	6.6582
30	9.8184	9.6907	9.9672
40	13.1386	13.1386	13.2879

Wideband systems with $B >> B_c$ mitigate the impact of Rice fading on channel capacity, because $\overline{c_{Rice}} = E\{c_{Rice}\}$ is constant for an ergodic fading process and follows with high accuracy from the average *SNR*.

IV. SYSTEM- AND SIGNAL-THEORETICAL PERSPECTIVE

The basic idea of RIS systems is described in Section II. Ideally, the channel transfer function should be frequency independent within the system transmission bandwidth *B*. The system capacity is maximized according to (7) and (8), if all multipath components are constructively super imposed. However, in Sections V and VI the frequency dependency with respect to the radio channel behavior is considered.

The physical radio channel is a causal system with a channel impulse response $h_{mp}(t) = 0$ for $t < 0$. Therefore, the impulse response of the channel will arrive at the output later as the excitation of the channel or ideally at the minimum propagation delay. This also needs to be considered for the RIS system approach. That means that a RIS system can only add phase shifts or delays per multipath component to ensure a constructive superposition of all multipath components.

Under ideal conditions the channel transfer function of the radio channel including RIS elements at the different reflectors should be frequency independent. With the causality condition the ideal RIS channel impulse response $h_{mp\,RIS}(t)$ and frequency transfer function $H_{RIS}(\omega)$ should then correspond to a single path model, which is shifted by the maximum path delay $\Delta\tau_{max}$ of the original channel impulse response without a RIS system. That requires that all multipath components will have the same delay $\Delta\tau_{max}$. The maximum path delay results in a linear frequency dependent phase of the channel transfer function.

$$h_{mp\,RIS}(t) = h_{sum} \cdot \delta(t - \Delta\tau_{\max}) \tag{45}$$

$$H_{RIS}(\omega) = h_{sum} \cdot e^{-j\omega\cdot\Delta\tau_{\max}} \tag{46}$$

The impulse response in (1) would then be transformed with path specific delay lines of $\Delta\tau_i = \Delta\tau_{max} - \tau_i$:

- without RIS system

$$h_{mp}(t) = h_d \cdot \delta(t) + \sum_{i=1}^{I} h_{r,i} \cdot \delta(t - \tau_i) \tag{47}$$

- with ideal RIS system

$$\begin{aligned} h_{mp,RIS}(t) = \\ = h_d \cdot \delta(t - \Delta\tau_{max}) + \sum_{i=1}^{I} h_{r,i} \cdot \delta(t - \tau_i - \Delta\tau_i) \\ = \left\{h_{sd} + \sum_{i=1}^{I} h_{r,i}\right\} \cdot \delta(t - \Delta\tau_{max}) \\ = h_{sum} \cdot \delta(t - \Delta\tau_{max}) \quad . \end{aligned} \tag{48}$$

Fig. 5 is showing a theoretical block diagram for the implementation of (48). The blocks $g_d(t)$ and $g_{r,i}(t)$ are delay lines to ensure that all multipath components are arriving at the receiver with the same delay $\Delta\tau_{\max}$. This corresponds to a spatial filter with path specific delay lines. However, Fig. 2 shows that under realistic conditions very long path lengths in the order of many meters or even several hundred meters would need to be equalized, which is not feasible in practice. Therefore, practical RIS systems are adjusting the phase of each path. In addition, the two different cases Rayleigh and Rice channel need to be distinguished.

- Delay equalization for Rayleigh channels

A Rayleigh channel does not have a direct component h_d. Each received multipath component is at least affected by one reflection. Only the elements $h_{r,i}$ in (47) and (48) are affected by reflection. Therefore, a RIS system can be applied for all relevant multipath components. In this case theoretically the ideal RIS setting is feasible according to (45) and (48). The resulting radio channel corresponds to a single path channel (49), where the received amplitude would be maximized independent of the frequency.

$$h_{RIS\,Rayleigh}(t) = h_{sum} \cdot \delta(t - \Delta\tau_{\max}) \tag{49}$$

- Delay equalization for Rice channels

A Rice channel does have a direct component h_d. Except the direct path each other received multipath component is at least affected by one reflection. Only the elements $h_{r,i}$ in (47) and (48) are affected by reflection. Therefore, a RIS system cannot be applied to the direct path h_d. In this case theoretically the ideal RIS setting results according to (50) in a two-path channel, where the received amplitude is fluctuating below the breakpoint depending on frequency and distance [3], pp 24.

$$h_{RIS\,Rice}(t) = h_d \cdot \delta(t) + \sum_{i=1}^{I} h_{r,i} \cdot \delta(t - \Delta\tau_{max}) \tag{50}$$

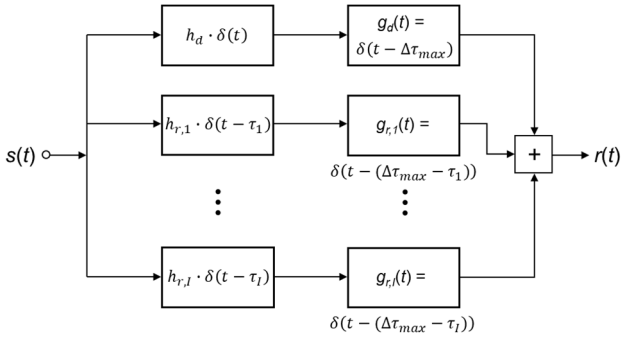

Fig. 5. Block diagram of an ideal RIS system with the same delay of all multipath components

V. PROPAGATION DELAY, PATH DIFFERENCE, PHASE DIFFERENCE AND IMPACT ON THE RADIO CHANNEL IMPULSE RESPONSE AND TRANSFER FUNCTION

In multipath propagation there are time delays τ_i between the direct and delayed paths. Especially in macro cells such delays may be under very special conditions up to the order of several tens of µs (e.g., 30 µs). However, at very high carrier frequencies in the millimeter wave or sub-Terahertz frequency range the radio range is much shorter than in standard macro cells at carrier frequencies below 1 or 2 GHz. Therefore, in the following the maximum considered delay is limited to $\Delta\tau_{max}$ = 1 µs (≙ 300 m in free space) (Fig. 2).

With (1) multiple delayed copies of the transmitted signal $s_t(t)$ and weighted with the channel impulse response $h_{mp}(t)$ arrive at the receiver. The time delays τ_i result in inter-symbol interference at the receiver, which needs to be mitigated by appropriate signal processing.

The path differences Δd_i follows from the speed of light c_0 and the time delays τ_i:

$$\Delta d_i = (d_{sr,i} + d_{rd,i}) - d_{LOS} = c_0 \cdot \tau_i \quad . \tag{51}$$

That results for the example $\Delta\tau_{max}$ = 1 µs in

$$\Delta d_{max} = c_0 \cdot \Delta\tau_{max} = 300 \text{ m} \quad . \tag{52}$$

For a given carrier frequency f this path difference Δd corresponds to a frequency dependent phase difference $\Delta\varphi$ between the delayed and direct path:

$$\Delta\varphi = 2 \cdot \pi \cdot \frac{\Delta d}{\lambda} = 2 \cdot \pi \cdot \frac{\Delta d}{c_0} \cdot f = 2 \cdot \pi \cdot \tau \cdot f \quad . \tag{53}$$

The path delay τ results for $\leq 1\,\mu s$ depending on the carrier frequency f in huge frequency dependent phase differences $\Delta\varphi$ according to (53) and Fig. 6. These huge phase differences will have a significant impact on the frequency dependency of the multipath radio channel.

The multipath propagation radio channel can be described by a tapped-delay-line model in (1), where each tap is characterizing a resolvable multipath component within the radio system bandwidth B. The reflection coefficient at a metallic plane is assumed as ϱ_i = -1 and is implicitly included in the tap weighting factors $h_{r,i}$. This phase shift by π is independent of the frequency.

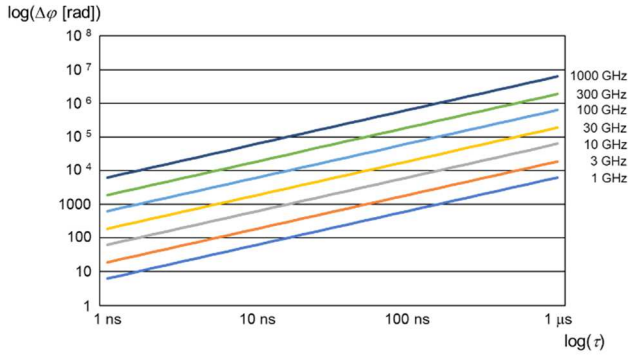

Fig. 6. Relation between delay difference τ and difference in path length Δd with carrier frequency f as parameter

The transmitted signal $s_t(t)$ is in general amplitude- and phase modulated at the carrier frequency $\omega = 2 \cdot \pi \cdot f$ with

$$s_t(t) = A(t) \cdot \sin(\omega \cdot t + \psi(t)) \quad . \tag{54}$$

The received signal $s_r(t)$ follows from the convolution of the transmitted signal in (54) with the channel impulse response in (1) [29], pp. 9.

$$\begin{aligned} s_r(t) &= s_t(t) * h_{mp}(t) = \\ &= \int_{-\infty}^{\infty} s_t(t - t_0) \cdot \left(h_d \cdot \delta(t_0) + \sum_{i=1}^{I} h_{r,i} \cdot \delta(t_0 - \tau_i)\right) dt_0 \\ &= A(t) \cdot \sin\left(\omega \cdot t + \psi(t)\right) \cdot h_d + \\ &+ \sum_{i=1}^{I} A(t - \tau_i) \cdot \sin(\omega \cdot (t - \tau_i) + \psi(t - \tau_i)) \cdot h_{r,i} \end{aligned} \tag{55}$$

The modulation terms $A(t)$ and $\psi(t)$ are slowly varying compared to the carrier signal.

The radio channel transfer function $H_{mp}(\omega)$ in the frequency domain is the Fourier transform of its impulse response $h_{mp}(t)$.

$$\begin{aligned} H_{mp}(\omega) &= \int_{-\infty}^{\infty} h_{mp}(t) \cdot e^{-j\omega t} dt = \\ &= \int_{-\infty}^{\infty} \left(h_d \cdot \delta(t) + \sum_{i=1}^{I} h_{r,i} \cdot \delta(t - \tau_i)\right) \cdot e^{-j\omega t} dt = \\ &= h_d + \sum_{i=1}^{I} h_{r,i} \cdot e^{-j\omega\tau_i} \end{aligned} \tag{56}$$

With respect to Fig. 6 there are very big phase shifts for each tap based on path delays, which are determined by the radio environment (path lengths and receiver location) for a given frequency. In the following the optimal RIS setting of phase shifts are determined to maximize the channel capacity in (8), where all incoming signal contributions are super imposed constructively.

VI. OPTIMAL RIS SETTINGS AND RADIO CHANNEL TRANSFER FUNCTION

A. *Optimal RIS settings*

The optimal settings to maximize the received power and channel capacity according (7) and (8) require, that for a carrier frequency ω_0 all path amplitudes show the same effective phase. This corresponds to a deterministic channel impulse response and not to random tap delays. With (56) it follows for the real and imaginary parts:

$$\text{Re}\left(H_{mp}(\omega_0)\right) = h_d + \sum_{i=1}^{I} h_{r,i} \cdot \cos(\omega_0 \tau_i) = max \tag{57}$$

$$\text{Im}\left(H_{mp}(\omega_0)\right) = \sum_{i=1}^{I} h_{r,i} \cdot \sin(\omega_0 \tau_i) = 0 \quad . \tag{58}$$

(57) and (58) can be fulfilled for adjusted delays τ_i'

$$\omega_0 \tau_i' = 2i \cdot \pi \qquad \text{for} \qquad i = 1, 2, 3 \ldots I \quad , \tag{59}$$

where I is limited by the maximum delay $\Delta\tau_{max}$. With (53) it follows

$$\Delta\varphi_i' = 2 \cdot \pi \cdot \frac{\Delta d_i'}{\lambda} = 2 \cdot \pi \cdot f_0 \cdot \tau_i' = 2i \cdot \pi \tag{60}$$

$$\tau_i' = \frac{i}{f_0} \tag{61}$$

$$\Delta\tau_{max}' = \frac{I}{f_0} \quad . \tag{62}$$

By appropriate settings of the individual RIS reflectors the phase shifts $\Delta\varphi_i'$ of the different paths or time delays τ_i' are adjusted by adding small delays to fulfill the closest value

in (61). All received paths are then in phase at ω_0. The allowed $2i$ or i follow from rounding or integer calculation:

$$\mathrm{Int}\left\{\frac{\Delta\varphi_i}{\pi}\right\} + 1 = \mathrm{Int}\left\{\frac{\omega_0 \cdot \tau_i}{\pi}\right\} + 1 = \frac{\Delta\varphi_{i'}}{\pi} = 2i \quad . \tag{63}$$

That means that the minimum difference between path delays corresponds to

$$\tau_{i+1} - \tau_i = \frac{1}{f_0} \quad . \tag{64}$$

This minimum time separation is the same between neighboring delays. Its resolution would require a receiver bandwidth equal to the carrier frequency.

B. *Radio channel transfer function*

The channel transfer function $H_{mp}{}'(\omega)$ for the optimally adjusted RIS channel impulse response at carrier frequency ω_0 with (61) to (64) can be represented in the time domain by the product of an infinite series of Dirac impulses and the envelope of the channel impulse response (Fig. 7 and (65)).

$$h_{mp}{}'(t) = h_{mp}(t) \cdot \sum_{i=-\infty}^{\infty} \delta\left(t - i \cdot \frac{1}{f_0}\right) \tag{65}$$

$H_{mp}{}'(\omega)$ corresponds to the convolution of the Fourier transform $\mathcal{F}\left(h_{mp}(t)\right)$ of the envelope of the impulse response $h_{mp}(t)$ and the Fourier transform of the infinite series of Dirac pulses [29], pp. 51; [30], pp. 209.

$$\mathcal{F}\left(\sum_{i=-\infty}^{\infty} \delta\left(t - i \cdot \frac{1}{f_0}\right)\right) = \tag{66}$$

$$= \sum_{i=-\infty}^{\infty} e^{-j\omega \cdot \frac{i}{f_0}} = \sum_{i=-\infty}^{\infty} \delta(\omega - i \cdot \omega_0)$$

$$H'_{mp}(\omega) = \mathcal{F}\left(h_{mp}(t)\right) * \mathcal{F}\left(\sum_{i=-\infty}^{\infty} \delta\left(t - i \cdot \frac{1}{f_0}\right)\right) =$$

$$= \mathcal{F}\left(h_{mp}(t)\right) * \sum_{i=-\infty}^{\infty} \delta(\omega - i \cdot \omega_0) \, . \tag{67}$$

The Fourier transform of $h_{mp}(t)$ is repeated around all frequencies $i \cdot \omega_0$, if the impulse response shows a resolution according to (64) for optimal RIS settings. However, that would require an unrealistic system bandwidth $B = {\omega_0}/{2\pi}$. For a carrier frequency of 10 GHz and $\Delta\tau'_{max} = 1$ µs that would correspond with (62) to $I = 10000$ paths with a delay difference $\tau_{i+1} - \tau_i = 0.1$ ns . For an assumed relative system bandwidth ${B_{system}}/{f_0} = 0.01 \mathrel{\widehat{=}} 1\,\%$ the resolution of the impulse response would be $\Delta\tau = 10$ ns and 100 resolved paths. (64) can then be expressed with reduced resolution as

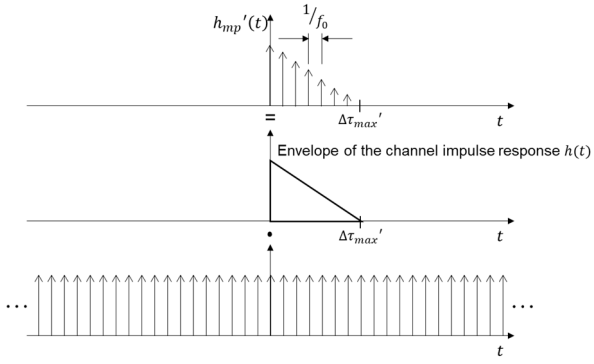

Fig. 7. Radio channel impulse response for optimal RIS settings at carrier frequency ω_0

$$\tau_{i+\mathrm{Int}\left\{{f_0}/{B_{system}}\right\}} - \tau_i = \Delta\tau = \frac{1}{B_{\mathrm{system}}} \quad . \tag{68}$$

With (66) this is described as

$$\mathcal{F}\left(\sum_{i=-\infty}^{\infty} \delta\left(t - k \cdot \frac{1}{B_{\mathrm{system}}}\right)\right) = \tag{69}$$

$$= \sum_{k=-\infty}^{\infty} e^{-j\omega \cdot \frac{k}{B_{\mathrm{system}}}} = \sum_{k=-\infty}^{\infty} \delta\left(\omega - k \cdot 2\pi B_{system}\right)$$

$$H'_{mp}(\omega) = \mathcal{F}\left(h_{mp}(t)\right) * \mathcal{F}\left(\sum_{k=-\infty}^{\infty} \delta\left(t - k \cdot \frac{1}{B_{\mathrm{system}}}\right)\right) =$$

$$= \mathcal{F}\left(h_{mp}(t)\right) * \sum_{k=-\infty}^{\infty} \delta\left(\omega - k \cdot 2\pi B_{system}\right) \tag{70}$$

The periodicity of the radio channel transfer function depends on the resolution of the channel impulse response or the system bandwidth, which is related to the sampling theorem. In the following (70) is evaluated for different envelopes (rectangular, triangular and exponential) of $h_{mp}(t)$.

C. *RIS transfer function for rectangular channel impulse response*

The envelope of the rectangular impulse response $h_{mp}(t)$ is described by

$$h_{mp}(t) = \begin{cases} h_d & 0 \le t \le \Delta\tau_{max} \\ 0 & t < 0 \quad \text{and } t > \Delta\tau_{max} \end{cases} \quad . \tag{71}$$

The Fourier transform follows as:

$$\mathcal{F}\left(h_{mp}(t)\right) = h_d \cdot 2 \cdot \frac{\sin\left(\omega \cdot \frac{\Delta\tau_{max}}{2}\right)}{\omega} \cdot e^{-j\,\omega \cdot \frac{\Delta\tau_{max}}{2}} \quad . \tag{72}$$

With (70) the radio channel transfer function is given as:

$$H'_{mp}(\omega) = h_d \cdot 2 \cdot \frac{\sin\left(\omega \cdot \frac{\Delta\tau_{max}}{2}\right)}{\omega} \cdot e^{-j\,\omega \cdot \frac{\Delta\tau_{max}}{2}} *$$

$$* \sum_{k=-\infty}^{\infty} \delta\left(\omega - k \cdot 2\pi B_{system}\right) \quad . \tag{73}$$

The absolute value of (73) is shown in Fig. 8 for the exemplary parameters

- f_0 10 GHz
- B_{system} 100 MHz
- I 100 for transfer function around f_0 = 10 GHz
- k 0
- $\Delta\tau_{max}$ 1 µs .

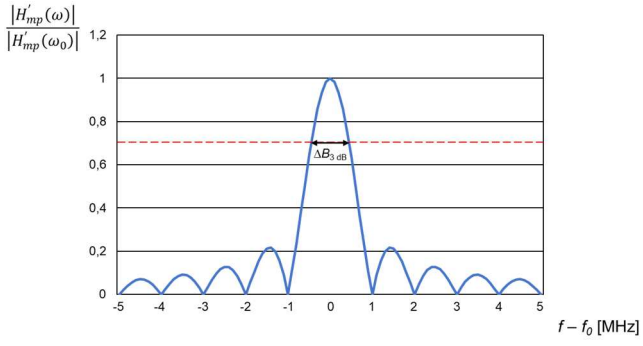

Fig. 8. Normalized channel transfer function for optimal RIS settings at carrier frequency f_0 = 10 GHz, B_{system} = 100 MHz, I = 100, $\Delta\tau_{\max}$ = 1 µs and rectangular impulse response

The absolute value of $H'_{mp}(\omega)$ around the carrier frequency f_0 for optimal RIS settings only depends on the envelope of $h_{mp}(t)$. It is periodic with the system bandwidth, because the tap delays are optimally adjusted to (68). The 3 dB bandwidth in the case of a rectangular envelope of the channel impulse response corresponds to 880 kHz, which can be approximated by

$$\Delta B_{3\,\mathrm{dB}} = B_{system,RIS} = 880\ \mathrm{kHz} \approx \frac{1}{\Delta\tau_{max}} = \frac{1}{1\,\mu s} = 1\ \mathrm{MHz}\ . \quad (74)$$

The RIS approach is very narrowband compared to the intended system bandwidth of 5G and 6G systems in the order of several 100 MHz to a few GHz. The bandwidth of optimal RIS settings can only be increased, if the impulse response is becoming much shorter. However, this length depends on the actual radio environment.

D. Received power for RIS and SISO approach for rectangular channel impulse response

According to (5) and (7) the phase shifts of all taps in the channel impulse response in a SISO approach without RIS are random, which result in a Rayleigh or Rice distribution. In the case of a narrowband system with $B_{system} < B_c$ (coherence bandwidth) the received amplitude follows these distribution functions (Section III.B.). If $B_{system} >> B_c$, the received power corresponds to the average power of the Rayleigh or Rice distribution (c.f. (19) or (27)). In the RIS approach all received tap amplitudes at the carrier frequency f_0 show the same phase and are summed up constructively. However, this high effective amplitude is only possible within the narrow bandwidth as in the example of Fig. 8.

For $L = I + 1$ resolvable paths in the channel impulse response within the system bandwidth (the "1" corresponds to a potential direct path) the ratio between the received RIS power $P_{r,RIS,narrowband}$ and the SISO power $P_{r,SISO,wideband}$ for a wideband receiver is given by:

$$\frac{P_{r,RIS,narrowband}}{P_{r,SISO,wideband}} = \frac{P_t \cdot G_t(\varphi,\theta) \cdot G_r(\varphi,\theta) \cdot \left(|h_d| + \sum_{i=1}^{I} |h_{r,i}|\right)^2}{P_t \cdot G_t(\varphi,\theta) \cdot G_r(\varphi,\theta) \cdot \left(|h_d|^2 + \sum_{i=1}^{I} |h_{r,i}|^2\right)} =$$

$$= \frac{\left(|h_d| + \sum_{i=1}^{I} |h_{r,i}|\right)^2}{\left(|h_d|^2 + \sum_{i=1}^{I} |h_{r,i}|^2\right)}\ . \quad (75)$$

If all paths have the same amplitude

$$|h_d| = |h_{r,i}| = |h| \quad \forall\ i \quad \text{and} \quad L = I + 1 \quad (76)$$

as assumed here for the rectangular shape of the impulse response, (75) can be written as follows:

$$\frac{P_{r,RIS,narrowband}}{P_{r,SISO,wideband}} = \frac{\left(|\underline{h}_{sd}| + \sum_{i=1}^{I} |\underline{h}_{r,i}|\right)^2}{|\underline{h}_{sd}|^2 + \sum_{i=1}^{I} |\underline{h}_{r,i}|^2} =$$

$$= \frac{\left(L \cdot |\underline{h}|\right)^2}{L \cdot |\underline{h}|^2} = L \mathrel{\widehat{=}} 10 \cdot \log L\ . \quad (77)$$

If a narrowband receiver with $B_{system,RIS}$ is used according to (74) with the RIS approach, the received power is L times bigger than for the SISO approach and a wideband receiver with $B_{system,SISO}$.

This difference in received power can also be derived from the RIS transfer function $H'_{mp}(\omega)$ in (73) and Fig. 8 with the relative frequency $\omega' = (\omega - k \cdot 2\pi B_{system})$ around the carrier frequency $\omega_0 = k \cdot 2\pi B_{system}$ and the average power transfer function $\overline{H'_{mp}(\omega)}^2$, which provides the average received power for a wideband system under multipath propagation conditions for a white transmit power spectral density.

$$\int_{-\omega_{system}/2}^{\omega_{system}/2} \left|H'_{mp}(\omega')\right|^2 d\omega = \overline{\left|H'_{mp}(\omega')\right|}^2 \cdot \omega_{system} \quad (78)$$

With [31], p. 119 and No. 14b) (78) follows with (73) as

$$\overline{\left|H'_{mp}(\omega)\right|}^2 =$$

$$= |h_d \cdot 2|^2 \cdot \frac{2}{\omega_{system}} \cdot \int_0^{\omega_{system}/2} \left| \frac{\sin\left(\omega' \cdot \frac{\Delta\tau_{max}}{2}\right)}{\omega'} \right|^2 d\omega' \approx$$

$$= |h_d \cdot 2|^2 \cdot \frac{2}{\omega_{system}} \cdot \frac{\frac{\Delta\tau_{max}}{2}\pi}{2 \cdot 0!} = |h_d \cdot 2|^2 \cdot \frac{\Delta\tau_{max}}{4 \cdot B_{system}}\ . \quad (79)$$

The maximum value of the square of the RIS transfer function at $\omega' = 0$ and the ratio of the average and the maximum of the RIS transfer functions follows

$$\frac{\overline{\left|H'_{mp}(\omega)\right|}^2}{\left|H'_{mp}(\omega'=0)\right|^2} = \frac{|\underline{h}_{sd} \cdot 2|^2 \cdot \frac{\Delta\tau_{max}}{B_{system} \cdot 4}}{|\underline{h}_{sd} \cdot 2|^2 \cdot \left(\frac{\Delta\tau_{max}}{2}\right)^2} = \frac{1}{B_{system} \cdot \Delta\tau_{max}} = \frac{1}{L}\ . \quad (80)$$

For the exemplary values in Section VI.C. $\overline{\left|H'_{mp}(\omega)\right|}^2 = 0.01 \mathrel{\widehat{=}} -20\ \mathrm{dB} = -20 \cdot \log L$ like in (77). Fig. 9 is showing the square of the RIS transfer function and the average transfer function. In the RIS case the good transfer conditions are concentrated in a narrow bandwidth around the carrier frequency and its periodic. Between the maxima the transfer function is showing very low values, which means a very uneven distribution of the received power versus frequency.

E. Channel capacity for RIS and SISO approach for rectangular channel impulse response

With (6) and (8) the respective available channel capacities are derived with the noise power density N_0:

$$C_{RIS,narrorband} =$$

$$= B_{system,RIS} \cdot \log_2\left(1 + \frac{P_t \cdot G_t(\varphi,\theta) \cdot G_r(\varphi,\theta) \cdot \left(L \cdot |\underline{h}|\right)^2}{N_0 \cdot B_{system,RIS}}\right) \quad (81)$$

$$C_{SISO,wideband} =$$

$$= B_{system,SISO} \cdot \log_2\left(1 + \frac{P_t \cdot G_t(\varphi,\theta) \cdot G_r(\varphi,\theta) \cdot L \cdot |\underline{h}|^2}{N_0 \cdot B_{system,SISO}}\right)\ . \quad (82)$$

With L resolvable path and $I = L - 1$, the system bandwidth for the RIS and SISO approach and (68) and (74) are related to each other like for $L >> 1$:

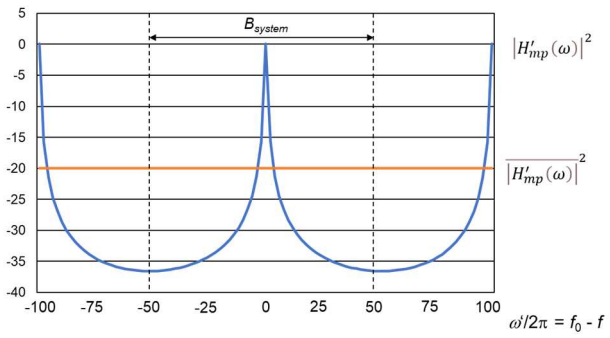

Fig. 9. Normalized radio channel transfer function for optimal RIS settings at carrier frequency f_0 = 10 GHz, B_{system} = 100 MHz, I = 99, 100 and 101 and $\Delta\tau_{max}$ = 1 µs

$$\Delta\tau_{max} = (L-1)\cdot\frac{1}{B_{system,SISO}} \approx \frac{1}{B_{system,RIS}} \quad (83)$$

$$B_{system,SISO} \approx (L-1)\cdot B_{system,RIS} \approx L\cdot B_{system,RIS} \quad (84)$$

as well as the system capacities and with their approximations in (36) and (44)

$$C_{RIS,narrorband} = \\ = \frac{B_{system,SISO}}{L}\cdot\log_2\left(1+\frac{P_t\cdot G_t(\varphi,\theta)\cdot G_r(\varphi,\theta)\cdot|\underline{h}|^2\cdot L^3}{N_0\cdot B_{system,SISO}}\right) \quad (85)$$

$$C_{SISO,wideband} = \\ = B_{system,SISO}\cdot\log_2\left(1+\frac{P_t\cdot G_t(\varphi,\theta)\cdot G_r(\varphi,\theta)\cdot|\underline{h}|^2\cdot L}{N_0\cdot B_{system,SISO}}\right) \quad (86)$$

$$SNR = \frac{P_t\cdot G_t(\varphi,\theta)\cdot G_r(\varphi,\theta)\cdot|\underline{h}|^2}{N_0\cdot B_{system,SISO}} \quad (87)$$

$$\frac{C_{SISO,wideband}}{C_{RIS,narrowband}} = \frac{L\cdot\log_2(1+SNR\cdot L)}{\log_2(1+SNR\cdot L^3)} \quad . \quad (88)$$

The effective signal/noise-ratio for the RIS approach is increased by L^2, because the received power is by a factor of L bigger than for the SISO approach and the system bandwidth is by a factor L smaller. Therefore, the argument of the logarithm for higher SNR for RIS is growing with L^2 faster than for SISO. However, the system bandwidth in front of the logarithm for RIS is by a factor L smaller than for SISO. Fig. 10 shows that $C_{SISO,wideband}$ is bigger than $C_{RIS,narrowband}$ for all practical cases.

F. RIS transfer function for triangular and exponential channel impulse response

The envelope of the triangular channel impulse response $h_{mp}(t)$ is described by

$$h_{mp}(t) = \\ = \begin{cases} h_d\cdot\left(1-\frac{t}{\Delta\tau_{max}}\right) & 0\le t\le\Delta\tau_{max} \\ 0 & t<0 \quad and \quad t>\Delta\tau_{max} \end{cases} \quad . \quad (89)$$

The transfer function follows with [32], p. 326:

$$H'_{mp}(\omega) = h_d\cdot e^{-j\,\omega\frac{\Delta\tau_{max}}{2}}\cdot\left\{3\cdot\frac{\sin\left(\omega\cdot\frac{\Delta\tau_{max}}{2}\right)}{\omega}+\right. \\ \left.+j\frac{\cos\left(\omega\frac{\Delta\tau_{max}}{2}\right)}{\omega}-j\frac{\sin\left(\omega\frac{\Delta\tau_{max}}{2}\right)}{\frac{\Delta\tau_{max}}{2}\omega^2}\right\}*\sum_{k=-\infty}^{\infty}\delta(\omega-k\cdot\omega_0) \quad . (90)$$

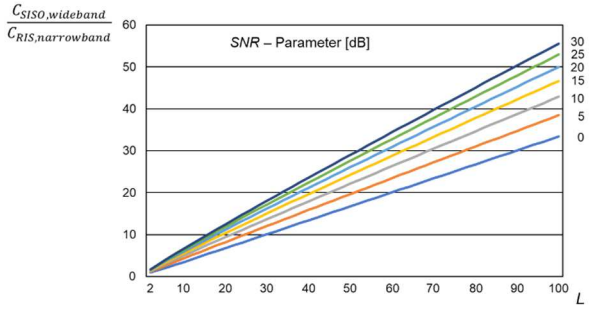

Fig. 10. Ratio of $C_{SISO,wideband}$ and $C_{RIS,narrowband}$ versus number of resolvable paths with *SNR* according to (87) as parameter

The absolute normalized value of (90) is shown in Fig. 11 for the exemplary parameters as in Section VI.C.

The 3 dB bandwidth in the case of a triangular envelope of the channel impulse response corresponds to 900 kHz, which can be approximated by

$$\Delta B_{3\,dB} = B_{system,RIS} = 900\ \text{kHz} \approx \frac{1}{\Delta\tau_{max}} = \frac{1}{1\ \mu s} = 1\ \text{MHz} \quad . (91)$$

This value is slightly higher than for a rectangular channel impulse response in (74).

The exponential envelope is described by

$$h_{mp}(t) = \begin{cases} h_d\cdot e^{-a\cdot t} & t\ge 0 \\ 0 & t<0 \end{cases} \quad . \quad (92)$$

The parameter a is determined that for $\Delta\tau_{max}$ the impulse response is decreased to 1 %: with $a = -\frac{\ln 0.01}{\Delta\tau_{max}}$, which means a = 4.605 1/µs for $\Delta\tau_{max}$ = 1 µs.

The transfer function follows as:

$$H'_{mp}(\omega) = h_d\cdot\frac{(a-j\omega)}{a^2+\omega^2} \quad . \quad (93)$$

The absolute normalized value of (93) is shown in Fig. 12 for the exemplary parameters as in Section VI.C.

The 3 dB bandwidth in the case of an exponential envelope of the channel impulse response corresponds to 1460 kHz, which can be roughly approximated by

$$\Delta B_{3\,dB} = B_{system,RIS} = 1460\ \text{kHz} \approx \frac{1}{\Delta\tau_{max}} = \frac{1}{1\ \mu s} = 1\ \text{MHz} \quad (94)$$

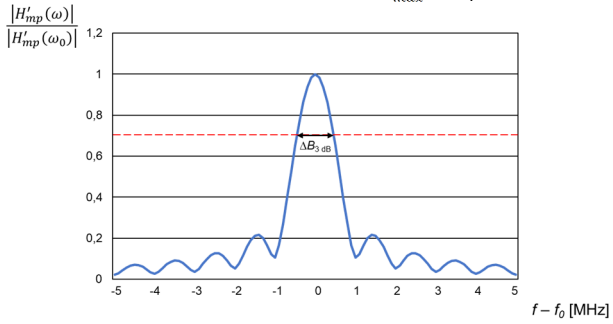

Fig. 11. Normalized radio channel transfer function for optimal RIS settings at carrier frequency f_0 = 10 GHz, B_{system} = 100 MHz, I = 100 and $\Delta\tau_{max}$ = 1 µs and triangular channel impulse response

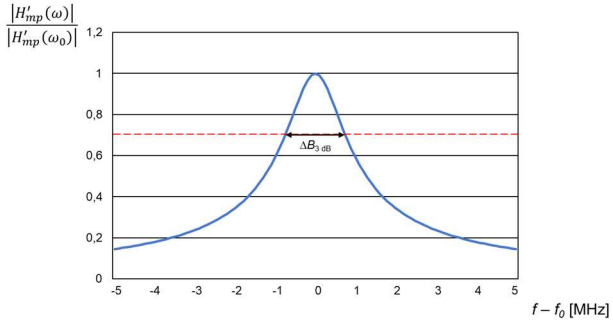

Fig. 12. Normalized radio channel transfer function for optimal RIS settings at carrier frequency f_0 = 10 GHz, B_{system} = 100 MHz, I = 100 and $\Delta\tau_{max}$ = 1 µs (a = 4.605 1/µs) and exponential channel impulse response

This value is somehow higher than for a rectangular or triangular channel impulse response in (74) and (91).

In general, the achievable bandwidth $B_{system,RIS}$ is rather narrow and can roughly be approximated by the inverse of the maximum relevant tap delay as in (74), (91) and (94).

VII. Impact of Displacements of the Mobile Station in the RIS Approach

The RIS settings are very sensitive versus frequency. The sensitivity versus displacements of the receiver is relevant in the case of mobility and the update rate for optimal RIS settings. The effective time delays and associated phase shifts according to (53) or (60) are changing with displacements of the mobile station in the deployment area. Fig. 13 shows a simple example of multipath transmission with a direct path and two reflected paths, where all three paths have the same amplitude. With a displacement of the mobile station the geometry is changing and thereby the path lengths. The changing relative phase shifts between the paths result in a different vectorial superposition of the different paths and thereby the channel transfer function. The RIS settings are optimized for the mobile location $x = x_1 = d_0$ and $y = y_1$, which is valid for a single user. For other users at different locations a different RIS system is needed. When the mobile station is moving, the RIS settings are not optimal anymore.

The path lengths are derived for the general receiver position as follows:

$$\begin{aligned} d_0 &= \sqrt{x^2 + (y_1 - y)^2} \\ d_1 &= \sqrt{x^2 + (y_1 + y)^2} \\ d_2 &= \sqrt{x^2 + (2 \cdot y_2 - y_1 - y)^2} \quad . \end{aligned} \tag{95}$$

For the receiver coordinates for optimal RIS settings (95) and the reflector positions y_0 and y_2 result in:

$$\begin{aligned} d_0 &= x_1 & y_0 &= 0 \\ d_1 &= \sqrt{{x_1}^2 + (2 \cdot y_1)^2} & y_1 &= \frac{\sqrt{{d_1}^2 - {x_1}^2}}{2} \\ d_2 &= \sqrt{{x_1}^2 + (2 \cdot y_2 - 2 \cdot y_1)^2} & y_2 &= \frac{\sqrt{{d_2}^2 - {x_1}^2}}{2} + \frac{\sqrt{{d_1}^2 - {x_1}^2}}{2} . \end{aligned} \tag{96}$$

With (96) the following exemplary figures are assumed for a numerical evaluation at the optimal RIS settings and a carrier frequency of $f = 10$ GHz:

- Delays in the impulse response

$$\begin{aligned} \tau_0 &= 0 \text{ µs} \\ \tau_1 &= 0.5 \text{ µs} \\ \tau_2 &= 1.0 \text{ µs} \end{aligned} \tag{97}$$

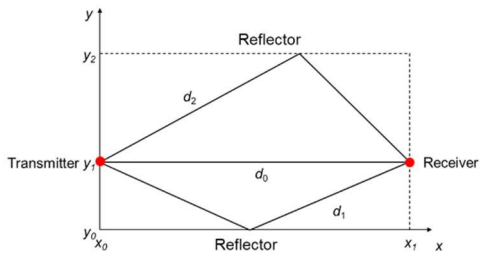

Fig. 13. Coordinate system between transmitter and receiver with a direct path and two reflected delayed paths

- Associated path lengths and receiver coordinates at optimal RIS settings

$$\begin{aligned} d_0 &= 1000 \text{ m} & & \\ d_1 &= 1150 \text{ m} & y_1 &= 283.9454 \text{ m} \\ d_2 &= 1300 \text{ m} & y_2 &= 699.2765 \text{ m} \quad . \end{aligned} \tag{98}$$

These path lengths including the reflection coefficient $\varrho = -1$ ensure that all delayed paths have a phase shift of an integer multiple of 2π for optimal RIS settings and that all paths are constructively super imposed ((53), (97) to (98)).

$$\begin{aligned} \Delta\varphi = 2 \cdot \pi \cdot \frac{\Delta d}{\lambda} = 2 \cdot \pi \cdot \frac{\Delta d}{c_0} \cdot f = 2 \cdot \pi \cdot \Delta\tau \cdot f \\ \Delta\varphi_1 = 2 \cdot \pi \cdot \Delta\tau_1 \cdot f = 2 \cdot \pi \cdot 5000 \\ \Delta\varphi_2 = 2 \cdot \pi \cdot \Delta\tau_2 \cdot f = 2 \cdot \pi \cdot 10000 \end{aligned} \tag{99}$$

A. Displacement along the x-axis

It is assumed that the mobile station is moving along the x-axis, i.e., y_1 remains. The position of the reflectors at $y = y_0$ and $y = y_2$ are not shifted. The receiver coordinates result in:

$$x = {d_0}' \qquad \text{and} \qquad y = y_1 \quad . \tag{100}$$

This provides the path lengths:

$$\begin{aligned} {d_0}' &= x \\ {d_1}' &= \sqrt{x^2 + (2 \cdot y_1)^2} \\ {d_2}' &= \sqrt{x^2 + (2 \cdot y_2 - 2 \cdot y_1)^2} \quad . \end{aligned} \tag{101}$$

The following observations are made:

- With deviating x from x_1 and thereby d_0, all three tap delays τ_0, τ_1 and τ_2 are changing.
- τ_0 is increasing with increasing x and vice versa.
- τ_1 and τ_2 are increasing slower than τ_0 with increasing x and vice versa.
- Thereby, the path delay differences are slightly changing with x.

The received electric field is described with the same tap amplitude E_r per path by vectorial superposition and the phase shifts according to (99) by

$$\underline{E} = E_r \cdot \left(e^{-j\Delta\varphi_1} + e^{-j\Delta\varphi_2} + e^{-j\Delta\varphi_3}\right) \quad \Delta\varphi_i = 2\pi \cdot \Delta\tau \cdot f \tag{102}$$

$$|\underline{E}| = E_r \cdot \sqrt{(\cos\Delta\varphi_1 + \cos\Delta\varphi_2 + \cos\Delta\varphi_3)^2 + (\sin\Delta\varphi_1 + \sin\Delta\varphi_2 + \sin\Delta\varphi_3)^2} \quad . \tag{103}$$

Fig. 14 shows the received amplitude $|\underline{E}|$ normalized to the maximum versus $\Delta x/\lambda$, where $|\underline{E}|$ is significantly varying compared to the optimal RIS settings at $\Delta x/\lambda = 0$ or $x = d_0 = 1000$ m according to (96). Within the considered displacement of 0.36 m (corresponding to 12λ at 10 GHz) or 3.6 m (corresponding to 120λ at 10 GHz) $|\underline{E}|$ is varying in a wide range on this short distance. Therefore, the RIS settings need to be adapted already for slight displacements at high carrier frequencies.

The 3 dB bandwidth versus displacement in x-direction of around 0.11 m corresponds to around 3.6λ wavelengths. In this case all path delays are moving in the same direction and their relative distance does only change slightly. However, the optimal RIS setting is very sensitive with respect to displacements of the mobile station.

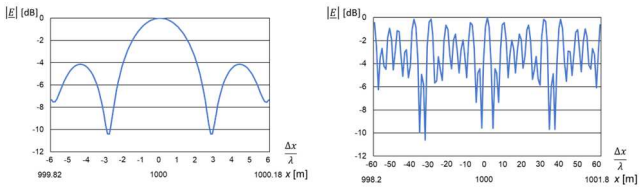

Fig. 14. Relative received amplitude $|\underline{E}|$ for displacement along the x-axis of 0.36 m or 12λ (left side) and 3.6 m or 120λ (right side) at 10 GHz

B. *Displacement along the y-axis*

Here it is assumed that the mobile station is moving along the *y*-axis, i.e., x_1 remains. The reflector positions at $y = y_0$ and $y = y_2$ are not shifted. The receiver coordinates result in:

$$x = x_1 = d_0 \qquad \text{and} \qquad y \quad . \tag{104}$$

This provides the path lengths:

$$\begin{aligned} d_0' &= \sqrt{{x_1}^2 + (y_1 - y)^2} \\ d_1' &= \sqrt{{x_1}^2 + (y_1 + y)^2} \\ d_2' &= \sqrt{{x_1}^2 + (2 \cdot y_2 - y_1 - y)^2} \end{aligned} \tag{105}$$

and phase shifts according to (99). The following observations are made:

- With deviating *y* from y_1 and thereby d_0', all three tap delays τ_0, τ_1 and τ_2 are changing.
- τ_0 is increasing with increasing and decreasing *y* compared to y_1.
- When τ_1 is increasing with increasing *y*, then τ_2 is decreasing slower and vice versa.
- Thereby, the path delay differences are slightly changing with *y*.

The received electric field is described with the same tap amplitude E_r per path by vectorial superposition and the phase shifts according to (102) and (103).

Fig. 15 shows the received amplitude $|\underline{E}|$ normalized to the maximum versus $\Delta y/\lambda$, where $|\underline{E}|$ is significantly varying compared to the optimal RIS settings at $\Delta y/\lambda = 0$ or $y = y_1 = 283.9454$ m according to (96). Within the considered displacement of 0.36 m (corresponding to 12λ at 10 GHz) or 3.6 m (corresponding to 120λ at 10 GHz) $|\underline{E}|$ is varying in a wide range on short distance. Therefore, the RIS settings need to be adapted already for slight displacements at high carrier frequencies. The fluctuation versus *y*-direction is much faster than versus *x*-direction.

The 3 dB bandwidth versus displacement in *y*-direction of around 0.022 m corresponds to around 0.75λ wavelengths. In this case the path delays are moving in different directions

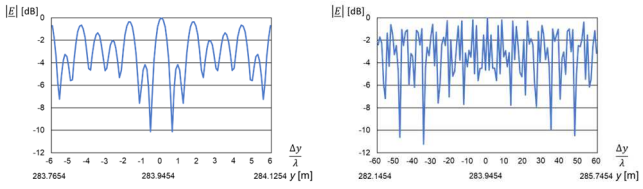

Fig. 15. Relative received amplitude $|\underline{E}|$ for displacement along the *y*-axis of 0.36 m or 12λ (left side) and 3.6 m or 120λ (right side) at 10 GHz

and their relative distance is changing. Therefore, the fluctuations versus y are faster than versus x. The optimal RIS settings are even more sensitive with respect to displacements of the mobile station.

The detailed shape of the impulse response is influencing the RIS settings versus mobile station position.

VIII. Means for Increasing Achievable Bandwidth

Broadband systems like 5G and 6G require a much wider bandwidth than provided by the limitation of the envelope of the channel impulse response according to Section VI and the approximation in (74). The effective bandwidth can be extended by an array of RIS elements, where different sets of RIS elements are optimized for different frequencies. The signals from the different RIS elements are summed up at the receiver antenna. As an outlook to further research the extension of (67) around the carrier frequency ω_0 provides the broadband transfer function $H'_{bb}(\omega)$ with RIS bandwidth $\Delta B_{3\text{dB}}$, system bandwidth B_{system} and tap spacing $\Delta\tau(\omega)$, which corresponds to a spatial filter bank with *L* elements:

$$\Delta B_{3\text{ dB}} \approx \frac{1}{\Delta\tau_{max}} \qquad B_{system} = L \cdot \Delta B_{3\text{ dB}} \tag{106}$$

$$\tau_{i+\text{Int}\left\{\frac{f_0 + l \cdot \Delta B_{3\,dB}}{B_{system}}\right\}} - \tau_i = \Delta\tau = \frac{1}{B_{\text{system}}} \quad . \tag{107}$$

$$H'_{bb}(\omega) = \sum_{-L/2}^{L/2} \mathcal{F}\left(h_{mp}(t)\right) * \delta(\omega - \omega_0 - l \cdot 2\pi \cdot \Delta B_{3\,dB}) \tag{108}$$

IX. Conclusions

The approach of Reconfigurable Intelligent Surfaces (RIS) is discussed in the research community in the context of post-Shannon activities to improve radio channel capabilities with the objective to increase the channel capacity (Section II). In this paper the RIS approach is compared with the classical SISO radio transmission under Rayleigh or Rice fading conditions (Section III).

For the investigation a multipath propagation environment is considered, where the reflection is described by ideal metallic reflectors with a reflection coefficient of $\varrho = -1$. Multipath propagation results in an impulse response of different delayed paths. In practice large delays or path length differences may occur depending on the 3 dB antenna beamwidth at transmitter and receiver. Within a wide frequency range, the path delays are rather independent of the frequency. However, the path delays are transformed in a frequency dependent phase shift. In the RIS approach the phase shifts of the different resolvable paths are adjusted in a way that all paths are super imposed constructively, i.e., they are all in phase at carrier frequency. This maximizes at the receiver the received signal amplitude and thereby the received power and the channel capacity (Section III).

System and signal theoretical considerations are made in Section IV. A frequency independent RIS system would only be feasible, if all received paths show the same delay corresponding to a single path model. This approach can only be applied to radio channels without a direct component and would require in the RIS system unrealistic long delay lines.

Therefore, in practice all path phase shifts are adjusted to modulo 2π instead of the same delay. However, this superposition is very sensitive with respect to the frequency and the maximized received power is only available in a very narrow bandwidth. The radio channel transfer function around the carrier frequency f_0, where the RIS settings are

optimized, depends on the envelope of the channel impulse response. With increasing length of the impulse response $\Delta\tau_{max}$ a high absolute value of the transfer function around f_0 (optimal RIS settings) is only achieved for a very narrow decreasing bandwidth. This 3 dB bandwidth can be estimated by the inverse value of the maximum tap delay. This is in the order of the radio channel coherence bandwidth in [2], pp. 163 and [10], pp. 44. A wider 3 dB bandwidth can be achieved by shorter impulse responses. The achievable bandwidth of a RIS system for practical lengths of the impulse response for outdoor scenarios and big halls is much smaller than required for LTE, 5G and 6G systems. Therefore, further means for increasing the effective bandwidth are required (Sections V and VI). The RIS approach assumes that a much higher power can be received by constructive superposition of the different path components. Therefore, the signal/noise-ratio within the RIS bandwidth can be increased to improve the channel capacity. However, this can only be achieved within a small system bandwidth. A wideband system with standard SISO transmission and without RIS provides a much higher channel capacity than the narrowband RIS system for the same transmit power (Section VI.E.). A wideband system with a much wider bandwidth than the radio channel coherence bandwidth is the preferred solution with less complexity and higher channel capacity.

Also, with respect to displacements of the mobile station the RIS approach is very sensitive with a 3 dB bandwidth versus displacement in the order of the wavelength of the carrier frequency (Section VII). This requires a very fast adaptation of RIS settings for moving mobile stations.

A spatial filter bank with RIS elements, which are optimized for different frequencies, can provide a wideband RIS system (Section VIII).

REFERENCES

[1] Meinke/Gundlach, "Taschenbach der Hochfrequenztechnik," Berlin: Springer-Verlag 1986.

[2] T.S. Rappaport, "Wireless Communications - Principles & Practice," New Jersey: Prentice Hall 1996.

[3] J.B. Parsons J.B, "The Mobile Radio Propagation Channel," Pentech Press, London, 1992.

[4] H. Brodhage and W. Hormuth, "Planung und Berechnung von Richtfunkverbindungen," 10th updated edition, Siemens AG, Berlin – Munich, 1977.

[5] Recommendations and Reports of the CCIR, "XVIth Plenary Assembly," Dubrovnik 1986, Vol. V: Propagation in Non-Ionized Media, Report 338-5, Propagation Data and Prediction Methods Required for Line-of Sight Radio Relay Systems, ITU, Geneva 1986.

[6] ITU-CCIR, "CCIR Rep. 721-1, Recommendations and Reports of the CCIR," 1982, XV Plenary Assembly, Geneva 1982, Vol. 5.

[7] V. Jung, V. and H.-J. Warnecke, "Handbuch für die Telekommunikation," Springer Verlag, Berlin, second edition, 2002.

[8] Federal Communications Commission, "Millimeter Wave Propagation: Spectrum Management Implications," Office of Engineering and Technology, New Technology Development Division, Bulletin Number 70, July 1997.

[9] W.C. Jakes, "Microwave Mobile Communications," John Wiley & Sons, New York, 1974.

[10] W.C.Y. Lee, "Mobile Communications Engineering," McGraw-Hill Book Company, New York, 1982.

[11] W.C.Y. Lee, "Mobile Communications Design Fundamentals," Second edition, John Wiley & Sons, New York, 1993.

[12] R. Steele, "Mobile radio communications," Pentech Press Publishers, London and IEEE Press, New York, 1994.

[13] Y.-C. Liang, R. Long, Q. Zhang, J. Chen, H.V. Cheng, and H. Guo, "Large Intelligent Surface/Antennas (LISA): Making Reflective Radios Smart," Journal of Communications and Information Networks, Volume: 4, Issue: 2, June 2019, pp. 40 – 50.

[14] E.N. Papasotiriou, A.-A. A. Boulogeorgos, A. Stratakou, and A. Alexiou, "Performance Evaluation of Reconfigurable Intelligent Surface Assisted D–band Wireless Communication," 2020 IEEE 3rd 5G World Forum (5GWF), 10-12 Sept. 2020.

[15] M.A. ElMossallamy., H. Zhang, L. Song, K. G. Seddik, Z. Han, and G Ye Li, "Reconfigurable Intelligent Surfaces for Wireless Communications: Principles, Challenges, and Opportunities," IEEE Transactions on Cognitive Communications and Networking, May 6, 2020, https://www.scinapse.io/papers/3021587675.

[16] S. Liu, L. Xiao, M. Zhao, X. Xu, and Y. Li, "Performance Analysis of Intelligent Reflecting Surface in Multi-user MIMO Systems," Journal of Physics: Conference Series, ISAI 2020, 1575 (2020) 012078, https://iopscience.iop.org/article/10.1088/1742-6596/1575/1/012078/pdf#:~:text=Intelligent%20Reflecting%20Surface%20(IRS)%20is,the%20wireless%20signal%20transmitting%20environment.

[17] Y. Liu, X. Liu, X. Mu, T. Hou, J. Xu, M. Di Renzo, and N. Al-Dhahir, "Reconfigurable Intelligent Surfaces: Principles and Opportunities," arXiv: 2007.03435 [eess], November 2020, accessed: April 22, 2021 [online]. http://arxiv.org/abs/2007.03435.

[18] A. Taha, M. Alrabeiah, and A Alkhateeb, "Enabling Large Intelligent Surfaces With Compressive Sensing and Deep Learning," IEEE Access, Vol. 9, 2021, pp. 44304 – 44321.

[19] R. Fara1, D.-T. Phan-Huy, P. Ratajczak, A.Ourir, M. Di Renzo, and J. De Rosny, "Reconfigurable Intelligent Surface-Assisted Ambient Backscatter Communications – Experimental Assessment," IEEE International Conference on Communications Workshop on Reconfigurable Intelligent Surfaces for Future Wireless Communications, 2021, Microsoft Word - 50622021002149Paper_05_v17.docx (arxiv.org).

[20] M. He, W. Xu, H. Shen, G. Xie, C. Zhao, and M. Di Renzo, "Cooperative Multi-RIS Communications for Wideband mmWave MISO-OFDM Systems," IEEE Wireless Communications Letters, Vol. 10, No. 11, November 2021, pp. 2360 – 2364.

[21] M. Saber, M. Chehri, R. Saadane, Y. El Hafid, A: El Rharras, and M: Wahbi, "Reconfigurable Intelligent Surfaces Supported Wireless Communications," Elsevier, Procedia Computer Science, Volume 192, 2021, pp. 2491-2501, https://www.sciencedirect.com/science/article/pii/S1877050921017555.

[22] I. Alamzadeh, G. C. Alexandropoulos, N. Shlezinger, and M. F. Imani, "A reconfigurable intelligent surface with integrated sensing capability," Scientific Reports, Volume 11, Article number: 20737 (2021), Cite this article (2237 Accesses, 4 Altmetric, Metricsdetails), https://www.nature.com/articles/s41598-021-99722-x.

[23] J.B. Thomas, J.B, "An Introduction to Statistical Communication Theory," John Wiley & Sons, New York.

[24] W.B. Davenport and W.L. Root, "An Introduction of the Theory of Random Signals and Noise," McGraw-Hill Book Company, New York, 1958.

[25] D. Middleton, "An introduction to statistical communication theory," McGraw-Hill Book Company, New York, 1960.

[26] M. Pätzold, "Mobile Fading Channels," John Wiley & Sons, Ltd, Chichester, 2002.

[27] M. Abramowitz and I.S. Stegun, "Handbook of mathematical functions," Dover Publications, Inc., New York, 1972.

[28] J. Dreszer, "Mathematik Handbuch für Technik und Naturwissenschaft," VEB Fachbuchverlag Leipzig, 1975.

[29] H-D. Lüke, "Signalübertragung – Einführung in die Theorie der Nachrichtenübertragungstechnik," Springer-Verlag, Berlin, 1975.

[30] O. Föllinger, "Laplace- und Fourier-Transformation," AEG-Telefunken, Elitera Verlag, 2. Auflage, Berlin, 1980.

[31] W. Gröbner and N. Hofreiter, "Integraltafel – Zweiter Teil Bestimmte Integrale," 5th edition, Springer-Verlag, Vienna, New York, 1973.

[32] I. Bronstein and K.A. Semendjajew, "Taschenbuch der Mathematik," Verlag Harri Deutsch, Zürich and Frankfurt/Main, 1974.

GDOP optimised LEO constellation for Positioning Estimation

Harshal More
Dept. Electronics Engineering
Torvergata University
Rome, Italy
catchmemore@hotmail.com

Mauro De Sanctis
Dept. Electronics Engineering
Torvergata University
Rome, Italy
mauro.de.sanctis@uniroma2.it

Ernestina Cianca
Dept. Electronics Engineering
Torvergata University
Rome, Italy
cianca@ing.uniroma2.it

Cosimo Stallo
Dept. Navigation Engineering
Thales Alenia Space
Rome, Italy
cosimo.stallo@uniroma2.it

***Abstract*—An emergence of new applications such as autonomous driving, UAVs, indoor positioning determination, low energy positioning, Robust Real Time Kinematics (RTK) estimation, infra referencing are demanding for robust, accurate, safe GNSS systems. On contrary conventional Medium Earth Orbit (MEO) or Geo Synchronised Orbit (MEO+GSO) based GNSS systems are facing limitation in terms of performance against growing threats such as spoofing, jamming and multipath.**

On the other hand, new space economy and race to launch Mega Constellations from private sectors such as Starlink, Oneweb, Kuiper, Iridium etc, for applications such as internet, IoT, telecommunication hint towards the Low Earth Orbit (LEO) satellites to be recognised as the promising positioning system in the near future where these piggybacked payloads can be used for Precise Positioning, Navigation and Timing (PNT) estimation. In fact, the versatility, small dimensions, short development period and high return-to-cost potential make LEO satellites attractive options not only for technology demonstration but also for navigation purpose. Moreover, considering relative proximity to the Earth compared to MEO satellites, high C/No ratio, high speed, the Doppler based positioning makes LEO systems good candidates for future positioning solutions to complement the existing GNSS and terrestrial navigation.

In this context, this paper presents the design of a dedicated LEO constellation optimized using a Genetic Algorithm (GA). The optimization aims to minimize the Geometric Dilution of Precision (GDOP). The paper demonstrates that the designed constellation provides good Geometrical Navigation Accuracy (GNAC) and global availability. The proposed constellation is a combination of sub-Walker constellations (hybrid) that can provide 100 % global coverage, with at least 4 visible satellites at given epoch. Using the proposed constellation, the position accuracy in a static and dynamic user scenario has been assessed.

***Index Terms*—LEO Positioning, GDOP, Global Availability, GNAC, Optimised LEO, GA.**

I. Introduction

The conventional Medium Earth Orbit (MEO) based Global Navigation Satellite System (GNSS) is prone to growing intentional and unintentional threats such as spoofing, jamming, multipath etc. On parallel, the emergence of new applications such as UAVs, Autonomous Driving etc, shows a clear tendency of even more demanding requirements for robust, accurate and safe GNSS system.

Current technological developments in small satellite industry and race to launch mega constellations from private sectors such as Starlink, Oneweb, Kuiper, Iridium for various applications such as internet, IoT, telephony, telecommunication hint towards the LEO satellites that can be recognised as the promising positioning system in the near future where these LEO constellations can be used for Precise PNT analysis and estimation.

There are several advantages where these LEO systems can be good candidates for future positioning solutions. The author [7] has shown that Doppler based positioning using LEO is complementary to the existing GNSS and terrestrial navigation. The relative proximity to the Earth compared to MEO satellites makes LEO signals 300 to 2400 times more powerful than GNSS signals. This strongly reduces static and persistent multipath in an urban canyon. The assessment study [4] of UHF/VHF has shown that lower altitude reduces space losses less than 10 dB w.r.t. MEO (includes antenna), lower frequency reduces free space losses with 24 dB (VHF) w.r.t. L Band. Similar studies show that the use of L/S/C bands can be used along with Ka/Ku to improve the performance. The comparison shown in [13] between MEO and LEO (Iridium) has proved that the spreading loss at zenith for LEO is -69 dB and for MEO is –97 dB while the multipath decorrelation time is 1 min and 10 min, respectively. Simulations with Signal of Opportunity (SoO) have shown that the convergence time for full operational capability multi GNSS PPP can be significantly shortened from 9.6 min to 7.0, 3.2, 2.1 or 1.3 min through augmentation with 2.4, 3.1, 6.3 or 9.5 visible LEO satellites respectively [10].

All the above mentioned studies are carried out using existing LEO mega constellations as SoO. Moreover considering the advantages of current LEO satellites for navigation purpose, constellation design is fundamental to improve the performance in terms of accuracy and availability. Several research have been done to design optimised constellations for different purposes. Author [2] shows the optimization of

classical MEO constellation for global coverage and hybrid LEO+GSO constellation to provide a navigation service over Europe. In [5] author has designed hybrid constellations for broadband internet access that can be used for augmented navigation purpose with global coverage and at most three visible satellites. Research [12] has shown optimization with combined GA and semi-analytical approach for regional coverage to reduce computational load of GA. Similarly, the paper [8] describes the application of an evolutionary optimization method to design a regional communication satellite constellation.

However, none of the above works proposes an optimal design for a LEO constellation dedicated to navigational services. The paper presents the design of a dedicated LEO constellation using GA which aims to minimize the GDOP and maximize the global coverage with at least 4 visible satellites at given epoch.

The paper is organized as follows: Section I reviews current LEO constellations used for PNT in recent. In section II, an analysis of some selected constellations is carried out which provides useful hints to define important properties of the constellation to be designed; the mathematical modelling of hybrid constellations is presented in section III. Section IV explains GA implementation with definition of fitness function, constraint function, selection of optimization variables and parameter selection for GA which includes population selection, generation size, probability of crossover, probability of mutation and search ranges. Section V and VI shows simulation and discussion of the achieved results respectively; conclusions are drawn in section VII.

II. Preliminary Choice of Some Orbital Parameters

Table I shows an overview of orbital parameters of mainstream GNSS [9] and some selected LEO mega constellations [9]. This is useful to get some initial hints on orbital parameters choices such as eccentricity, argument of perigee, altitude, type of configuration etc. In particular, a combination of circular sub-Walker constellation has been chosen. As a matter of fact, circular constellations are better for navigation and communication purpose due to the constant velocity in the given orbits. Therefore, eccentricity (e) and argument of perigee (w) are set to 0. The choice of hybrid configuration with combination of sub-Walker constellations is motivated by the fact that higher inclination orbits offer better coverage at poles and lower inclination offers greater coverage in equatorial areas [14]. For an instance, to get global coverage Starlink uses a hybrid constellation (different altitude, inclinations) as shown in I.

About the altitude LEO constellations are classified as follows:

1) **Low LEO orbit** (**<1000 Km):** Currently, there are more than 300 satellites at this altitude. Most of them with small and low cost platforms (Nanosat/Cubesat). The New Space Economy is focused here.
2) **High LEO orbit** (**>1000 Km):** At this altitude, there are less than 150 satellites, with moderately bigger platforms, higher reliability and larger lifetime compared to low LEO orbits.
3) **Higher orbit** (**>1200 Km):** There are very few satellites with medium size platforms, higher reliability and longer lifetime with respect to other two orbits.

As shown in the Table I, most of the selected LEO mega constellations are in orbit lower than 1200 Km. Therefore, Low LEO and High LEO orbits are crowded with large number of satellites. Moreover considering other effects such as distribution of space debris, the radiation environment, Total Ionizing Dose (TID) and other orbital perturbation, the higher orbit LEO are considered a better choice [5]. Therefore, we have set the altitude to 1250 Km.

III. Mathematical Model for LEO Constellation Design

We aim to design a hybrid constellation. A Walker constellation is represented by the notation $a : i : T/P/F$ where: a is semi-major; i is the inclination; T is the total number of satellites per plane; P is the total number per orbital planes; F is the phasing between satellites in adjacent planes; $S = T * P$ is total number of satellites. A hybrid constellation is represented as follows based upon different inclinations:

- **Sub-Walker – I (Polar Orbits,** $i = 90°$ **)**
- **Equatorial Orbit** ($i = 0°$)
- **Sub-Walker – II (Optimize,** $0° < i < 90°$)

Mathematical modelling of polar, equatorial orbits and sub-Walker – II are presented in the next sub-sections.

A. Designing of Polar and Equatorial Orbit

Fig. 1 shows the single satellite coverage on the Earth's surface.

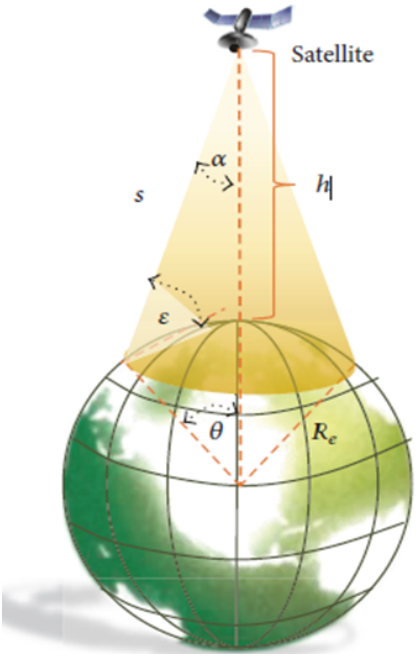

Fig. 1. Single Satellite Coverage with Earth's central angle of visibility [12]

Constellation	Application	Altitude Per Orbit (Km)	Mean Velocity (Km/s)	Period (min)	Planes per Orbit	Satellites per Plane	Total Number of Sat	Inclination (deg)	e	Frequency Bands Downlink
GPS	Navigation	20200	3.88	720	6	4	24	55	0	L1 - 1575.42 Mhz L2 -1227.60 MHz
GALILEO	Navigation	23222	3.66	845	3	6	24+6	56	0	E -1176-1207 MHz
Starlink	Global Internet Broadband	335.9 340.8 345.6 550 1110 1130 1275 1325	7.5576 7.5839 7.6098 7.4984 7.2139 7.2696 7.2128 7.1679	91-112	9 7 9 24 32 8 5 6	77 354 283 66 50 50 75 75	11943	42 48 53 53 53.8 74 81 70	0	K-band: 17.8-18-5 GHz 18.8-19.3 GHz 19.7-20.2 GHz V-band: 37.5-42.0 GHz
Oneweb	Global Internet Broadband	1200	7.24	110	18	36	358	87.9	0	Ku-Ka Bands
Iridium Next	Narrowband Communication	780	7.4628	97	6	11	66	86	0	L-band: 1.616-1.63 GHz K-band: 19.3-19.7 GHz
LEO 288*		1000	7,37	105	12		192	90	0	Not defined
LEO 192*		600	9.97	96	12			90		Not defined
LEO 192*		1000	7,37	105	12		288	90		Not defined

TABLE I

OVERVIEW OF MAINSTREAM APPLICATIONS, ORBITAL PARAMETERS, TYPE OF FREQUENCY BANDS OF SELECTED CONSTELLATIONS, * SOME SELECTED LITERATURE CONSTELLATIONS [10]

Based upon the sensor half angle and maximum swath width of the satellite, a coverage circle with a radius can be calculated by the following Eq.1, [12]:

$$\theta = \arccos\left(\frac{R_e + h}{R_e}\cos\epsilon\right) - \epsilon \tag{1}$$

where θ is the Earth's central angle of visibility viewed from its center, R_e is the radius of the Earth, h is the altitude of satellite, ϵ is the elevation mask angle.

For a given constellation, to get a continuous and uniform coverage over desire point, the minimum number of P and S can be deduced by the Eq.2 & Eq.3, [8]:

$$P_{min} = \left\lceil \frac{2\pi}{\theta} \right\rceil \tag{2}$$

$$S_{min} = \left\lceil \frac{\pi}{\theta} \right\rceil \tag{3}$$

In order to define the complete configuration for both polar and equatorial orbits, S and P in both orbits at given angle ϵ are given by Eq.4, [5]:

$$\Big\{(P_p - 1).\arcsin[\tan(\alpha)\cos(\pi/S_e)] + (P_p + 1)\arcsin\left[\frac{\sin(c)\cos(\pi/s_e)}{\cos(\alpha)}\right]\Big\}\eta = \pi \tag{4}$$

where;

$$c = \arccos\left[\frac{\cos(\alpha)}{\cos(pi/S_p)}\right] \tag{5}$$

P_p are the number of polar planes, S_p are the number of polar satellites in P_p, S_e are satellites in equatorial planes, α is sensor half cone angle, η is the multiplication factor set to 1. Non-linear Eq.4 can be solved using conditions from Eq.2 & Eq.3. Using Eq.1 to Eq.5 the complete configuration of polar and equatorial orbit is designed.

B. Designing of Sub-Walker - II

A Walker configuration can be sub divided into the following configuration based upon the satellite distribution of the Right Ascension of the Ascending Node (RAAN) between the planes of the constellation [1]:

- **Delta configurations:** This configuration have orbital planes distributed evenly over a span of $360°$ in RAAN.
- **Star configurations:** This configuration have orbital planes distributed over a span of $180°$ in RAAN.

In order to narrow the scope of optimization and increase efficiency of GA, the optimization is performed over a sub-Walker - II with delta configuration with inclined orbits. Eq.6 shows the modelling for sub-Walker II [5]:

$$\begin{cases} a_{k,j} = a_0 \\ e_{k,j} = e_0 \\ i_{k,j} = i_0 \\ \Omega_{k,j} = \Omega_0 + \frac{360^0}{P} * (k-1) \\ w_{k,j} = w_0 \\ M_{k,j} = M_0 + \frac{360^0}{P*S} * F * (k-1) + \frac{360^0}{S}(j-1) \end{cases} \tag{6}$$

where, k & j are the indices of k^{th} satellite in its j^{th} orbit plane, Ω is the $RAAN$, w is the Argument of Periapsis, M is the Mean Anomaly (MA). Suffix 0 represents nominal reference satellite. Initial Ω_0 and M_0 is set to 0 for the reference satellite of each sub constellation.

IV. Optimization Using Genetic Algorithm

GA is an optimization method inspired by the Principle of Natural Selection (Darwin's theory of Natural Evolution). It is population based technique. From population, a GA selects individuals with good chances of reproduction (best fitness function) and reproduces the new generation of individuals using operations such as crossover and mutation. In GA solutions are terms as chromosomes. There are two types of chromosomes, one is parent chromosome and other is offspring chromosome. From parents chromosomes new solutions are generated where as from offspring chromosomes contains newly generated solutions. Better candidate has more chance to survive in an environment of limited resources. Good solutions are retained where as bad solutions are eliminated. The process is repeated several times until it runs a certain number of generations or until a solution considered as optimum is reached [6].

A. Fitness Function and Constraints Functions

The first step of the optimization is the definition of the fitness function and constraints functions. The fitness function is defined to take into account both the minimization of the GDOP and the maximization of global visibility.

1) GDOP
   In navigation, precise positioning accuracy of user depends upon the geometrical configuration of the satellites i,e. Dilution of Precision (DOP). Several definitions of the DOP exist [3]:
   a) Geometric (GDOP): $\left(\sqrt{\sigma_x^2+\sigma_y^2+\sigma_z^2+\sigma_t^2}\right)/\sigma$
   b) Position (PDOP): $\left(\sqrt{\sigma_x^2+\sigma_y^2+\sigma_z^2}\right)/\sigma$
   c) Horizontal (HDOP): $\left(\sqrt{\sigma_x^2+\sigma_y^2}\right)/\sigma$
   d) Vertical (VDOP): $\left(\sqrt{\sigma_z^2}\right)/\sigma$
   e) Time (TDOP): $\left(\sqrt{\sigma_t^2}\right)/\sigma$

   where, σ is root mean square (rms) pseudorange error of a satellite, $\sigma_x, \sigma_y, \sigma_z$, are rms errors of the user position, σ_t is user clock bias error, which is assumed to be known. An evenness in satellite geometry is important to improve accuracy. Table II shows that typically ideal GDOP is less than 1. Excellent values for GDOP are in the range 1-2 and good ones are in the range 2-5. Mainstream GNSS has on the average excellent GDOP [4]. The objective of the optimization is to achieve performance in terms of GDOP that range between ideal and excellent values.

GDOP	Rating
< 1	Ideal
$1 < 2$	Excellent
$2 < 5$	Good
$5 < 10$	Moderate

TABLE II
GDOP RATINGS CLASSIFICATION [9]

2) Visibility of at least 4 satellites at global level
   To evaluate the user position, there is a need of at least four pseudoranges from visible satellites at given epoch. In case of more than 4 visible satellites accuracy in user location estimation can be further improved. Pseudorange errors are also function of elevation angle, free space losses and varies from satellite to satellite. In this paper, the LEO constellation is optimised for different elevation angles assuming no atmospheric losses. In order to calculate 100% visibility of satellites at global level as a function of design variables, some ground points of interest must be selected. Assuming that the Earth is perfectly symmetrical along both hemispheres, 18 Points are selected from $0°$ - $90°$ latitude and $0°$ longitude as shown in fig. 2. A 10 × 10 grid is generated along each point with further assumption of zero ellipsoidal height.

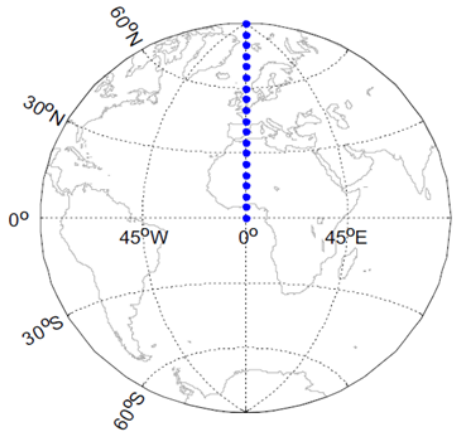

Fig. 2. Mapping of selected ground points for global coverage [5]

Therefore, we have defined the following fitness function:

$$J = min\big((1-\beta).f_1(x) + \beta.(1-f_2(x)\big), x \in C \quad (7)$$

where $f_1(x)$ is the GDOP, $f_2(x)$ is a function of the visibility and β is the parameter to define the weights for $f_1(x)$, $f_2(x)$. C represents the following constraints for optimization.

$$\begin{cases} \delta(x) = 100\% \\ F_o \leq P_o - 1 \\ P_o \in Z, \\ S_o \in Z, \\ F_o \in Z, \\ P_o.S_o = T_o \end{cases} \quad (8)$$

being $\delta(x)$, the global visibility of at least 4 satellites function of P_o, T_o, F_o, which are the important factors for evenness in satellite configuration. Z is an integer number. For a given set of satellites, different combinations of P_o, T_o, F_o and i_o are possible to design a constellation. Therefore, the optimization variables are:

$$x = [S_o, P_o, F_o, i_o] \quad (9)$$

Suffix o stands for optimization. Using the mathematical modelling from section III, the optimization process is finally performed using the GA toolbox of MATLAB.

B. Parameters selection for GA

GA tool box is setup as Table III. GA is computationally demanding hence, search is started with initial population 50 and gradually increased based upon Pareto graph. For extensive search, the population size is set to 300, 400 & 500. Similarly number of generations are chosen from 30, 40, 50 & 100. Optimization variables S_o, P_o, F_o must be integers, whereas i_o can be non-integer. To solve this mixed-integer constrained optimization problem, Mixed Integer Nonlinear Programming (MINLP) is used. The probabilities of crossover and mutation are 0.8 & 0.194 respectively [5]. To evaluate the score of each chromosome, a penalty function is used internally instead of the objective function due to the presence of the constraints. The penalty value is equal to the objective value for a feasible individual, while it is equal to the sum of the objective value of the worst feasible individual plus the violation score for an infeasible individual. Additionally, the optimization procedure is set to not terminate until the end of the generation.

Parameters	value
Population Size	300/400/500
Max generations	30/40/50/100
MINLP	S,P,F
Probability of crossover	0.8
Probability of mutation	0.194
Penalty	5

TABLE III
GA PARAMETER SETTINGS

The search ranges for optimization variables are shown in Table IV. Scenarios S1, S2, S3, S4 represent ϵ angles $7°$, $10°$, $15°$, $20°$ respectively with search ranges are chosen as per the reference [5]. Scenarios S5 and S6 are for ϵ angle $20°$ with search range for P_o from 10 - 20, F_o from 1 - 15 and i_o from $70°$ - $90°$. S5 explicitly represents only Walker constellation. Selection of search ranges follow the constraint defined in eq.8.

X/ϵ	S1($7°$)	S2($10°$)	S3($15°$)	S4($20°$)	S5($20°$)	S6($20°$)
S_o	4-12	4-12	4-15	4-12	4-15	4-15
P_o	1-10	1-10	1-10	1-10	10-20	10-20
F_o	1-9	1-9	1-9	1-9	1-15	1-15
i_o	$45°$-$60°$	$45°$-$60°$	$45°$-$60°$	$45°$-$60°$	$70°$-$90°$	$70°$-$90°$

TABLE IV
SEARCH RANGES FOR OPTIMIZATION VARIABLES FOR EACH CASE

V. SIMULATION

Initially, a two body propagator is simulated at the epoch 1 January, 2000 for 2 complete orbits, which defines the simulation period. Visibility is calculated only when the angle between the given ground point and satellite is less than the Earth's central angle. At given epoch, if the number of visible satellites at a given location is at least 4, the GDOP is estimated. If the mean of GDOP for all points is higher than 5 or the satellite does not cover any target latitude, the algorithm automatically assigns a high value to the fitness function.

The fitness function of each individual solution is evaluated for every generation, and while the evaluation does not hit the stopping criteria, the selected parents continue to meet and reproduce new generations via crossover and mutation. The stopping criteria is set as default in MATLAB (tolerance) and testing of all generations and population to minimize the objective function.

VI. RESULTS AND DISCUSSION

The GA algorithm has been applied using the ϵ angle $7°$, $10°$, $15°$, $20°$ obtaining the satellites configurations S1, S2, S3, S4, S5, S6 described in Table V. Parameters P_p, S_p, S_e are obtained based upon the condition from Eq.4. While S_o, P_o, F_o, i_o are the achieved optimised parameters obtained for the sub-Walker - II constellation. Case S5 shows a complete Walker constellation without polar and equatorial orbits. The obtained results are sensitive to the different search ranges and GA parameter settings. Hence, cases S4, S5, S6 have varying configurations for the same elevation angle.

Param	S1	S2	S3	S4	S5	S6
S_p	6	6	7	7	0	7
P_p	7	8	9	9	0	9
S_e	7	8	9	10	0	10
S_o	5	7	13	10	16	16
P_o	9	10	8	13	10	10
F_o	1	3	5	5	8	8
i_o	$50.37°$	$46.58°$	$46.52°$	$50.50°$	$70.23°$	$70.23°$
T_{sat}	94	120	176	203	160	233

TABLE V
OBTAINED CONFIGURATION FOR HYBRID CONSTELLATION FOR DIFFERENT ELEVATION ANGLES

The obtained constellations from Table V are then simulated in STK. In Fig. 3 only cases S1, S2, S3, S4 are shown. S5 and S6 could be added but the results are very similar and the readability of the Fig.3 would decrease. Moreover, we have calculated the position accuracy on the following two scenarios:

1) Static user located in Rome
2) Dynamic user travelling from Rome to Milan by Uniform Rectilinear Motion (URM) with constant velocity of about 96.3 Km/h.

For both scenarios, geometric ranges are imported in MATLAB from the visible satellites at each epoch. A standard normal distribution noise of 1 m, 5 m, 10 m & 20 m is added to simulate code measurements for positioning estimation using Least Square (LS) solution. Velocity estimation is done using the rate of change of position estimation. In this way, the performance in terms of navigation accuracy for both cases is determined using the optimized LEO constellations. Different graphs are plotted for all cases.

Fig. 4 shows the visibility of average number of satellites at an interval of 60 seconds over latitude from $0°$ to $90°$ North.

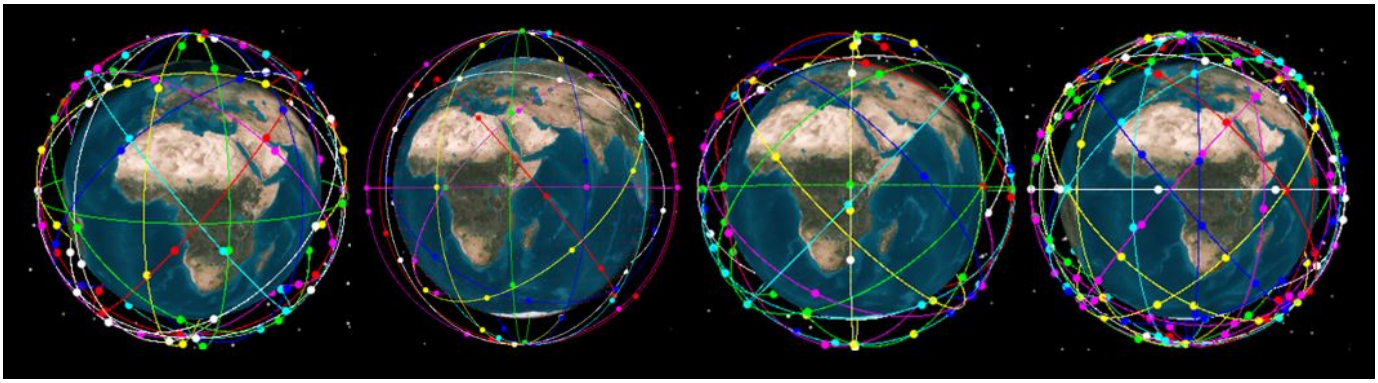

Fig. 3. Cases S1 (7°), S2 (10°), S3 (15°), S4 (20°) with respective elevation mask angles from left-right

Case S6 has maximum number of average visible satellites due to maximum number of satellites in the constellation. For S5 average number of visible satellites are lesser than S6 due to absence of polar and equatorial orbits. S1, S2, S3 shows constant results in terms of availability over entire region. On an average at least 5 satellites are visible at each latitude. The good visibility is achieved at lower latitude. Case S4 has the highest visibility among all solutions at lower latitude while at higher latitude, the visibility is reduced but it is still sufficient.

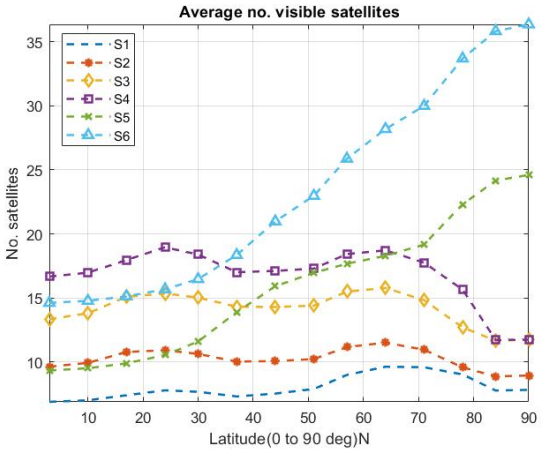

Fig. 4. Average number of visible satellites over latitude

Fig. 5 shows the GDOP over the latitude (0° - 90°) North. For all configurations GDOP is less than 2 except for S1. For Cases S3, S4, S6 average GDOP is about 1.5, which means that GDOP results are in the excellent range (Table III). For S6, GDOP further goes below 1 after 55° latitude, so ideal GDOP value can be achieved. S1 has worst GDOP among all configurations but it is still in the range of good GDOP (Table III). Similar results are achieved for HDOP, PDOP, VDOP, TDOP.

Similarly, GNAC is computed for the optimized configurations as shown in Fig. 6, which has a similar behaviour as the GDOP (Fig. 5). S6 GNAC is the lowest among all cases. It goes below 5m after 57° latitude. S3, S4, S6 performance are better i.e. less than 8m. Similarly position (PNAC), horizontal

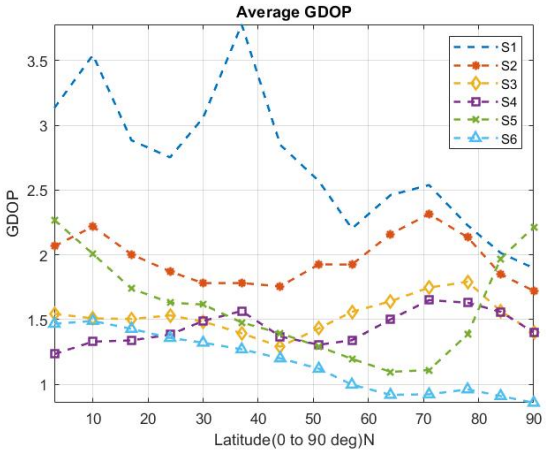

Fig. 5. GDOP over latitude

(HNAC), verticle (VNAC), time (TNAC) navigation accuracy show similar results. Based upon the assumption of symmetry of the Earth, Fig. 4, Fig. 5, Fig. 6 show symmetric behavior for latitude (0° - 90°) South.

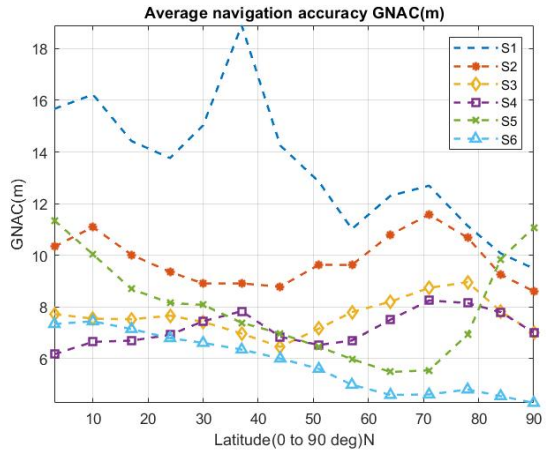

Fig. 6. GNAC over latitude

Stationary and dynamic scenarios are simulated in STK for

60 minutes. Fig. 7, Fig. 8 and Fig. 9 show results using only S5 case. Fig. 7, shows average GDOP for both scenarios. Dynamics user is moving with velocity 96.3 Km/h so, GDOP is shows more variation with respect to stationary one. Average GDOP for both scenarios is about 1.187.

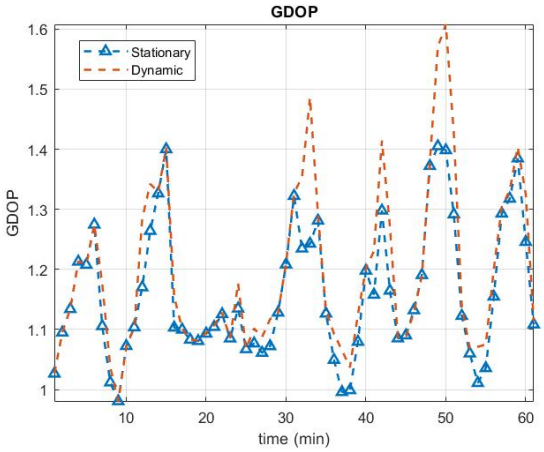

Fig. 7. GDOP for stationary and dynamics user for 60 min

Fig. 8 and Fig. 9 represents GNAC for both scenarios respectively. Each scenario shows GNAC values for uncertainties 1 m, 5 m, 10 m, 20 m in code measurements. For lower uncertainties, GNAC is on an average 5 m, and 8 m for static and dynamics user scenarios respectively.

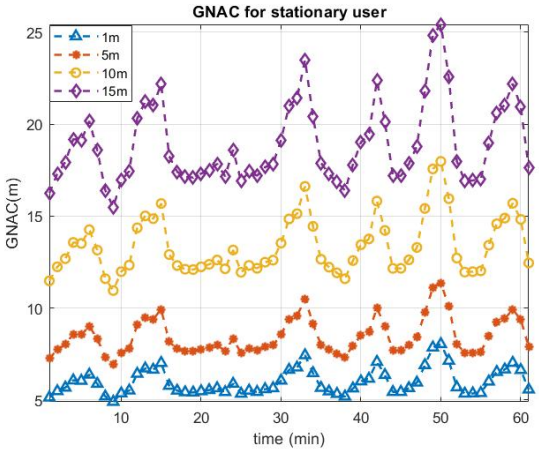

Fig. 8. GNAC for stationary user for 60 min

Further, Fig. 10 shows errors in LS positioning estimation (x,y,z) of stationary user using LEO (S5) and MEO (GPS) measurements. The graph is for worst case scenarios with the standard normal distribution noise of 10 m. The average absolute position error in x, y, z directions is 5.7857 m, 3.4933 m, 6.5981 m for S5 whereas that for GPS is 10.294 m, 3.7825 m, 4.7727 m respectively.

Fig. 11 shows the normalized positioning estimation error. The average error in square root of all 4 components i.e. x, y, z, t is 10.3606 m and 12.7264 m for S5 and GPS respectively.

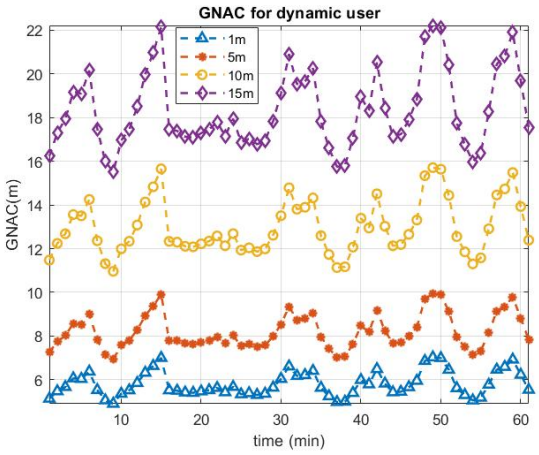

Fig. 9. GNAC for dynamics user for 60 min

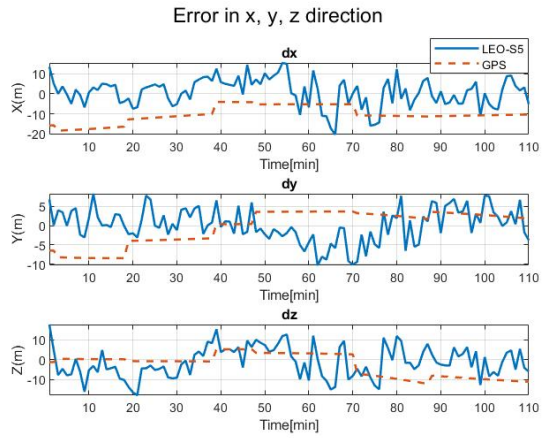

Fig. 10. LS estimation error in x,y,z directions

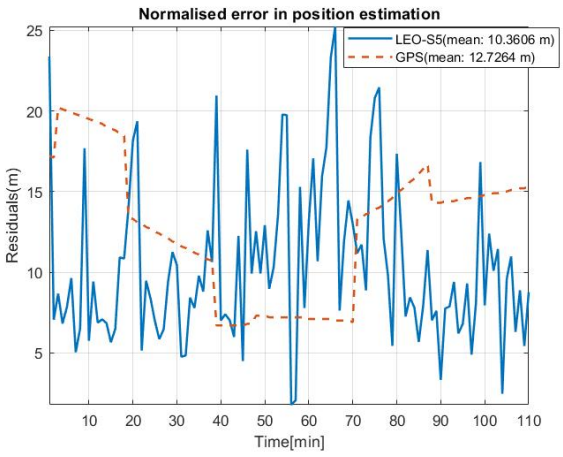

Fig. 11. Normalised error in positioning estimation

It is assumed that in the both cases ephimeris of satellites are already known. Errors in the case of S5 seem to be more fluctuating than GPS due to the rapid change in geometry of

LEO (faster velocity) and more visible satellites at given epoch than GPS. Moreover these errors in positioning estimation also depends upon the level of standard normal distribution measurement noise. Similarly, positioning estimation using LS for other cases (S1, S2, S3, S4, S6) is found to be satisfactory for different level of standard normal distribution noise.

VII. Conclusion and future work

The paper has presented the design of a dedicated PNT LEO constellation optimized to minimize the GDOP and maximize the satellite visibility at global level. The achieved optimised constellation provides good navigation accuracy (GNAC) and global availability. The proposed solution is a combination of sub-Walker constellations which can provide 100% global coverage with at least 5 visible satellites at given epoch. Higher orbit zone (>1200 Km) is a good choice for these constellations. The GDOP values of all obtained solutions are in the excellent range ($1 < 2$). Cases S3, S4 and S6 can be good choices for improving the performance as GDOP is lower than 1.5. S6 is best among all with GDOP in ideal range but number of satellites in constellation are maximum. Positioning estimation for static and dynamic scenarios is effective using proposed constellations. For higher latitude GDOP is further improved to 1.187 for S5. Even for worst case (std noise of 10 m), final average error in positioning estimation is 10.3606 m and 12.7264 m for LEO and MEO respectively.

GA is stochastic approach but computationally demanding. Final results depend upon various factors such as population size, generation size, step size, orbital propagator, mutation and crossover probabilities, search ranges etc. In future, analysing the LEO signals considering factors such as type of signal, clock synchronization biased, ephemeris etc, which is considered to be known already may yield more meaningful results and make this problem closer to a real case. Other considerations about orbital parameters such as altitude, RAAN, mean anomaly are considered same for complete hybrid constellation which should be changed slightly to avoid collisions between satellites. Moreover, subsequent increase in mainstream GNSS satellites, optimised LEO based navigation can be complimentary solution/standalone solution in presence of threats. It would be also interesting to investigate the integration of LEO+MEO, LEO+INS signals or LEO code+Doppler measurements to improve the accuracy in Urban Canyon environment.

References

[1] Designing of Walker constellation using STK. Help documentation, https://help.agi.com/stk/11.0.1/Content/stk/tools-12.htm

[2] Dufour, F., Bertrand, R., Sarda, J., Lasserre, E., and Bernussou, J. (2019).“Constellation Design Optimization with a Dop Based Criterion.” 14^{th} International Symposium On Space Fligt Dynamics.

[3] Elliott D Kaplan, Christopher J Hegarty. (2017). ”Understanding GPS: Principles and Applications.” (Second Edition 2nd Revised ed. Edition), Artech House.

[4] Francis Soualle. (2018). ”Perspectives of PNT Services Supported by Mega-Constellations.” ITSN, GPS World.

[5] Fujian Ma, Xiaohong Zhang1, Xingxing Li, Junlong Cheng, Fei Guo, Jiahuan.(2020).”Hybrid constellation design using a genetic algorithm for a LEO-based navigation augmentation system.” GPS Solutions Volume 24.

[6] Goldberg, D. E. (1989). ”Genetic algorithms in search, optimization, and machine learning.” (13th ed. Edition). Addison-Wesley Publishing Company.

[7] Hamza Benzer, rouk Quang Nguyen Fang, Xiaoxing abdess, amadam-rhar, Hamza Rasaee, Rene. JrLandry. (2019). ”LEO satellites Based Doppler Positioning Using Distributed nonlinear Estimation.” IFAC-PapersOnLine Volume 52, Issue 12, 2019, Pages 496-501

[8] I. Meziane-Tani, G. Métris, G. Lion, A. Deschamps, F. T. Bendimerad & M. Bekhti. (2016). ”Optimization of small satellite constellation design for continuous mutual regional coverage with multi-objective genetic algorithm.” International Journal of Computational Intelligence Systems, 9:4, 627-637, DOI: 10.1080/18756891.2016.1204112.

[9] Isik OK, Hong J, Petrunin I, Tsourdos A. (2020). ”Integrity analysis for GPS-based navigation of UAVs in urban environment.” Robotics, Volume 9, Issue 3, Article number 66.

[10] Li Xingxing, Ma Fujian, Li Xin, Lv Hongbo, Bian Lang, Jiang Zihao, Zhang Xiaohong. (2018). ”LEO constellation-augmented multi-GNSS for rapid PPP convergence.” Journal of Geodesy, Volume 93, Issue 5, pp.749-764.

[11] Ruben Morales-Ferre, Elena Simona Lohan, Gianluca Falco, Emanuela Falletti. (2020). ”GDOP-based analysis of suitability of LEO constellations for future satellite-based positioning.” IEEE International Conference on Wireless for Space and Extreme Environments (WiSEE).

[12] Tania Savitri, Youngjoo Kim, Sujang Jo, and Hyochoong Bang. (2017). ”Satellite Constellation Orbit Design Optimization with Combined Genetic Algorithm and Semianalytical Approach. International Journal of Aerospace Engineering.” Hindawi, article ID 1235692.

[13] Tyler G.R. Reid,Andrew M. Neish,Todd Walter,Per K. Enge. (2018). ”Broadband LEO Constellations for Navigation. NAVIGATION: Journal of the Institute of Navigation.” Volume 65, Number 2, Pages: 205 - 220.

[14] Yang M, Dong X, Hu M.(2016). ”Design and simulation for hybrid LEO communication and navigation constellation.” Proceedings of the IEEE CGNCC. Chinese Society of Aeronautics and Astronautics, China, pp 1665–1669.

Dynamic Resource Block Allocation in Network Slicing

Nidhi *‡, Bahram Khan†§, Albena Mihovska *¶, Ramjee Prasad *‖,
Vladimir Poulkov ‡††, Fernando J. Velez †**
*AU – Department of Business Development and Technology, Aarhus University, Herning, Denmark
†Instituto de Telecomunicações and Universidade da Beira Interior,
Faculdade de Engenharia, Departamento de Engenharia Electromecânica Covilhã, Portugal
‡TU – Technical University Sofia, Bulgaria
Emails: ‡nidhi@btech.au.dk, §bahram.khan@lx.it.pt, ¶amihovska@btech.au.dk, ‖ramjee@btech.au.dk,
††vkp@tu-sofia.bg, **fjv@ubi.pt

***Abstract*—Network slicing is crucial in 5G and its evolution concerning user-centric services. By allocating independent resources, like link bandwidth, computing/processing capabilities and spectrum, to address users' requests, slicing serves the end-to-end verticals or services. gNodeB (gNB) allocates the bandwidth resources to transmit/receive data to User Equipments (UEs). Resources Blocks (RBs) are the smallest resource entities assigned to a single user. In 5G New Radio (NR), the time-domain resource allocation defines the allocated symbols (OFDM symbols), while the frequency-domain allocation illustrates the RBs (sub-carriers) allocation to the UE. RB comprehends 12 sub-carriers in the frequency domain with a flexible RB bandwidth, unlike LTE-A. It is critical to provide enhanced services to different users. There have been several works on challenges to enable a multi-tenant and service RAN while providing isolation to the slices. This work proposes a detailed approach for creating slices based on the demanded services, resource virtualization and isolation. The focus is on resource sharing algorithms at the Slice Orchestrator (SO) level. These virtual network slices support a wide range of services and applications categorized into the Enhanced Mobile Broadband, Ultra-Reliable and Low-Latency Communications and Massive Machine-Type Communications megatrends. The paper also provides an overview of standardization activities and evolving requirements to support use cases and services like Holographic Telepresence, Automotives, among other.**

***Index Terms*—Network Slicing, Communication Service Providers, RB Allocation, Slice Isolation, Holographic Communication, Industry 4.0.**

I. Introduction

The roll-out of fifth-generation (5G) wireless networks has embarked on the concept of Network Slicing (NS) as one of its fundamental technologies. NS facilitates a segmented layer of networks as slices or network slices in addition to the base network architecture [1]. As an integral part of the virtual network, these network slices offer full end-to-end connectivity for user-specific services [2]. The slices forming isolated virtual network layers exhibit all the required functionalities of the shared physical network. It enables the Communication Service Providers (CSPs) to address various inventive business models, use cases, and tailor-made user-specific solutions with guaranteed performance over a prevailing infrastructure. NS diminishes the requirement for new physical networks for dedicated services. The network orchestration helps CSPs to automate the communication on and across the network providing tailored services with guaranteed Quality of Service (QoS) for various usage scenarios, in association with Service Level Agreements (SLAs) [3].

NS Framework was first proposed by the Third Generation Partnership Project (3GPP) in Release 15 [4]. It has gradually evolved, with the technical details and enhancements in the following releases. By employing NS, CSPs can create multiple virtual slices to acknowledge enormous data traffic increases and specific user requirements. Each slice in isolation, i.e., without interfering with the coexisting slices, hosts individual network functions and application services [5]. Various Standard Development Organizations (SDOs) have backed NS to support multi-vendor services [6]. The Next-Generation Mobile Network (NGMN) [1] laid out the detailed principle of creating and managing multiple independent logical mobile networks over shared physical infrastructure.

This work focuses on resource-sharing algorithms at the Slice Orchestrator (SO) level and computing slice's radio resource requirements and usage. The resources are periodically adjusted based on the current Channel Quality Indicator (CQI). The scheduler needs to handle the demand and service quality. As it is essential to efficiently allocate radio resources in dynamic environments, allocating resources to slices distinguishes services to meet user QoS. The proposed method tracks adaptive behaviors of communication services based on the number of active users, data buffer status, and channel condition. Additionally, the paper also provides different use cases enabling future networks and an overview of the standardization activities towards NS.

The remaining paper is organized as follows. Section II discusses the state-of-the-art concerning resource management, NS standardization activities, and requirements. Section III

This work was supported by FCT/MCTES through national funds and when applicable cofounded EU funds under the project UIDB/50008/2020, ORCIP (22141-01/SAICT/2016), COST CA 20120 INTERACT, SNF Scientific Exchange-AISpectrum (project 205842) and TeamUp5G. TeamUp5G has received funding from the European Union's Horizon 2020 research and innovation programme under the Marie Skłodowska-Curie ETN TeamUp5G, grant agreement No. 813391.

summarizes our methodology and assumptions, along with the discussion of the results. Finally, Section IV presents the main conclusions of this work and discusses topics for further research.

II. State-of-the-Art

The evolving services are categorized broadly into the following four classes: (i) enhanced Mobile Broadband (eMBB), (ii) Ultra-Reliable Low-Latency Communications (URLLC), (iii) massive Machine-Type Communications (mMTC), and (iv) Vehicle to Everything (V2X). These services set the Key Parameter Indicators (KPIs) to evaluate the user requirements enabled through network slicing. In 4G networks, NS was limited to service isolation [7]. However, with 5G and beyond networks, NS can facilitate CSPs to provide guaranteed QoS services via virtual network slices, also called "5G Slice". The resources are allocated on-demand with a valid session using existing virtualization techniques. Thus, it adds additional scalability and flexibility to conventional networks. By facilitating resource sharing and automation among independent 5G slices, virtualization and Orchestration technologies are the key enablers of NS [8], [9]. NGMN defined a 3-layer NS framework [1] enabling a flexible and scalable End-to-End (E2E) architecture, consisting of the Radio Access Network (RAN) and core networks [10]. 5G Infrastructure Public-Private Partnership (5G-PPP) proposed an exhaustive 5-layer NS Framework in addition to the NGMN definition, depending on different use cases [6], [11]. To manage the slice sessions and resource management, ETSI defined the Network Function Virtualization (NFV) Management and Network Orchestration (MANO) architecture [9] to facilitate NF management and orchestration, its virtualization and resource allocation through the three following functional blocks: i) the NFV orchestrator, ii) the VNF manager, and iii) virtualized infrastructure manager [12]. Figure 1 illustrates the various layers that conceptualize the NS technology.

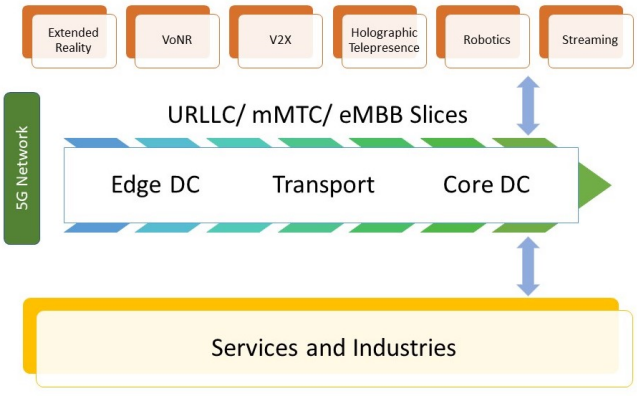

Fig. 1. Layered approach and concept of Network Slicing

A. Resource Block Allocation in Network Slicing

In wireless networks, Dynamic Resource Allocation (DSA) of data packets is critical to support different dynamically active services like real-time (RT), non-real-time (NRT), and control signaling. The gNodeB (gNB) allocates the bandwidth resources to the User Equipment (UE) to facilitate data transmission and reception in both downlink and uplink. The Resource Block (RB) is the smallest resource entity assigned to a single user. The time-domain resource allocation in 5G New Radio (5G NR) defines the allocated symbols (OFDM symbols) from different sub-carriers. In contrast, the frequency domain allocation illustrates the Resource Block (RB) (sub-carriers) allocation to the UE. An RB comprehends 12 sub-carriers in the frequency domain with a flexible RB bandwidth, unlike LTE-A. RB bandwidth depends on sub-carrier spacing. NR provides a higher bandwidth efficiency (up to 99%) than the LTE (90%) [13] and operates at a channel bandwidth of 100 MHz, in the sub-6 GHz bands, and 400 MHz, in the mmWave range, without any reserved Direct Current (DC, the sub-carrier whose frequency is equal to the RF center frequency of the transmitting station) sub-carrier for uplink and downlink. The UEs use a DC subcarrier to identify the OFDM frequency band's center and do not contain any information. The maximum and minimum RBs are defined by means of the 5G New Radio numerology. Hence, the channel bandwidth can be calculated by knowing the given bandwidth of the RB.

Finally, it is worthwhile to mention that the 3GPP specifications define two types of resource allocation in the frequency domain:

- Resource Allocation Type #0 (RAT#0);
- Resource Allocation Type #1 (RAT#1).

Network Slicing scenario deployed with slices created over the same infrastructure demands sharing the same network resources. The Slice Manager (SM) is responsible for allocating resources to individual slices while coordinating with the infrastructure providers. The Virtual Network Operator (VNO) services the slices, commonly known as the slice tenants. SLA is created between SMs and VNOs to regulate the required resources [14]. Authors in [15] have presented an efficient approach for statistical resource distribution among the network slices with strong SLAs. This approach provided a higher trade-off between the resource distribution and system complexity and thus, opened new research questions on the data and cost continuum. In [14], the authors addressed the slicing of RAN resources in multi-tenant scenarios. The resource allocation approach focused on the optimized fairness index, utility gains, and capacity savings. Following this, authors in [16] explored the Deep Reinforcement Learning (DRL) approach to allocate resources in dynamic multi-tenant systems. In [17], authors have proposed an adaptable and flexible 5G network architecture to support cross-domain E2E slicing with well-defined inter-slice control and management functions.

B. Standardization Activities on Network Slicing

Standards administrate the development of products and technologies to ensure requirements, interoperability, and quality [18]. Organizations like Global System for Mobile Communications Association (GSMA) and NGMN have gradually contributed to the high-level system requirements and architecture for Network Slicing. They also regulate the fundamentals for creating slices in an E2E 5G NS framework [19]. GSMA [20] highlighted the need for collaboration in the standardization process from the giants of different verticals, namely academia, industries, CSPs, etc.

3GPP is actively involved in multiple initiatives to support 5G network slicing like SA1 (requirements and use cases), SA2 (NS Architecture) [19], SA3 (Security), SA5 (Slice Management) [21], etc. Similarly, the Internet Engineering Task Force (IETF) contributes to the requirements and applications. The European Telecommunications Standards Institute (ETSI) is working towards NS services, configuration, delivery, assurance of deployment, etc. [9]. The 13th study group (SG13) of International Telecommunication Union - Telecommunication (ITU-T) focuses mainly on the orchestration, network management, and horizontal slicing [22]. Furthermore, the focus group FG-ML 5G defines Machine Learning developments and scopes to the requirements and services [23]. Authors from [6] have mentioned different relevant groups working on NS standardization activities.

C. Requirements for Future Networks

The use cases, service requirements, business models and application areas constantly evolve to meet the diverse demands. This sub-section lists some characteristic use cases and services for 5G and beyond networks [24].

- The underlying requirements are as follows:
  - Holographic Communication - Holographic Telepresence (HT) or communication is the next frontier to provide an immersive experience of distant communication with or without using the Head Mount Devices (HMDs) [25]. It focuses on amalgamating sensory information like touch, smell, and taste into the audio and visual transmission and reception. To facilitate HT, ultra-low latency of 1ms [26] and ultra-high data rate (Tbps) to support 30fps [27] are required, with high computing capabilities.
  - Industrial Automation - The upcoming generation of mobile communication foreseen an industrial revolution and dominance of automated services. The everything-to-everything connection will rule the networking paradigm with an enormous amount of devices. The services demand high QoS and Quality of Experience (QoE). The requirements to support Industry 4.0 and future 5.0 will be Ultra-low latency of 0.1 ms, ultra-high reliability, and ultra-low delay jitter [26], [28].

Figure 2 illustrates the classes of use cases for upcoming communication networks [29].

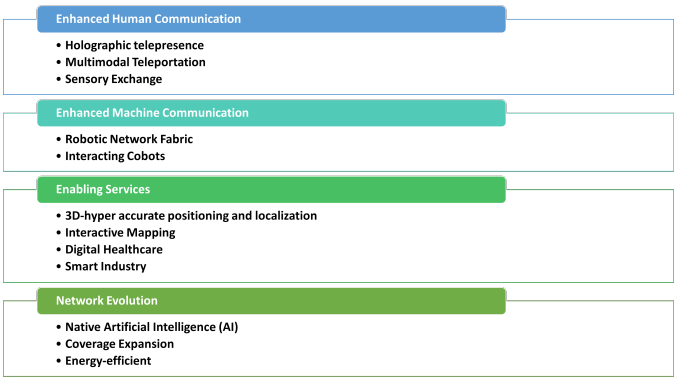

Fig. 2. High-level Use Cases Categorization [29]

III. Methodology and Results

Network slicing enabled the Infrastructure/Slice Providers (SP) to offer resources to the customers as a service for a given cost to maximize the resource usage by accepting slice requests. The customer requests a network slice from SP to get customized services. There is a need for a mechanism/ scheduling scheme in which SPs can entertain the requests, as the SPs are subject to limited resources. Authors from [15] and [30] introduced a two-level scheduler to share the Physical Radio Blocks (pRB) among slices by abstracting pRBs and using two scheduler levels. Two-level schedulers operation is as follows:

- The first level is slice-specific, allowing each slice to use its internal scheduler and schedule each UE with Virtual Resource Blocks (vRB).
- The second level considers the slice-specific (virtual) resource assignment and maps it to actual pRBs. It controls the number of NpRBs (number of pRBs) assigned to each slice and indicates the maximum NpRB to dedicate to each slice after executing an intra-slice physical resource sharing algorithm.

The aim is to compute the radio resources required in each slice. The resources are periodically adjusted based on the current Channel Quality Indicator (CQI) estimates from the users of the different slices. Assumptions are as follows:

- 5G network which including a SO, to initiate and configure slice resources based on the use case types (eMBB, mMTC or URLLC) and a set of eNBs deployed covering an area.
- The SO communicates with the eNBs using a protocol that allows remote interaction and management.
- The eNB management process consists of
  - RAN information (CQI);
  - eNB configuration.
- A set of UEs is served by/associated with a network slice, spanning a set of eNBs (i.e., different physical locations).
- There are three types of Slices: eMBB and URLLC Slices
- The SO receives the request to instantiate a slice. The Slice request includes
  - Slice type;

– Duration;
– Requirements like data rate, application, or latency;
– List of associated UEs.

We simulated on MATLAB the two-level scheduler for eMBB and URLLC slices for a varying number of users in each slice, keeping the other constant to observe CQI variations. The goal is to improve network performance and introduce flexibility and optimization of the network resources by accurately and dynamically provisioning the activated network slices with the appropriate resources to meet their diverse requirements. The aim is to have a flexibility in RAN resource allocation concerning slicing.

A. Slice Definition and Requirements

- eMBB Slice Requirements - High Data Rate

$$N_{pRB_{max}}(i) * d_{pRB} = N_{users}(i) * d_{App/user}$$

- URLLC Slice Requirements: Ultra-Low Latency

$$\mu = \frac{N_{pRB} * d_{pRB}}{\text{Average packet size}}$$

where,
$N_{pRB_{max}}(i)$: Required pRBs for each eNB;
$d_{App/user}$: Required Data rate per slice.;
N_{users} : the number of active users;
d_{pRB} : maximum data rate provided by one pRB;
pRB : Physical Radio Blocks.
Ideal channel conditions correspond to the maximum CQI = 15.

B. Simulation Results and Discussion

The performance has been evaluated in Matlab as an extension to the referenced work in [15]. We modified the SO and considered eMBB and URLLC slice. We defined each slice with the required data rate, number of users and latency in URLLC slice. The simulations were carried out at varying CQI level, i.e. ,medium (7) to high (13). The eMBB slice users were fixed to 5 and varied users (up to 20 for medium CQI and up to 30 for high CQI values) in URLLC slice.

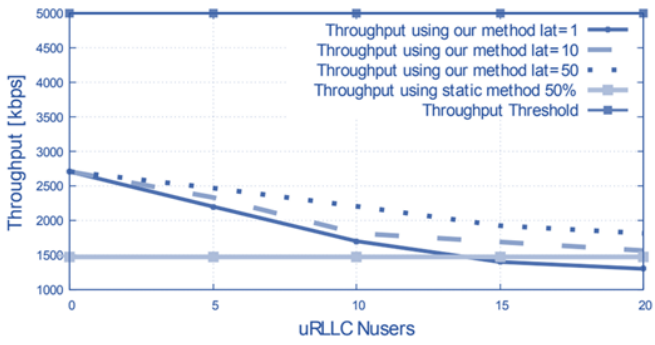

Fig. 3. Throughput variations as a function of the number of users (with Medium CQI value).

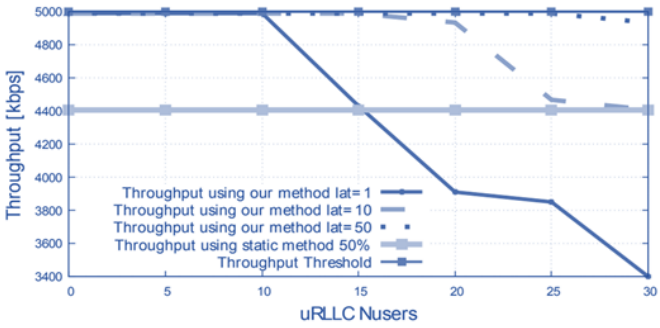

Fig. 4. Throughput variations as a function of the number of users (with High CQI value).

Figures 3 and 4 present the throughput for the URLLC slice at varying CQI values. Beyond the threshold, slice performance degrades (more in case of high CQI) but it guarantees the required bandwidth until 25 users.

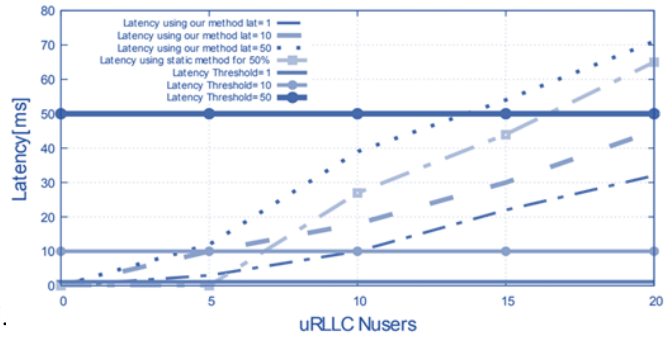

Fig. 5. Latency variations as a function of the number of users (with Medium CQI value).

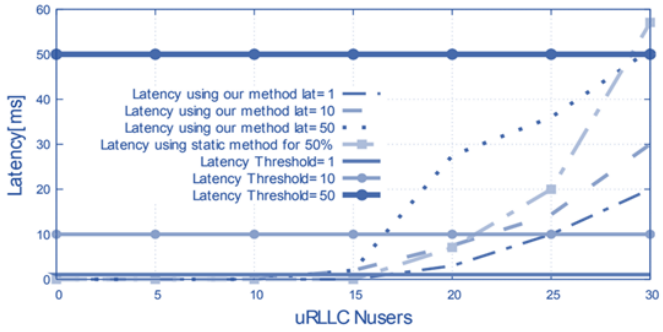

Fig. 6. Latency variations as a function of the number of users (with High CQI value).

Figures 5 and 6 illustrate the experienced latency in case of the uRLLC users for varying CQI values from 7 to 13. We considered different maximum values for latency, i.e., 1 ms, 10 ms and 50 ms. We observed that the max. latency value was near about maintained for both the value of CQI. Good CQI allows higher NpRB compared with the medium CQI by allowing more users. We also observed that fixed number of pRBs cannot guarantee the very low latency requirement.

The results in Figures 7 and 8 show the estimated NpRB and used by the eNBs for the URLLC slices with varied CQI values. In 7 and 8, we observed that the estimated NpRB is similar to the one communicated to the eNB until reaching the identified thresholds as in Figures 4 and 5. The communicated NpRB to eNB is lower than the estimated value on increasing the threshold values.

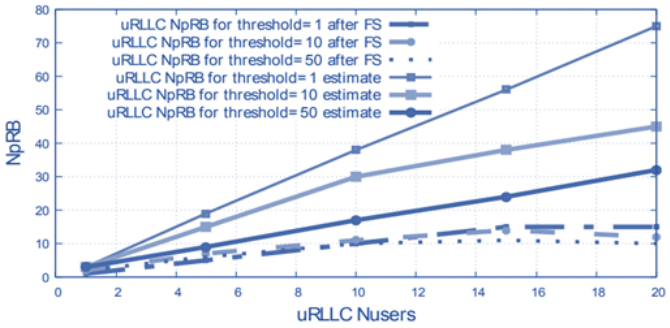

Fig. 7. NpRB of the URLLC slice as a function of the number of users.

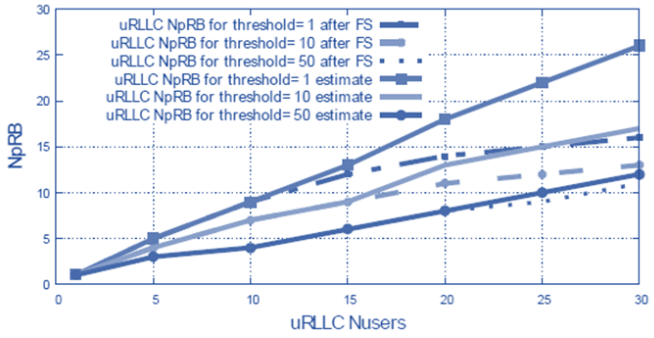

Fig. 8. NpRB of the URLLC slice as a function of the number of users.

The results in Figures 9 and 10 show the estimated NpRB used by the eNBs for eMBB slices with varied CQI values. We observed that the estimated NpRB could not be satisfied in case of medium channel quality and required NpRB is higher. Lower dpRB is expected at higher CQI values.

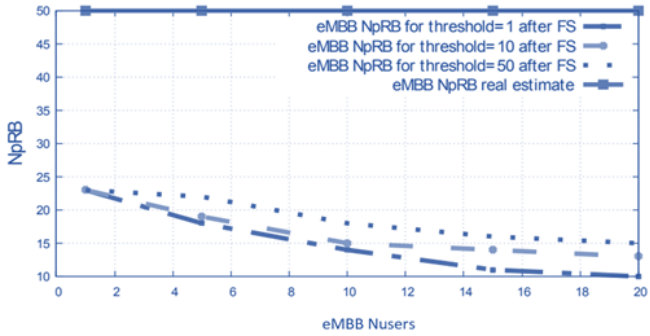

Fig. 9. NpRB of the eMBB slice as a function of the number of users.

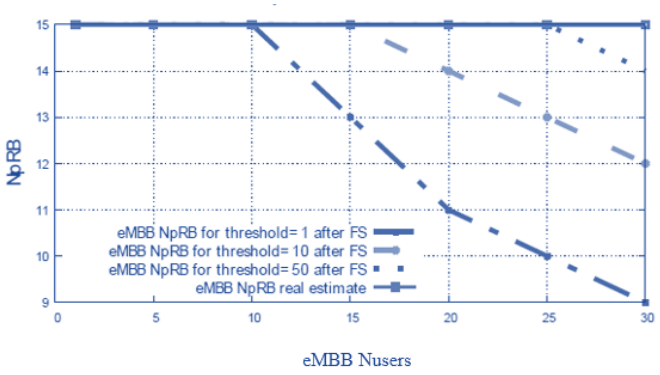

Fig. 10. NpRB of the eMBB slice as a function of the number of users.

The results show that our proposed algorithm to estimate the required NpRB for eMBB and URLLC slices is accurate and permits sharing of the RAN resources among slices. Hence, the practical feasibility of our proposed solution is verified.

IV. Conclusions and Future Work

This paper proposes slice creation and allocation of resource blocks while isolating the slices for eMBB and URLLC by using the two-level scheduling introduced in the referenced work. We have introduced algorithms to estimate the required RAN resources for the eMBB and URLLC slices while evaluating the performance under varying CQI values at the SO level. Heterogeneous Networks (HetNets) optimization is an open research area concerning Network Slicing. Also, 3GPP's functional splits [20] have huge potentials to be implemented with slicing to manage the network function virtualization and softwarization of RAN resources. Besides, there is a need to develop novel meta-learning models for ML-enabled network slicing, an open research area.

The main foreseen challenge in 5G New Radio dynamic resource allocation is the associated overhead when we extract the information from the base station (UE provides CQI to the base stations) to the SO. Thus, to eliminate/ minimize the communication overhead, we will simultaneously propose the following steps:

- A machine learning approach to infer the stability of UE channel conditions;
- Propose a predictive scheme to efficiently reduce the dependency on the network's configuration to address the various service and demands;
- Admission Control Policy/ Decision based on Q-Learning and Regret Matching for the SP to manage the slice requests (we will then validate the mechanism concerning the SP serving the network requests).

References

[1] N. Alliance, "5G White Paper (Final Deliverable)," 2015.
[2] H. Zhang, N. Liu, X. Chu, K. Long, A.-H. Aghvami, and V. C. Leung, "Network slicing based 5G and future mobile networks: mobility, resource management, and challenges," *IEEE communications magazine*, vol. 55, no. 8, pp. 138–145, 2017.

[3] "Network slicing explained," Nov 2020. [Online]. Available: https://www.nokia.com/about-us/newsroom/articles/network-slicing-explained/

[4] K. Flynn. (2019) A global partnership. [Online]. Available: https://www.3gpp.org/release-15

[5] A. Nakao, P. Du, Y. Kiriha, F. Granelli, A. A. Gebremariam, T. Taleb, and M. Bagaa, "End-to-end network slicing for 5g mobile networks," *Journal of Information Processing*, vol. 25, pp. 153–163, 2017.

[6] B. Khan, Nidhi, A. Mihovska, R. Prasad, and F. J. Velez, "Overview of network slicing: Business and standards perspective for beyond 5g networks," in *2021 IEEE Conference on Standards for Communications and Networking (CSCN)*, 2021, pp. 142–147.

[7] Samsung, "Samsung Technical White Paper: Network Slicing," 2020.

[8] N. Alliance, "Description of network slicing concept," *NGMN 5G P*, vol. 1, no. 1, 2016.

[9] N. ETSI, "Network functions virtualisation (NFV); terminology for main concepts in NFV," *Group Specification, Dec*, 2014.

[10] X. Foukas, G. Patounas, A. Elmokashfi, and M. K. Marina, "Network Slicing in 5G: Survey and Challenges," *IEEE Communications Magazine*, vol. 55, no. 5, pp. 94–100, 2017.

[11] S. Redana, Ö. Bulakci, A. Zafeiropoulos, A. Gavras, A. Tzanakaki, A. Albanese, A. Kousaridas, A. Weit, B. Sayadi, B. T. Jou *et al.*, "5G PPP architecture working group: View on 5G architecture," 2019.

[12] A. Devlic, A. Hamidian, D. Liang, M. Eriksson, A. Consoli, and J. Lundstedt, "NESMO: Network slicing management and orchestration framework," in *2017 IEEE International Conference on Communications Workshops (ICC Workshops)*. IEEE, 2017, pp. 1202–1208.

[13] X. You, C. Zhang, X. Tan, S. Jin, and H. Wu, "Ai for 5g: research directions and paradigms," *Science China Information Sciences*, vol. 62, no. 2, pp. 1–13, 2019.

[14] P. Caballero, A. Banchs, G. de Veciana, and X. Costa-Pérez, "Multi-tenant radio access network slicing: Statistical multiplexing of spatial loads," *IEEE/ACM Transactions on Networking*, vol. 25, no. 5, pp. 3044–3058, 2017.

[15] A. Ksentini, P. A. Frangoudis, P. Amogh, and N. Nikaein, "Providing low latency guarantees for slicing-ready 5g systems via two-level mac scheduling," *IEEE Network*, vol. 32, no. 6, pp. 116–123, 2018.

[16] F. Mason, G. Nencioni, and A. Zanella, "A multi-agent reinforcement learning architecture for network slicing orchestration," in *2021 19th Mediterranean Communication and Computer Networking Conference (MedComNet)*. IEEE, 2021, pp. 1–8.

[17] M. Shariat, Ö. Bulakci, A. De Domenico, C. Mannweiler, M. Gramaglia, Q. Wei, A. Gopalasingham, E. Pateromichelakis, F. Moggio, D. Tsolkas *et al.*, "A flexible network architecture for 5g systems," *Wireless Communications and Mobile Computing*, vol. 2019, 2019.

[18] N. Abdelkafi, R. Bolla, C. J. Lanting, A. Rodriguez-Ascaso, M. Thuns, and M. Wetterwald, "Understanding ICT standardization: Principles and practice," 2019.

[19] P. Rost, C. Mannweiler, D. S. Michalopoulos, C. Sartori, V. Sciancalepore, N. Sastry, O. Holland, S. Tayade, B. Han, D. Bega *et al.*, "Network slicing to enable scalability and flexibility in 5G mobile networks," *IEEE Communications Magazine*, vol. 55, no. 5, pp. 72–79, 2017.

[20] GSMA. (2021) E2E Network Slicing Architecture Version 1.0. [Online]. Available: https://www.gsma.com/newsroom/wp-content/uploads//NG.127-v1.0-2.pdf

[21] X. De Foy and A. Rahman, "Network slicing-3GPP use case," *Working Draft, IETF Secretariat, Internet-Draft draft-defoy-netslices-3gpp-network-slicing-02*, 2017.

[22] ITU-T. (2019) Progress of 5G studies in ITU-T: overview of SG13 standardization activities . [Online]. Available: https://www.itu.int/en/ITU-T/Workshops-and-Seminars/20180604/ Documents/Session1.pdf

[23] "Focus Group on Machine Learning for Future Networks including 5G." [Online]. Available: https://www.itu.int/en/ITU-T/focusgroups/ml5g/Pages/default.aspx

[24] Y. Zhou, L. Liu, L. Wang, N. Hui, X. Cui, J. Wu, Y. Peng, Y. Qi, and C. Xing, "Service-aware 6g: An intelligent and open network based on the convergence of communication, computing and caching," *Digital Communications and Networks*, vol. 6, no. 3, pp. 253–260, 2020.

[25] A. Vlahov, V. Poulkov, and A. Mihovska, "Analysis of open ran performance indicators related to holographic telepresence communications," in *2021 24th International Symposium on Wireless Personal Multimedia Communications (WPMC)*. IEEE, 2021, pp. 1–5.

[26] C. Han, Y. Wu, Z. Chen *et al.*, "Network 2030 a blueprint of technology applications and market drivers towards the year 2030 and beyond," 2018.

[27] R. Li *et al.*, "Towards a new internet for the year 2030 and beyond," in *Proc. 3rd Annu. ITU IMT-2020/5G Workshop Demo Day*, 2018, pp. 1–21.

[28] G. Berardinelli, N. H. Mahmood, I. Rodriguez, and P. Mogensen, "Beyond 5g wireless irt for industry 4.0: Design principles and spectrum aspects," in *2018 IEEE Globecom Workshops (GC Wkshps)*. IEEE, 2018, pp. 1–6.

[29] N. Alliance, "6G Use Cases and Analysis," 2022.

[30] A. Ksentini and N. Nikaein, "Toward enforcing network slicing on ran: Flexibility and resources abstraction," *IEEE Communications Magazine*, vol. 55, no. 6, pp. 102–108, 2017.

Stateless Paradigm for Resiliency in Beyond 5G Networks

Savita Sthawarmath*‡, Eric Renault†, Thierry Lejkin‡
*Telecom SudParis, Evry, France
†LIGM, Univ. Gustave Eiffel, CNRS, ESIEE Paris, Noisy-le-Grand, France
‡Orange Innovation Networks, Chatillon, France

***Abstract*—An unprecedented surge in communication capabilities to things, in general, is challenging the traditional internet service providers. Telecommunication operators played a major role in connecting people to the internet and are now compelled to accommodate communicating things with traffic demands that are diverse and unpredictable in nature. To that end, sofwarization and virtualization of network entities have extensively helped to achieve a high degree of flexibility and scalability. Complementing this, separating the computing from the storage as a second degree of decoupling is required to make network functions highly resilient. Our work introduces the stateless network function paradigm by proposing a *Quasi-Local model* which is a fetch and cache model in order to achieve resiliency. We justify the proposed model with the state analysis, design, and derivation of state metrics. Furthermore, we assess various network architectures suitable for future stateless network functions to maintain the End-to-End delay budget of diverse telecom use cases.**

***Index Terms*—Stateless Network Functions, Network Function Virtualization, In-memory data-stores, Resilience, Future networks, 5G.**

I. Introduction

The promising objectives of next-generation networks as defined by the global telecom standardization body have exposed endless potential use-cases by embedding communicating capabilities in things. Internet of Things (IoT), Autonomous vehicles (V2X), Industry 4.0, and enhanced mobile broadband (eMBB) are some of the popularly heard buzzwords in today's communication society. A plethora of use-cases envisaged is in function of latency, bandwidth, and coverage requirements, in line with the promises of the future 5G network. Industry 4.0 may require continuous monitoring of robots and their critical parts, though the requirement of coverage is not significant for these sensors, any compromise in latency would affect revenue. So, is the case in telesurgery, where latency could equate to potential fatality. Some applications like autonomous vehicles have strict requirements of latency, coverage, and bandwidth to be able to sense its environment and operate without human involvement. These diverse applications of communicating things along with existing human adoption of mobile devices will likely change the service demand distribution from previously established Poisson behaviour. The fusion of traffic consumption distribution by various applications is going to define and test the robustness factor of the core network.

Fig. 1: Network entity evolution.

It is time to accept the fact that the traditional telecom core network was never designed for foreseen use-cases of 5G and thus incorporating the new technological advancement is the new mandate. To meet the requirements of 5G, telecom operators are adopting an openness attitude with the content producers (CPs) as well as equipment vendors. By facilitating Mobile Edge Computing (MEC) platforms as an Infrastructure as a Service (IaaS) at the edge of the core network, CPs are allowed to operate close to content consumers (CCs) thereby meeting the latency demands. Encouraging equipment vendors to softwarize the network and further virtualize the core network entities meets the scalability and resiliency demands. These changes make the current core network simpler and in line with the Internet architecture with Service Based Architecture (SBA) over HTTP for communication between network entities. Virtualization has successfully demonstrated the ways of exploitation of the underlying hardware for various applications at a given time, virtualizing network functions breaks this tight dependence of network entities with the hardware by being able to deploy on commodity hardware. We define these new generation of network functions as Virtual Network Functions (VNFs).

Though virtualization best addresses the scalability of future networks, network resilience can be further improved, for example by breaking the tight coupling between the computation and the data in a VNF. Introducing a novel data-plane by limiting VNFs to computation-only aims to address the network resilience effectively. This adds one more step in the network entity evolution, as shown in Fig. 1. Designing the data plane needs a) very good knowledge about control traffic volume between network functions for service provisioning and also the data traffic, b) defining the various data models coherent with the functioning of network functions, c) careful selection of data store providers in function to rate of change

of control data.

In this paper, we first highlight some interesting efforts by various research teams with similar objectives, as discussed in section II. We try to answer the basic questions required for the design of stateless network functions in section III. Later in section III-B, we do traffic analysis and estimation between various network entities considering 4G specifications. In section IV, we discuss our experimental scenario, highlighting a few critical parameters and estimating the latency due to network entity failure considering the best possible values. We conclude our discussion in section V

II. Related Work

The traffic speed promised by 5G demands a highly robust core and access network. To that end, the ability of the solutions and architectures to ensure traffic continuity at the lowest possible end-to-end latency defined as *Resilience* is of paramount importance for the network operators.

A. Resilience

Conventional methods used in mobile core networks generally include Active/Standby and Active/Active redundant pair systems. In both cases, an active node continuously synchronizes the memory to a standby node or dedicated partner active node. In the event of a failure of an active node, the standby node or partner active node takes over the traffic to ensure high availability of service. Both these solutions prove to be expensive as every active network entity needs a backup and the active node always need to be engaged in the synchronization process with its standby node consuming significant amount of computational resources [1].

In addition, auto-healing or restoration is considered in virtualized environments, in which redundant systems are rebuilt by removing failed elements and adding new Virtual Machines (VMs) as standby nodes [2]. However, restoration of Network Function (NF) failure impacts a potential number of users, leading to signalling overhead.

In a stateless environment, the resilience of network functions is achieved by decoupling the computational part and data part, as discussed in [3]. In case of network function failure, externalized state is pulled and used, thereby reducing the service disruption time notably.

B. Architecture for stateless Virtual Network Functions

Several architectural choices have been discussed while addressing the operation resilience aspects for VNF, for example, authors in [4] presents the ratio of virtual function versus compute instances as, *1:1*, *1:N*, *N:1*, *N:2* mapping with different characteristics, advantages, and disadvantages.

1:1 mapping, signifies one functional entity of 4G Evolved Packet Core (EPC) network over one VM. For example, one Mobility Management Entity (MME) over one running VM, and one Packet Gateway Entity (P-GW) on another running VM. Though the design is simple, it has some limitations in terms of scalability i.e, scaling up is easy but scaling down is a complex operation as the virtual EPC components are stateful,

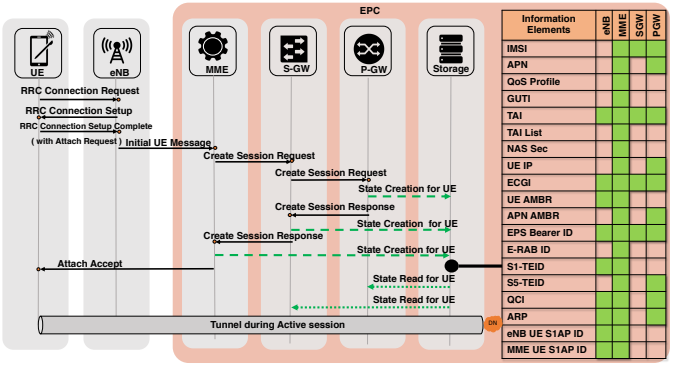

Fig. 2: Initial Attach with transaction level stateless model

and they cannot be simply shut down without disrupting the active user sessions and if a VM fails, all the sessions need to be re-established.

1:N mapping, several replicas of one EPC component are deployed on VMs, but may appear as a single logical entity to other peer components. Stateless EPC components in this implementation ensure the high availability of nodes, but are prone to synchronization issues and latency due to passing through multiple nodes.

N:1 mapping, all the EPC components are merged and deployed over one VM and N:2 is the extension of the N:1 model where control and data plane components are split and with stateless design introducing short delay processing.

1:N architectural choice is discussed in most of the related works as it enables high scalability requirements, availability of the nodes, and the resiliency to failure of nodes. However, the synchronization issues that possibly exists between different instances of VM is addressed in [5] with various state synchronization design choices being *always sync*, *session sync* and *no sync* designed for both control and data plane operations.

We plan to consider 1:1 and 1:N mapping architecture in our discussion and experimentation.

III. Prerequisites

The complexity of telecom networks is such that any upgrade or changes to existing architecture needs several rounds and types of validation. To initiate the *Stateless* concept in telecom network functions, we try to clarify the *3Ws*, i.e, *What*, *When* and *Where* to store?. It is also important to discuss *How* to store?. Answers to these questions are the foundation of the stateless concept.

A. Stateless Model

What to store Decoupling the data from computation at network functions appears to be feasible, but choosing an optimal scheme from various possible configurations is a real challenge. When it comes to data, the first question to be answered is; *What needs to be decoupled and stored?* or *How do we define data or state in a network function?*. Let us consider the Initial Attach Procedure in LTE shown in Fig. 2, the table on the right summarises the information pertaining to a user and bearer associated with the user session as generated

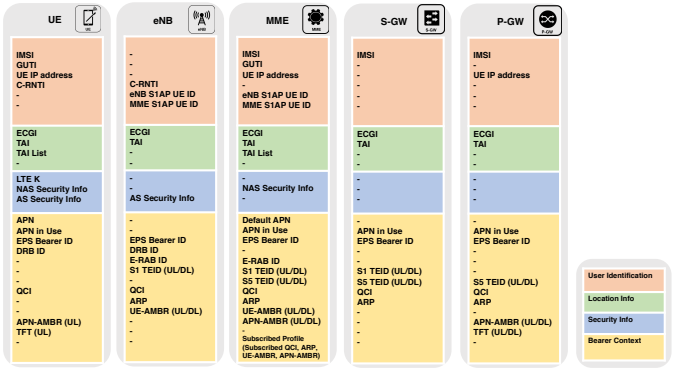

Fig. 3: Context at each network function after Initial Attach Procedure in LTE.

at the end of the attach procedure in 4G LTE network. These user contexts define the state or states being stored locally at each network function needs a state template for pushing the state to a datastore. These states either can be configured as a one big state or grouped as smaller substates as user identity, security, location and bearer context as shown in the Fig. 3. We consider LTE network procedures over 5G for two main reasons, First, to take advantage of availability of real-world network data that helps us to estimate the user-context metrics discussed in Sec. III-B. Secondly, the traffic we considered are mostly human-type communication, which remains as one of the future 5G diverse traffic types.

When to store The stateless concept can be introduced at different instants during the course of a signalling procedure, hence the challenge is identifying the optimal level to introduce statelessness. Possible options that we can think of are at,

- Message level.
- Transaction level (with state update).
- Procedure level.

Each level has its own pros and cons, like persisting the data after every message at a network function is considerable but introduces a lot of update traffic to the data store. Transaction and Procedural level look meaningful, as any failure of network function during a procedure setup does not mandate re-initialization of the whole process.

Where to store 3GPP has standardized the concept of control and user plane separation (CUPS) [9] because of various scalability and flexibility advantages. The core objective is to reduce latency of an application service, hence the network entity that handles user application traffic is made of two functional and independent parts i.e, the control-plane part and the data-plane part. The control part creates and updates the user context, which can later be used for packet processing in the data-plane. A network entity that does not handle user application traffic has their own copy of user context that will be useful in case of session creation error or other failures.

In order to make 5G architecture flexible, 3GPP Technical Specification [10] defines Unstructured Data Storage Function (UDSF) that allows any network entity to store and retrieve unstructured data. Standardization outlines certain core

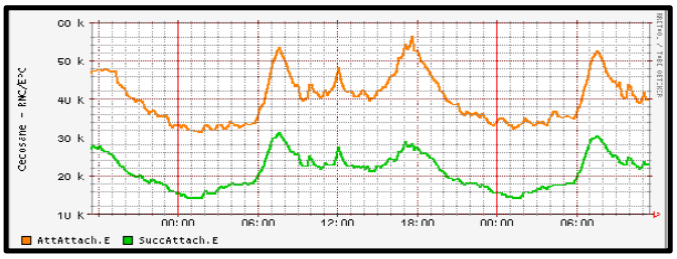

Fig. 4: Volume of Attach Request to a MME on a weekday in some site.

requirements which equipment vendors must adhere to like data concurrency and atomic consistency, subscribable service APIs, ensuring very low latency, multiple logical spaces, guidelines on UDSF sharing by multiple network entities, etc.

Fig. 2 illustrates the potential call flow of the Initial Attach procedure in stateless mode. A state is created by each network function after a transaction, i.e, after every request-response pair, and the final state is written to the data store at the end of the procedure. Once the initial attach is completed and state is pushed to the externalised datastore, the serving data-plane network function processes user packets by reading the user state from the datastore. This process of fetching the state to process each packet can overwhelm the data-plane thereby questioning the network latency and high bandwidth.

Given all the discussion above, we propose our stateless model to have,

- 1:1 or 1:N functional architecture.
- 1:1 user context storage template model.
- Procedure level of context persistence.

Let us call this stateless model as *Quasi-Local* since user context is made available locally (cached) only during the user session. In such a setup, when a network function fails, a new instance can be spinned up to process the redirected packet flow by fetching the user state from the datastore thereby meeting the resilience objective.

B. Traffic Analysis

To validate an optimal stateless scheme for virtual network functions, we need to have a very good understanding of the magnitude of traffic managed by the current core network. For the sake of discussion, we consider the Attach Request procedure in the 4G LTE network, which is the first communication of the User Equipment (UE) with the 4G LTE Evolved Packet System (EPS) to request any service. We try to evaluate the traffic per network entity w.r.t *state metrics* like *Volume*, *Size* and *Frequency* of requests.

Volume of requests can represent 1) the number of data session requests made by the UE to EPS 2). In a stateless network function context, it could mean - the number of datastore operations.

We assume that a UE is attaching itself to the telecom network to request a data session. Let N be the total number of attach requests, n be the number of successful attach attempts in a unit time, and n_w be the number of writes to the datastore. Fig. 4 shows the pattern of attach requests attempted at the

MME of EPS in one location for a weekday. This data is received from a telecom provider just to have an idea about the magnitude of requests. As we see, there are two to three distinguishable peak time of the day where the request is around $50K$ (with a 5K spread) with an average of 40.236 K requests. It is also evident that around 39% of requests are rejected for various reasons, hence average successful attach requests $n = 21.244K$. Considering Procedure wise stateless concept, a success rate of 61% means, on an average $n_w = n$ writes are performed from MME to datastore per second.

Size of Information represents 1) the size in bytes of signalling information per entity when requesting for a procedure 2) In stateless network function context, the size in bytes of the state written to or read from the datastore.
Traffic at MME following Attach Requests can be formulated as,

$$T_{MME} = S_{MME} \times n \times 60$$

where, T_{MME} represents the traffic at MME, S_{MME} represents the Information Elements (IE) size in the attach request. S_{MME} received by MME range around 239 bytes at the lower bound, the actual/exact number might vary depending on the length of the Access Point Name (APN), number of IP addresses used to construct the Traffic Flow Template (TFT), size of the security key, etc. Hence, plugging in the values gives $T_{MME} = 304.6MB/min$ or $18.27GB/hour$.
Similarly, Traffic at S-GW following attach requests can be formulated as,

$$T_{S-GW} = S_{S-GW} \times n \times 60$$

where, T_{S-GW} represents the traffic at S-GW, S_{S-GW} represents the IE size in the Attach Request. To calculate traffic T_{S-GW} at S-GW and T_{S-GW} at P-GW, it is safe to consider the Average Attach Success n. S_{S-GW} received by S-GW is 107 bytes at lower bound. Hence, we estimate traffic T_{S-GW} to be roughly $136MB/min$ or $8.18GB/hour$.

Likewise, Traffic at P-GW following Attach Requests can be formulated as,

$$T_{P-GW} = S_{P-GW} \times n \times 60$$

where, T_{P-GW} represents the traffic at P-GW, S_{P-GW} represents the IE size in the Attach Request. S_{P-GW} received by P-GW is 150 bytes during at lower bound, giving us T_{P-GW} estimate of $191.19MB/min$ or $11.47GB/hour$.

Frequency of information is influenced by both Volume of requests with time and size of information between entities. During the Initial Attach Request for bearer setup and considering procedure wise stateless mode, the number of state equals the number of Attach success i.e. n. Now for three EPS entities i.e, MME, S-GW and P-GW, assuming that they maintain their own copy of user context,

$$n_{w,Total} = \sum(n_{(w,MME)}, n_{(w,S-GW)}, n_{(w,P-GW)}) \times 60$$

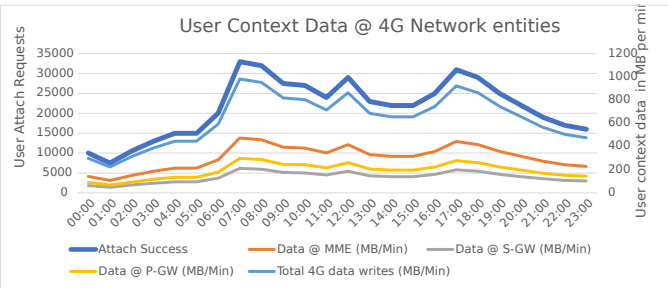

Fig. 5: Volume of information at network entities over 24hours following Initial Attach request.

where, $n_{(w,MME)}, n_{(w,S-GW)}, n_{(w,P-GW)}$ represents the state writes triggered by MME, S-GW and P-GW respectively. This estimates a total writes $n_{w,Total} = 3.823Mwrites/min$.

Now, the traffic to the data store T_{Total} during Attach procedure can be formulated as,

$$T_{Total} = \sum(T_{MME}, T_{S-GW}, T_{P-GW})$$

which gives us an estimate of $631.79MB/min$ or $37.92GB/hour$ at the lower bound considering the values calculated earlier. Although these analyses is limited to a geographic area, it is sufficient for a data store qualification study.

Forecasting the 5G traffic behaviour helps us to adapt to hugely varying patterns of 5G traffic which not only constitutes cellular traffic but also from varied 5G scenarios like IoT, V2X, Industry Automation. Considering these varying sources, the traffic pattern could possibly follow the poisson process of random arrivals as it is composed of some constant behaviour coming out of IoT devices along with the normal periodic/cyclic behaviour of cellular traffic.

Ericsson mobility report 2019 [11] estimates that by 2024, 5G networks will carry 25% of the world's mobile data traffic i.e., mobile data traffic is expected to increase by five folds (x5). Applying this estimation to our 4G traffic analysis in Fig. 4, we can roughly assume that the volume of the 4G traffic will be multiplied by 5 times, which drastically increments the number of bytes to be fetched/written to the data store, i.e,

$$T_{AMF} = T_{MME} \times 5$$

where T_{AMF} is the traffic at 5G Core Access and Mobility Management Function (AMF). Using the earlier numbers gives us T_{AMF} could swell to 1.523 GB/Min or 91.3 GB/hour. In Fig. 5, we present the detailed traffic pattern at network entities versus the number of successful attach requests as presented in Fig. 4.

This could mean that in addition to data store qualification, we may also need to look at data store hierarchical designs to meet future demands.

IV. Results and Discussion

In this section, we highlight the significance of our proposed model with real network data collected from an operator core network around a certain geographic area. Fig. 6 shows the

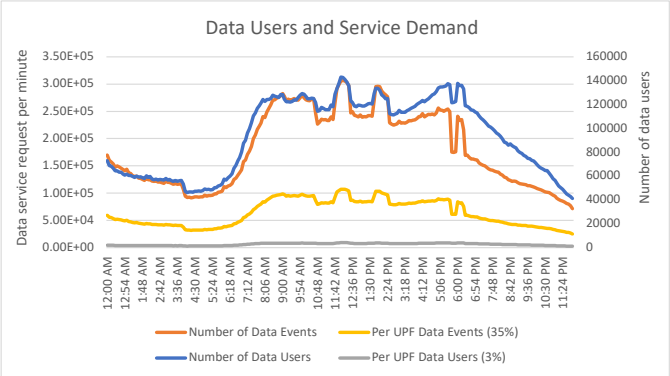

Fig. 6: Data Users and Service Demand

number of data users versus number of data requests made by those users over a period of $24h$. Due to confidentiality reasons, we are unable to publish the exact number of core network entities handling these requests. Due to this reason we assume some values from an interesting study by SK Telecom and Intel Corporation on designing next generation data-plane functions for 5G [12]. In this study, authors prove that a 5G UPF implementation with FD.io Vector Packet Processor (VPP) framework [13] with Data Plane Development Kit (DPDK) [14] plugin shows improved performance in latency and jitter for high priority traffic while still running best effort for lower priority traffic at high throughput rates and high infrastructure utilization. In this experiment, data packets from 50000 users were processed with various combination of packets belonging to high priority and normal traffic category. We consider the best possible values from a profile - where 50% traffic is from high priority group and the rest belonging to normal group. They state that per packet processing time when UPF CPU load is at 50% with average downlink packets (DL) per second per user of 295 packets is 40μs. Assuming that we employ such UPFs in our network, we uniformly distribute the number of data users and data events. In such scenario, each UPF handles around 3% of data users and handles 35% of data requests as shown in the Fig. 6.

Considering the above values, in Fig. 7, we show the number of DL packets at a given time versus the amount of time in seconds required to process those packets with various packet processing schemes. An important assumption here is that buffer-length in a given time does not affect the packet processing time in the next time step, in reality, this will greatly have an impact on the throughput. This assumption is made because of the values considered from [12], in real world telecom network, high performance UPF servers handles data requests and traffic from more than 50000 users. In addition to the values of packet processing, we experimented with various in-memory databases like Redis [15], VoltDB [16] and found that the data fetching times range between 20μs to 200μs. For this comparative study, we consider 20μs as access times by UPF.

Our objective in this study is to compare the packet processing time with three packet processing schemes,

- *True Stateless* - where user context is fetched to process each packet.
- *Quasi-Local Stateless* - where user context is fetched when UPF encounters the user packet for the very first time.
- *Stateful* - where user context is pushed from SMF to UPF as a part of PDU session establishment procedure.

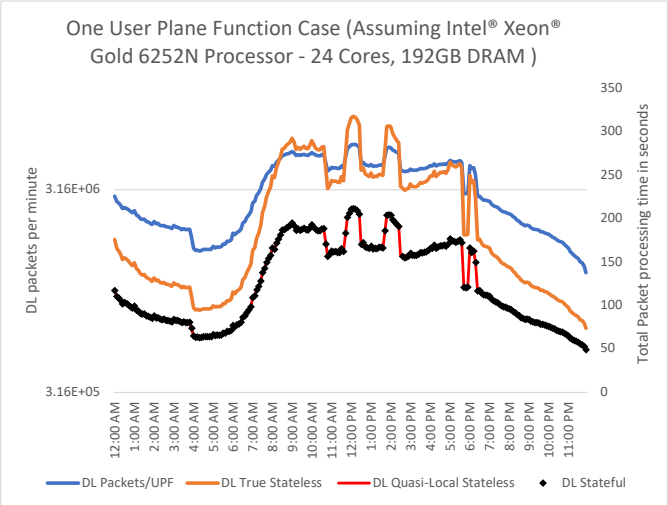

Fig. 7: VPP based User Plane Function case

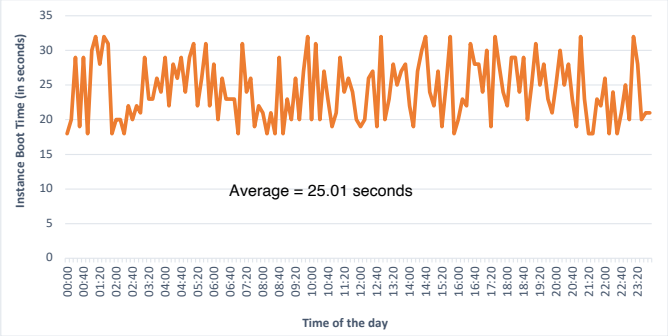

Fig. 8: Instance boot time benchmarking

From the Fig.7, it is clear that *True Stateless* scheme is the most expensive model towards stateless network functions and hence is not recommended for use-cases with critically low delay budget despite offering high degree of service continuity. *Stateful* scheme on the other hand provides the best latency but are not immune to system failures. The best compromise between these two schemes is presented by our *Quasi-Local Stateless* scheme, where UPF fetches the user context only when there is a user packet to process and a cache miss is encountered. Once fetched, user context is cached up to a certain time threshold. Upon failure of a Stateless UPF, a new instance can be booted to resume the operation, hence equating the service restoration time to boot time of a system. To have a realistic idea about the instance boot time, we experimented with Google Cloud Platform [17] considering Google MemoryStore as in-memory database. We achieved the average instance boot time to be around $25s$ as shown in Fig. 8. These values were derived when we instantiated an

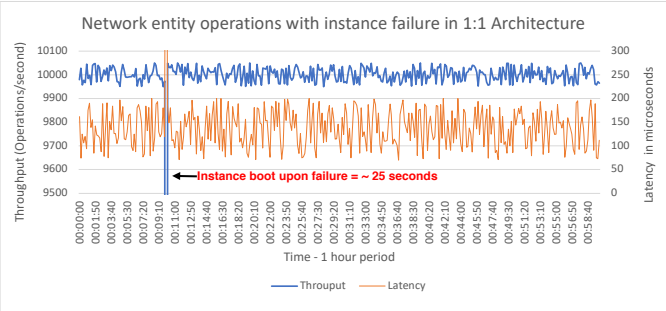

Fig. 9: Failure Scenario with Stateless UPF with 1:1 Architecture

instance at different times of the day with $10min$ frequency over a period of $24h$.

Furthermore, we constructed a functional stateless system to work with Quasi-Local Stateless scheme with 1:1 architecture. The objective of this study is to see the impact of instance downtime on service delivery, so we considered launching a basic non-telecom service that fetches the required data from an in-memory database to process each requests. This triggered around $9K$ database operations for an identical number of service requests. Over the period of $1h$, we simulated a failure event and, we confirmed that service downtime equates to system boot time with infinitesimal small delta fetch time of $20\mu s$ per user as discussed above and shown in Fig. 9.

V. Conclusion and Future Works

In this work, we discussed the significance of stateless network functions to address the resilience aspects in telecom networks. Our proposed *Quasi-Local Stateless Model* can easily be scaled and provides faster failure recovery compared to currently existing expensive solutions like Active-Standby and Active-Active which measures in several seconds. Our experimentation with Google Cloud has presented some promising results that motivate us to port the functional stateless network implementation to telecom network functions.

References

[1] Visibility Architectures: The ABCs of Network Visibility. 2020.

[2] Cisco S-GW Restoration, Ultra Services Platform Release N5.5.

[3] Murad Kablan and Azzam Alsudais and Eric Keller and Franck Le, "Stateless Network Functions: Breaking the Tight Coupling of State and Processing," 14th USENIX Symposium on Networked Systems Design and Implementation (NSDI 2017).

[4] T. Taleb et al., "EASE: EPC as a service to ease mobile core network deployment over cloud," in IEEE Network, vol. 29, no. 2, pp. 78-88, March-April 2015, doi: 10.1109/MNET.2015.7064907.

[5] P. Satapathy, J. Dave, P. Naik and M. Vutukuru, "Performance comparison of state synchronization techniques in a distributed LTE EPC," 2017 IEEE Conference on Network Function Virtualization and Software Defined Networks (NFV-SDN), Berlin, Germany, 2017, pp. 1-7, doi: 10.1109/NFV-SDN.2017.8169832.

[6] Tamura, M., Tetsuya Nakamura, T. Yamazaki and Y. Moritani. "A Study to Achieve High Reliability and Availability on Core Networks with Network Virtualization." (2013).

[7] F. Ojala, A. Rao, H. Flinck and S. Tarkoma, "NoSQL stores for coreless mobile networks," 2017 IEEE Conference on Standards for Communications and Networking (CSCN), Helsinki, Finland, 2017, pp. 200-206, doi: 10.1109/CSCN.2017.8088622.

[8] L. Abdollahi Vayghan, M. A. Saied, M. Toeroe and F. Khendek, "Deploying Microservice Based Applications with Kubernetes: Experiments and Lessons Learned," 2018 IEEE 11th International Conference on Cloud Computing (CLOUD), San Francisco, CA, USA, 2018, pp. 970-973, doi: 10.1109/CLOUD.2018.00148.

[9] 3GPP TS 23.214 Architecture enhancements for control and user plane separation of EPC nodes.

[10] 3GPP Technical Report 29.598 V16.0.0 Unstructured data storage services.

[11] Ericsson, "Ericsson Mobility Report", 2019.

[12] SK Telecom and Intel Corporation; White Paper "Low Latency 5G UPF Using Priority Based Packet Classification" 2020.

[13] FD.io. 2016. Fd.io /dev/boot. 2016.

[14] Intel Corporation. Intel DPDK vSwitch: Performance Report, 2014.

[15] Redis, "Redis benchmark", 2021.

[16] VoltDB, "VoltDB Benchmarks Report", 2018.

[17] Google Cloud Platform, https://cloud.google.com

How Tourists Move in a City

Catarina Castanheira
Bachelor in Data Science
Iscte University Institute of Lisbon
Lisboa, Portugal
catarina_cordeiro@iscte-iul.pt

Rita Almeida
Bachelor in Data Science
Iscte University Institute of Lisbon
Lisboa, Portugal
rita_alexandra_almeida@iscte-iul.pt

Duarte Marques
Bachelor in Data Science
Iscte University Institute of Lisbon
Lisboa, Portugal
duarte_marques@iscte-iul.pt

Guilherme Firmino
Bachelor in Data Science
Iscte University Institute of Lisbon
Lisboa, Portugal
guilherme_firmino@iscte-iul.pt

Luís B. Elvas
Instituto Universitário de Lisboa
(ISCTE-IUL), ISTAR-IUL, 1649-026
Lisboa, Portugal
0000-0002-7489-4380

Joao C Ferreira
Instituto Universitário de Lisboa
(ISCTE-IUL), ISTAR-IUL, 1649-026
Lisboa, Portugal
0000-0002-6662-0806

***Abstract*— Little is known about the spatial behaviour of urban visitors, even though travellers create a massive amount of data (Big Data) when they visit cities. Using their behaviours, these data sources may be utilised to monitor their existence. Using Big Data, this article aims to analyse the digital footprint of urban visitors. Unlike others that rely on mobile device operators in Lisbon, this article establishes a partnership with Lisbon Municipality. We developed a Python approach to clean and prepare visualisation dashboards to understand tourists' movement in a city. The analysed case study (Lisbon) demonstrates how tourists tend to gather around a set of parishes during a specific time of the day during the months under study as well as how unusual circumstances, namely international events, impact their overall spatial behaviour.**

The aim of this paper is to identify these patterns so that local entities can better manage the allocation of resources in Lisbon. Keywords—Roaming, tourists, Data Analytics, Cellular networks

I. INTRODUCTION

After a year marked by a severe pandemic scenario (2020) in which Portugal registered a sharp drop in international tourism, we witnessed a recovery in international tourism starting in the second half of 2021. [1] This trend continued in the first two months of 2022 (January and February) with a 769.2% increase in guests from abroad in February 2022 compared to February 2021 [1].

To get a better understanding of how tourists move in a city, we collaborated with the Lisbon City Council who provided us with data from a mobile carrier company – Vodafone, on the mobility of people (roaming and non-roaming) in the city of Lisbon based on cell phone data over September to December 2021 and January 2022. Later, we collected data of the weather from a national atmospheric organization – IPMA, in the same timeline and in the same city: Lisbon, Portugal.

Understanding human mobility and its patterns through cell phone data allows us to quickly and accurately analyse the mobility of those who move around the city of Lisbon and has great potential to support the organization of large events and the use of public transportation, for example.

Considering the theme previously addressed, the development of this study aims, using data provided by Lisbon City Hall and IPMA, to analyse the spatial-temporal behaviour of visitors to the city of Lisbon, more specifically people using cell phones in Roaming (possible tourists), to explain patterns observed by them:

- Understand main tourist places of interest, where tourists eat and where they stay;
- Identify main places of concentration and their variation over the months under study;
- Understand how mobility patterns in tourists change with the weather;
- Discover unusual mobility patterns in international events happening in Portugal during the months under study.

II. STATE OF THE ART

A. Search strategy and inclusion criteria

PRISMA (Preferred Reporting Items for Systematic Reviews and Meta-Analysis) Methodology [2] was used to conduct a systematic literature review with the research question "What is the state of the art on the tourists' behaviour analysis and tourism mobility in smart cities?"

The database used for the search was Scopus, and the study took place between May 8 and 12, 2022; all of the findings had to be publications published within the past five years and written in English.

The search method was based on a single query with many research focuses.

This approach allowed researchers to count the number of articles that existed while considering the subject, context, and population under investigation.

Only papers were considered for this review.

Reviews, conference papers, workshops, books, editorials, and publications not linked to the topic were removed.

B. Study Selection

The title and abstract were used to make the first selection of articles, and in certain situations when that information was insufficient, the whole text was examined.

C. Data Extraction and Synthesis

Zotero and Microsoft Excel were used to handle and store the data. The information included the title, author, year, journal, topic area, keywords, and abstract.

A qualitative assessment was undertaken based on the results reported above for data synthesis and analysis.

Scopus was thoroughly searched for published work on the topic related with the concept "Data Analysis" or "Behaviour Analysis", the target population "Smart cities" or "Cellular

network" or "Tourist" or "Roaming" and within a "Mobility" context of the study.

D. Results

The research was made by searching the existing literature regarding the concept, target population and the context of this study in Scopus detailed in Table 1. The query was made in the database and with the same restrictions and filters.

Table 1. Keywords Definition.

Concept	Population	Context	Limitations
Data Analysis Behavio#r Analysis	smart cities cellular network Touris* Roaming	Mobility	2018-2022
453.106 Documents	220.301 Documents	642.769 Documents	Only journal papers, articles, and reviews
3,156 Documents			
44 Documents			

We can see that when we use the keywords from each column in the query (Concept AND Population AND Context AND Limitations) resulting in 44 documents.
16 papers were retrieved after a manual procedure was completed in order to determine major subjects on their research questions and define the outcomes.
Year, region, RQ topic, and a brief description were all factors in our study systematization.

E. Study Characteristics

The 16 studies included in the review were chosen using the above-mentioned criteria.

The trend line in Figure 1 shows that the issue we're examining is growing in popularity, demonstrating its importance.

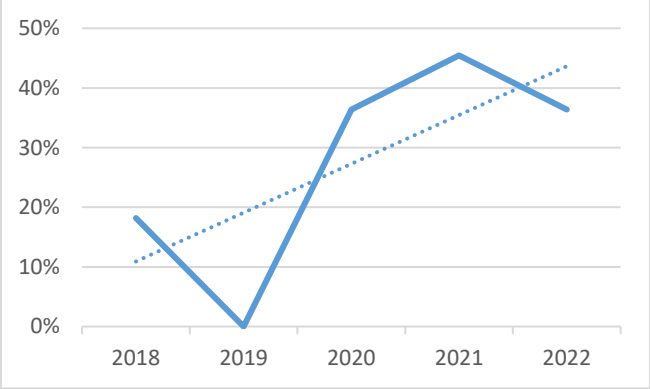

Fig 1. Evolution of the eligible studies by year

Given that the purpose of this study is to identify the use of tourist behaviour analysis and tourism mobility in Smart Cities, Table 2 and Figure 2 explain theoretically subjects mentioned in each of the evaluated papers, with a particular emphasis on the use of mobile phones and Behaviour Analysis on tourism and using mobile phones.

Figure 2 shows that most of the research focused on behaviours and used mobile phones and information and communications technology infrastructure (ICT).

Our research is predicated on both of these concepts since we not only investigate people's behaviour using the communication infrastructure of the city of Lisbon as an operator, but we also comprehend it and build a strategy to meet their demands.

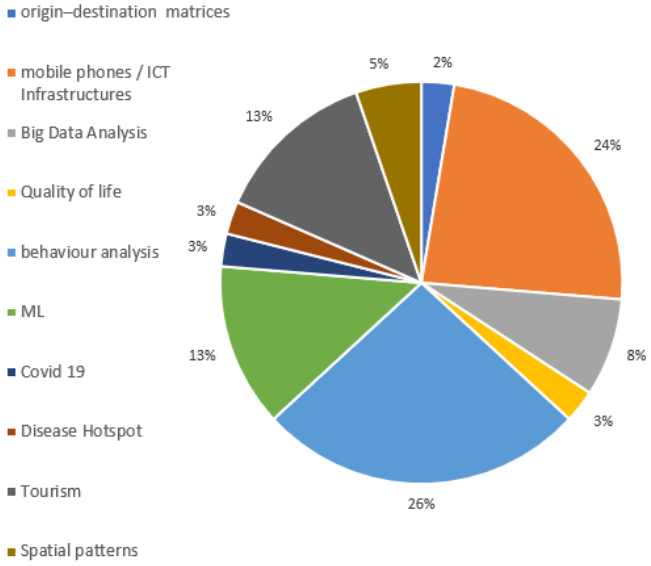

Table 2 summarises a more extensive examination of this review.

The issues were clearly described, and the writers of the publications did not need to be contacted for clarification.

The result categorization of the studies is not mutually exclusive, as they were assigned based on their existence or absence in the research.

Table 2. Keywords Definition.

Topic	Reference
(1) origin–destination matrices	[3]
(2) mobile phones / ICT Infrastructures	[3]–[11]
(3) Big Data Analysis	[3], [5], [10]
(4) Quality of life	[12]
(5) behaviour analysis	[4], [8], [10], [11], [13]–[18]
(6) ML	[4], [6], [7], [9], [13]
(7) Covid 19 / Disease Hotspot	[13]
(8) Tourism	[11], [13]–[15], [17]
(9) Spatial patterns	[14], [15]

After reading all of the publications, it was clear that the amount of behavioural research on tourist mobility has expanded dramatically in recent years all over the world.

Authors from [3] present a method for estimating origin–destination (O–D) matrices using passively obtained cellular network signalling data from millions of anonymous mobile phone users in the Rhône–Alpes region of France, enhancing and revolutionizing the field of travel demand and traffic flow modelling.

Still on the subject, the authors of study [5] can identify pedestrian hotspots and provide future traffic signal and street layout information to make the city more pedestrian friendly, as well as apply the knowledge gained to other data sets, such as bicycle traffic, to guide city infrastructure initiatives.

In a similar vein, but focusing on behaviour analysis, study [4] identifies a number of metrics for determining whether a person on the move is stationary, walking, or riding in a motorized private or public vehicle, with the goal of providing city users with personalized assistance messages for, among other things, sustainable mobility, health, and/or a better and more enjoyable life, with this applied to Tuscany and Florence. The goal of [8] in this chapter (combination of topics 2 and 5) is to study and compare the density of users in Shanghai city using Weibo geolocation data and univariate and bivariate density estimation approaches, such as point density and kernel density estimation (KDE), where the main findings are based on characteristics of users' spatial behaviour, such as the centre of activity based on check-ins, and the feasibility of using check-in data to explain the relationship between users and their social media accounts. Continuing in this vein, a research [10] based on long-term mobile phone data (from 2007 to 2012) of Beijing participants gives a means to visualize individual mobility patterns.

Study [6] aims to provide a taxonomy of 5G CN mobility prediction frameworks, from data gathering to model provisioning, while taking into account the 3GPP architecture and interfaces; and we provide two critical use cases in 5G CNs, in which the benefits of mobility predictions are assessed using information from real networks, whereas study [9] focuses on building a mobile sequential recommendation system to assist auto services (e.g., taxi drivers).

On the subject of behavioural analysis, study [16] presents an urban travel behaviour model and assesses its feasibility for creating a greener, cleaner environment for future generations, whereas study [18], based on a trip survey from the So Paulo Metropolitan Area, one of the world's busiest traffic locations, supplements a current bundling approach to enable multi-attribute trail datasets for the visual study of urban mobility, aiding in the identification and analysis of urban mobility.

In terms of quality of life, the authors of research [12] want to investigate the structural equation model of smart city elements that influence global management of world heritage sites as well as the quality of life for Thai tourists and inhabitants in Ayutthaya province.

Focusing on tourism, and behaviour analysis, author from [13] use machine learning to determine the most relevant parameters in influencing COVID-19 transmissions across different Chinese cities and clusters, researchers used a data-driven hierarchical modelling technique, being among this variables the “Number of tourists”. Following the same line, study [14] has the goal to assess the structure of tourist flows and \examine the variables that impact their regional distribution. Similarly, study [15] by using geographical and statistical analytic tools, the authors examine distinct intercity transportation patterns across different holidays and finds the driving factors, in order to optimize city hierarchical structure and allocate transportation resources. Study [7] using machine learning and the ICT, offer a position prediction system that takes into account both the spatial and temporal regularity of object movement. The object's historical trajectory data is utilized to derive personal trajectory patterns in order to determine possible future placements.

Using Airbnb data, author from [17] study visitors' mobility behaviour in relation to local public transportation access in tourist destinations. The author examines the attractiveness profile of 25 major tourist destination areas throughout the world using a "big data" analysis of the determinants of visitors' mobility behaviour and public transportation use in these tourist destinations.

Study [11] goal is to present novel techniques for studying pedestrian mobility aspects over the whole road network using the ICT and study the influence of visitor flows on the quality of life of locals and the preservation of cultural assets is exemplified by Venice.

III. METHODOLOGY: CRISP-DM

Cross Industry Standard Process for Data Mining (CRISP-DM), the methodological approach for the development of our project, is based on a standard method for designing data mining projects to reduce costs, increase reliability, execution, and manageability, making the data mining process more efficient [19].

However, for this project, given the data in question and our main goals, we opted for a modified version of this methodology consisting of 4 phases (see Fig 2):

- Data Understanding
- Data Preparation
- Analysis
- Visualisation

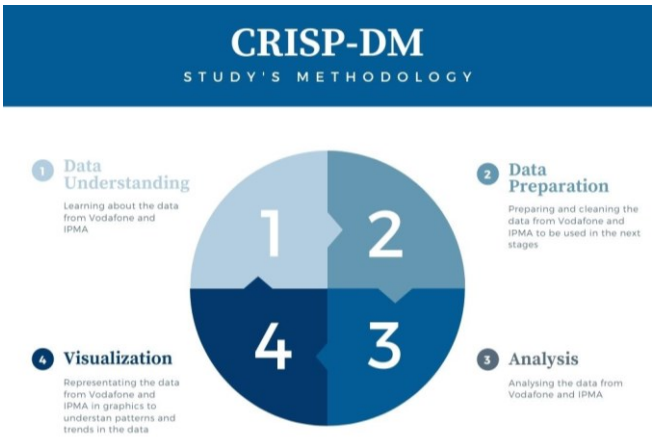

Fig 2 - Study’s Methodology

A. Data Understanding

After we gathered the data for our study, we explored it thoroughly and investigated each variable to understand the potential of our data and how we could maximize the added value of this study.

As stated previously, our main goal was to understand mobility patterns in tourists. To achieve that, we were given, by the Lisbon City Council, a dataset related to the mobility of people (roaming and non-roaming) in the city of Lisbon based on cell phone data, created by Vodafone, a British multinational telecommunications company. As it was explained to us, the data was collected from people who have Vodafone as a mobile carrier and later anonymized. To get a more accurate representation of the mobility of the all the people who circulated in Lisbon between September 2021

and January 2022, Vodafone extrapolated the data, originating the dataset we have available now (Vodafone dataset).

To get more accurate insights on the mobility of international tourists and how weather conditions change their mobility patterns, we reached out to the Portuguese Sea and Atmosphere Institute (IPMA) and requested data on the meteorological conditions in Lisbon between the months of September 2021 and February 2022.

There are two different datasets (Vodafone dataset and IPMA dataset), so they will be addressed separately.

1) Vodafone Dataset

The dataset provided by Vodafone was divided into several files in csv format separated by months, having 26 variables and 126 443 863 records in total, see Table I. As for the size of observations per month, see Table II.

TABLE I. VODAFONE DATASET VARIABLES

ID	Variable Name	Variable Description	Variable Type
0	Grid_ID	Number of grids There are 3743 squares of 200 by 200 meters in order to cover the metropolitan area of Lisbon	Nominal
1	Datetime	Time and date of occurrence	Datetime
2	C1	Number of distinct terminals counted on each grid cell during the 5 minute period – Measured every 5 minutes	Metric
3	C2	Number of distinct terminals in roaming counted on each grid cell during the 5 minute period– Measured every 5 minutes	Metric
4	C3	No. of distinct terminals that remained in the grid cell counted at the end of each 5 minute period	Metric
5	C4	No. of distinct terminals in roaming that remained in the grid cell counted at the end of each 5 minute period	Metric
6	C5	No. of distinct terminals entering the grid	Metric
7	C6	Terminals leaving the grid – These are the distinct terminals that left the grid. The calculation is made using the previous 5-minute interval as reference, also considering the crossings of the grid in the same interval	Metric
8	C7	Number of entries of distinct terminals, in roaming, in the grid	Metric
9	C8	Number of exits of distinct terminals, in roaming, in the grid	Metric
10	C9	Total no. of distinct terminals with active data connection in the grid cell – Measurement every 5 minutes	Metric
11	C10	Total no. of distinct terminals, in roaming, with active data connection in the grid cell – Measurement every 5 minutes	Metric
12	C11	No. of voices calls originating from the grid cell	Metric
13	C12	Entering the city: No. of devices that for 5 minutes enter the 11 street sections considered for analysis. For this purpose, a section of track is considered to be a route with	Metric

TABLE II. NUMBER OF OBSERVATION PER MONTH (IPMA DATASET)

MONTH	OBSERVATION NUMBERS
September 2021	17 233 318
October 2021	32 627 337
November 2021	21 619 292
December 2021	33 121 658
January 2021	33 344 624

2) IPMA Dataset

We performed an aggregation of the IPMA dataset by months and obtained a database consisting of 19 variables and 392 290 observations. The variables in this database are presented in Table II, as well as their descriptions:

TABLE III. IPMA DATASET VARIABLES

ID	Variable Name	Variable Description	Variable Type
0	Date_time	Date and time	Datetime
1	Entity_id	Entity type and id of the weather station (contains the values of the entity_type and station variables)	Nominal
2	Entity_location	Location of the station	Coordinates
3	Entity_ts	-	-
4	Entity_type	Entity type (present in variable entity_id)	Nominal
5	Station	Station id (present in variable entity_id)	Nominal
6	Fecha	Date and time of occurrence	Datetime
7	Fiware_service	firmware	-
8	Fiware_servicepath	Path of firmware service	-
9	Humidity	Relative humidity	Numeric
10	Wind_direction	Wind direction (represented by heading classes in weather reports: N, NE, E, SE, etc.)	Ordinal
11	WindIntensity_txt	Wind intensity (coding of the values of the variable Wind_direction)	Ordinal
12	WindIntensityKm	Wind intensity in km/h	Metric
13	Position	Location of station	Coordinates
14	PrecAccumulated	Accumulated precipitation in millimetres	Metric
15	Pressure	Atmospheric pressure in hPa	Metric
16	Radiation	Solar radiation	Metric
17	Temperature	Temperature in Celsius	Metric
18	Validity_ts	-	-

B. Data Preparation

Now that we have a better understanding of the data, we move to the second phase. This phase consists of four subphases: data selection, data cleaning, resource selection and data integration. Originally the dataset was spread over several files in csv format, each month consisting of 4 to 9 files of the same format. To handle the data more efficiently on personal computers and to proceed with preparation of the data, we decided to merge the csv files by months, rather than compiling all the files provided into one file. Later, we did the same to the IPMA dataset which was divided by months.

1) Vodafone Dataset

a) Data Selection

Mobile roaming data is obtained by means of radio waves, which are sent and received by the telecommunications base station and automatically stored in the memory or in the log files of the mobile network operators, in this case Vodafone. When a cell phone is registered in one country but used in another, its user can be recognized as a potential tourist, and the corresponding information such as the country of origin and location coordinates are registered as mobile roaming.

The information collected by Vodafone was aggregated over 3743 squares of 200 by 200 meters, with no values of less than 10 devices reported, and collected in 5-minute periods. The data becomes available after a processing period of approximately 45 minutes. This information is very important to study the mobility of tourists and is one of the most accurate.

b) Data Cleaning

In the primary clean-up of the dataset, we discarded missing values and removed duplicate rows. When that was complete, we moved on to the next subphase.

c) Resource Selection

One of the first things we did after cleaning the dataset was selecting the variables weren't of interest to our objective and eliminating them from the dataset. Thus, the original dataset was minimized to only a few variables of interest for our objectives.

Subsequently we created a dataset with only the mobility data of people in roaming (tourists) from the Vodafone dataset. We achieved that by keeping only the variables related to people in roaming.

d) Data Integration

The variable Datetime was in the format %Y-%m-%dT%H:%M:%S.%fZ. In order to facilitate its visualisation and also the manipulation of the data, we converted this variable from the object format to datetime, through the datetime library, and subsequently created separate columns for the date, time and created a new column with the corresponding day of the week.

As the goal of our work focuses on the mobility of people, it was also important to distinguish between holidays and weekdays/weekends in our dataset. To do this we used the holidays library, and only marked holidays on weekdays, since at the weekend they will not have much impact on mobility in general. Thus, using Python's Numpy library, a matrix was created for both the Weekday column - 1 is weekday, 0 weekend, and the new Holidays column - 1 is a holiday, 0 is not a holiday.

To check some events during the different times of the day, a column with distinct time intervals was also created.

To the Vodafone dataset we coupled the Vodafone Grid dataset, to have information about the parish and latitudes and longitudes of each Grid_ID. From the junction of this dataset, it was possible to build new columns to facilitate a posterior data analysis and visualisation in PowerBI. A column with zones of Lisbon was then created, in which the 24 parishes of Lisbon were grouped into 5 distinct zones (visible in fig 2), according to the administrative reorganization of the parishes in 2012, namely (https://www.am-lisboa.pt/451600/1/008910,000505/index.html):

- North Zone (Green Zone) - Santa Clara, Lumiar, Carnide, São Domingos de Benfica, Benfica;
- Western Zone (Yellow Zone) - Alcântara, Ajuda, Belém;
- Center Zone (Orange Zone) - Campolide, Alvalade, Avenidas Novas, Santo António, Arroios, Areeiro;
- Historic Downtown Area (Purple Zone)- Campo de Ourique, Estrela, Misericórdia, Santa Maria Maior, São Vicente, Penha de França;
- Eastern Zone (Blue Zone) - Beato, Marvila, Olivais, Parque das Nações.

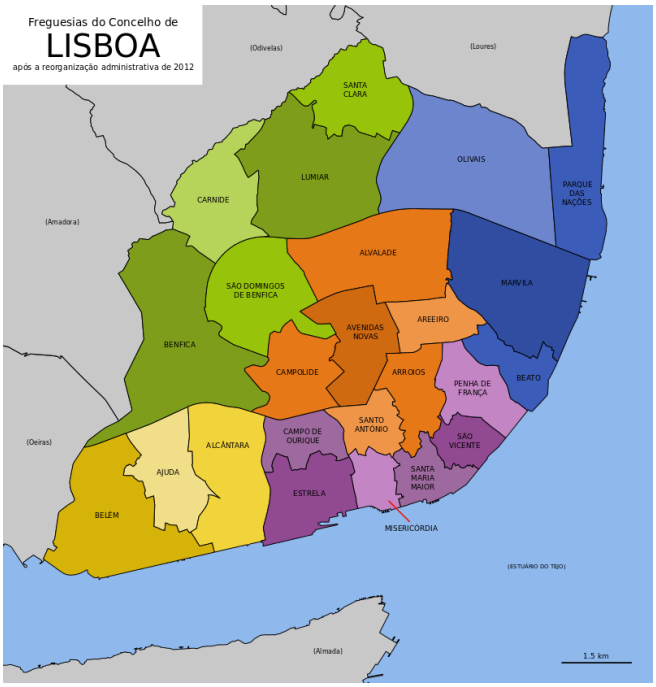

Fig 3 - Municipalities of the County of Lisbon

Regarding a variable (D1), which presents the TOP10 of equipment origin (cell phones) by order of representativeness, a split was applied in order to separate the countries that belonged to that column by distinct columns: TOP1 to TOP10, and then decreasing the TOP10 to only one TOP3 of representativeness of the countries in that location, so that instead of creating 10 additional columns, only 3 columns were created, making data manipulation more efficient.

For a facilitation of the visualisation of the mobility of tourists through the city of Lisbon, the countries represented in the columns TOP1 to TOP3 were grouped by territorial zones, except the main nationalities of tourists in Portugal: Spain, France, United Kingdom (Refª Tourism Statistics

2020) and other countries that in our perspective it would not make sense to be grouped together. Three new columns were then created (zonasnacionalidade1, zonasnacionalidade2 and zonasnacionalidade3), which represent the TOP1, TOP2 and TOP3, respectively, of different nationality groupings, as follows:

TABLE IV. COUNTRY GROUPS

Country	Group
Spain	Spain
France	France
Germany	Germany
Italy	Italy
U. S. A	U. S. A
South Africa	South Africa
Russia, Belarus	Eastern Europe
Bulgaria, Romania, Lithuania, Estonia, Latvia, Ukraine, Slovakia	Eastern Europe
Denmark, Sweden, Finland, Norway, Iceland, Faroe Islands	Nordic Europe
Belgium, Luxembourg, Andorra	Central Europe
Malta, Slovenia, Croatia, Greece, Serbia, Bosnia and Herzegovina, Albania, Montenegro, Macedonia.	Southern Europe
Hungary, Poland, Czech Republic	Visegrad Group
Austria, Switzerland, Liechtenstein	Alpine Countries
Kuwait, Iraq, Afghanistan, Israel, United Arab Emirates, Turkey, Saudi Arabia, Cyprus, Iran, Egypt, Qatar, Oman, Jordan, Bahrain	Middle East
Singapore, Indonesia, Georgia, Philippines, Malaysia, Thailand, Armenia, Vietnam	Southwest Asia
Nigeria, Azerbaijan, Ghana, Cameroon, Ivory Coast, Benin	West Africa
Tunisia, Morocco, Kenya, Gibraltar, Mozambique, Uganda, Algeria, Mauritius, Reunion	North and East Africa
India, Bangladesh, Pakistan, Kazakhstan, Sri Lanka	South, Central and South Asia
Hong Kong, Japan, South Korea, Macau, Taiwan	Eastern Asia
Costa Rica, Panama, Puerto Rico, Mexico, Guatemala, Dominican Republic, Bermuda, Nicaragua	Central and North America
Brazil, Peru, Uruguay, Chile, Paraguay, Netherlands Antilles, French Guyana	South America
Australia, New Zealand	New Zealand and Australia
Ireland, United Kingdom	Ireland and United Kingdom
Nan, None	Unknown

2) IPMA Dataset

a) Data Selection

IPMA, the Portuguese Sea and Atmosphere Institute holds the largest national meteorological observation infrastructure network which generates data about the weather conditions in real-time. This data is then grouped into datasets to be studied and analysed by professionals qualified to know the weather and its variations, to aid in prediction models, time series, i.e. In this case the data is being used to complement the main dataset due to its importance in understanding the mobility patterns in tourists.

b) Data Cleaning

To clean the dataset, we discarded missing values, removed duplicate rows, and deleted all rows which had an observation with the number -99 (Error Code). After that, we moved on to the next subphase.

c) Resource Selection

We proceeded to eliminate the variables that weren't of interest to our objective and the variables that had no variance. Thus, the original dataset was minimized to only a few variables of interest (see table V), the most important ones being humidity, wind intensity, accumulated precipitation, and temperature.

TABLE V. REMAINING VARIABLES (IPMA DATASET)

ID	Variable Name	Variable Description	Variable Type
0	Day	Day of observation	Datetime
1	Hour	Hour of observation	Numeric
2	Month	Month of observation	Numeric
3	Month_txt	Month of observation in text format	Nominal
4	Station	Station where the data was collected from	Nominal
5	Position	Coordinates of the Station	Coordinates
6	Humidity	Relative Humidity in %	Numeric
7	Humidity_txt	Categorized version of the variable Humidity	Categorical
8	WindIntensity	Wind intensity Index used by IPMA	Ordinal
9	WindIntensity_txt	Categorized version of the variable WindIntensity	Categorical
10	WindIntensityKm	Wind Intensity in km/h	Metric
11	PrecAccumulated	Accumulated Precipitation in mm	Metric
12	PrecAccumulated_txt	Categorized version of the variable PrecAccumulated	Categorical
13	Temperature	Temperature in °C	Metric
14	Temperature_txt	Categorized version of the variable Temperature	Categorical

d) Data Integration

The variable fecha was in the format %Y-%m-%dT%H:%M:%S.%fZ. For the same reason as the Vodafone dataset, we converted this variable from the object format to datetime, through the datetime library, and subsequently created separate columns for the month, hour, and day of the observation. Having completed that we then created new

columns that were the categorical version of our numeric variables of interest (see Table VI), basing our categories in the metadata from IPMA and the measuring system of each variable, and created a text version of the variable month to aid in the visualisation.

TABLE VI. NEW CATEGORICAL VARIABLES (IPMA DATASET)

Variable Name	Categories	Scale
Humidity_txt	No humidity	0–5 (%)
	Low humidity	6–20 (%)
	Moderate humidity	21–60 (%)
	High humidity	61–100 (%)
WindIntensity_txt (Index used by IPMA from 0 to 12)	No wind	0-1
	Low wind	1-4
	Moderate Wind	4-7
	Intense wind	7-12
AccPrecipitation_txt	No rain	0-5 (%)
	Low rain	6-20 (%)
	Moderate rain	21-60 (%)
	Abundant rain	61-100 (%)
Temperature_txt	Very Cold	-5-0 (°C)
	Cold	1-20 (°C)
	Pleasant	21-28 (°C)
	Warm	29-40 (°C)

IV. VISUALISATION

After the data analysis, we moved on to data visualisation. In this stage, we represented the data in graphics, as it's a quick way to see trends and patterns in the mobility of the tourists and to focus on the most important points. Graphs and charts let us explore and learn more about data [20].

We found that of the months under review, October had the most tourists (see Fig 4).

Fig 4 - Tourists in Lisbon

As for the presence of tourists in the various periods of the day, the month of October was analysed since it is the month that presents more tourist visits, as seen in the previous graph (see Fig 4). We found that in the lunch hour period the parishes that tourists frequent the most are Belém, Alvalade and Parque das Nações; in the afternoon and evening periods the most visited parishes are Belém, Alvalade and Avenidas Novas; finally, during the early morning hours the most frequented parishes are Avenidas Novas, Belém and Arroios.

Good data visualisations also makes it easier to communicate our ideas and insights to other people [20]. With PowerBI we represented each parish and used the data available to visualise the movement of tourists and to identify major patterns.

A) Case 1 – Mobility Patterns in Different Weather

One interesting case is the influence of tourists' movements based on weather conditions and the places they prefer to go to when it's raining and when it's sunny. In Fig 4 and 5 we represented tourists' movements on sunny and rainy weeks to depict their movements. When it is raining tourists tend to concentrate in certain places (The historic downtown area, the airport, near Carnide where we found a lot of hostels and apartments for rent and in the Eastern zone). Tourists tend to stick to monuments, their places of stay and shopping centres in rainy days (see Fig 5). When it's sunny, rather than concentrating in some places, tourists tend to spread out more and visit more areas than the "hotspots" (see Fig 6). It's clearly visible the effects of the weather on the mobility of tourists.

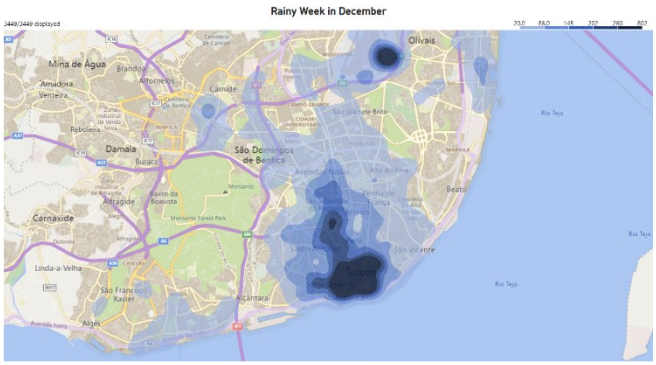

Fig 5 – Tourists' mobility on a rainy week in December

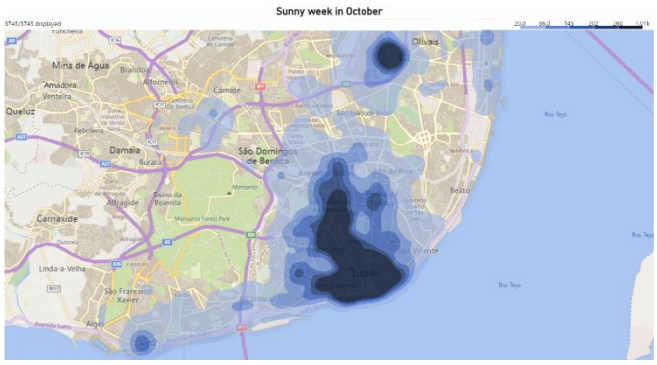

Fig 6 -Tourists' mobility on a sunny week in October

B) Case 2 – Web Summit

Web Summit is an annual technology conference held in Lisbon, Portugal and the biggest in Europe [21]. In 2021, still under the effects of the COVID-19 pandemic, the event gathered over 40,000 visitors. This influx of people allowed us to visualise the impact that the event had in the area where it was held (FIL – Lisbon International Fair).

To analyse this, we mapped the movement of Roaming users and considered those who were staying in the same grid for more than 5 minutes when the event was taking place and put those results side by side with the remaining days of the month. On the Web Summit period (1st – 4th November 2021), we were able to register an average of 2852 tourists at any given time in the event area. Compared to the 262 for the rest of the month of November (4th – 30th November 2021). This is a 987% increase in tourist activity (Figure 7 shows this example).

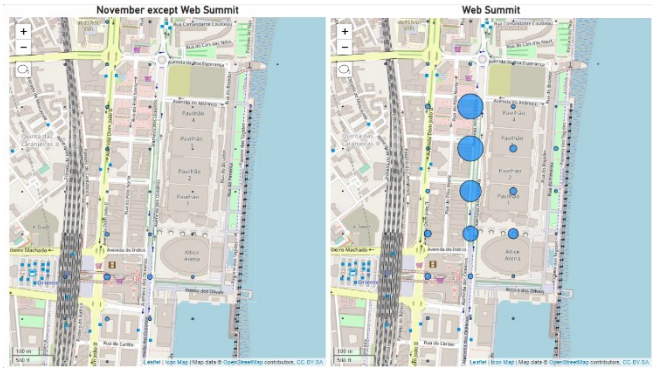

Fig 7 - Comparison of Tourist Mobility Before, and After vs. During Web Summit

C) Case 3 – Big Events Monitor Process – Case of a Game Day

Football tourists are those who travel to attend a football event, often a game. Within this group, it is feasible to identify three important categories of football tourists, the most common of which are travelling football teams.

The proposed approach allows for a real time monitoring of the tourist's movements in the city. Since the UEFA Champions League games create big movements of people from around the world. We monitored 4 major games in Portugal.

From the 4 games we monitored we chose the one which brought tourists from a nationality a lot less present throughout Lisbon, throughout the months in study, than the nationalities of other football fans that came to Portugal to see the other games (for privacy purposes, in this paper, we will call it nationality A). This aspect allowed us to monitor the football fans' movements a lot more effectively and clearly, than if we had a considerable number of tourists just visiting the city in general.

We were able to identify the time of arrival of the football fans at Lisbon Airport – 9 am – the day of the match, as can be seen in Figure 8 (big dot in the Humberto Delgado Airport).

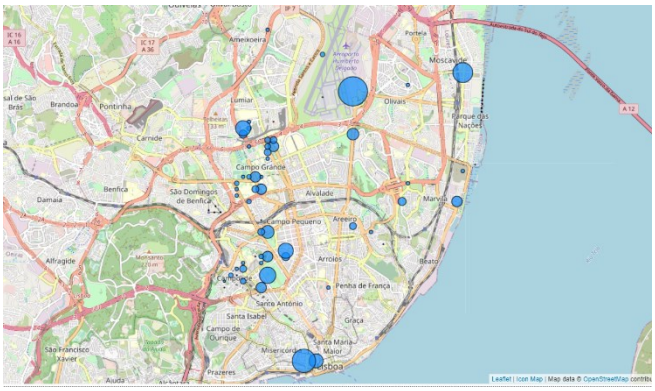

Fig 8 - Arriving time of football fans from nationality A in Lisbon Airport at around 9h

During the day they went mainly to the historic downtown area, as we can see in Fig 9.

Then at the game time we identify around 5000 tourists from nationality A at Sporting stadium (see Fig 10). After the game, since there are no flights, they stay and sleep in Historic Downtown Area (see Fig 11) and next day around 9h they leave Lisbon (see Fig 12). This case shows the importance of this study for parishes to understand tourists' movements and to better manage big events.

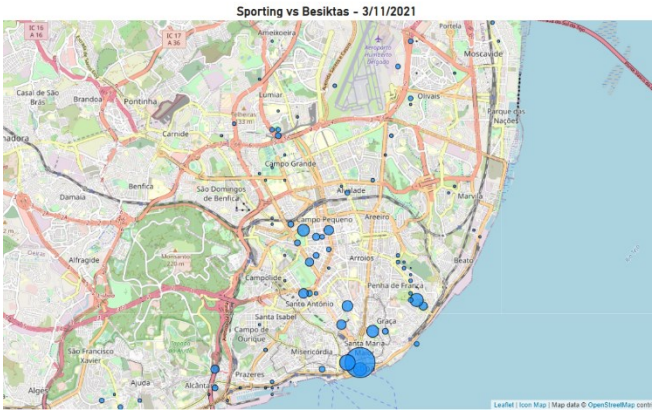

Fig 9 – Fans from nationality A at 14h in the Historic Downtown Area

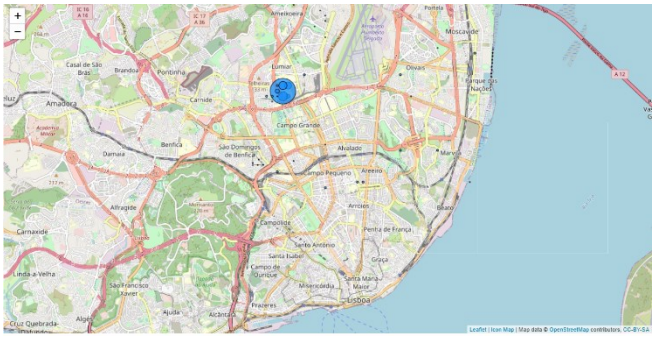

Fig 10 – Fans from nationality A during football match

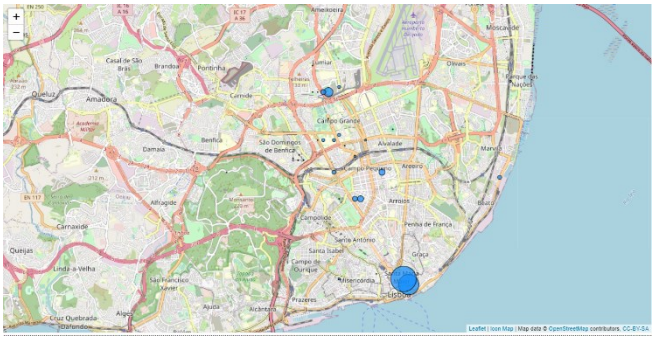

Fig 11 - Fans from nationality A after football match

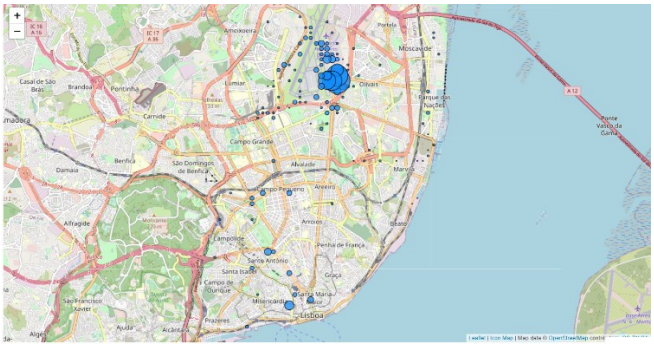

Fig 12 – Fans from nationality A the day after the match at 9h leaving Lisbon

A) Case 4 –Shopping activity

Shopping activity can be checked using the communication antennas that cover the shopping mall. The number of tourist visitors is useful information for authorities

and store owners. Visit patterns and understanding abnormal behaviour during promotion days like black Friday is useful information. We can check where tourists shop more and see if these promotions also influence their behaviour. The data collected shows this influence and it is possible to witness this behaviour based on the nationality. Figs 13 and 14 show this influence and also the main place where tourists shop.

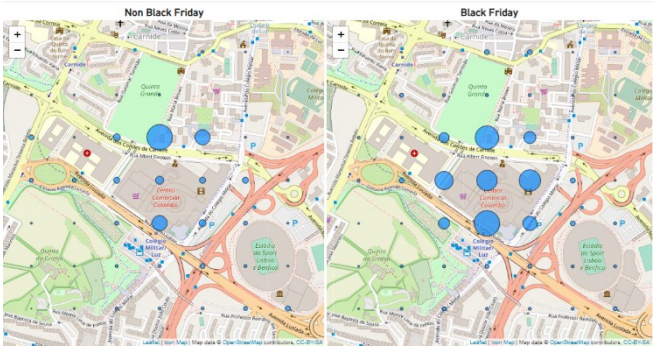

Fig 13 – Effect of Black Friday in Colombo Mall

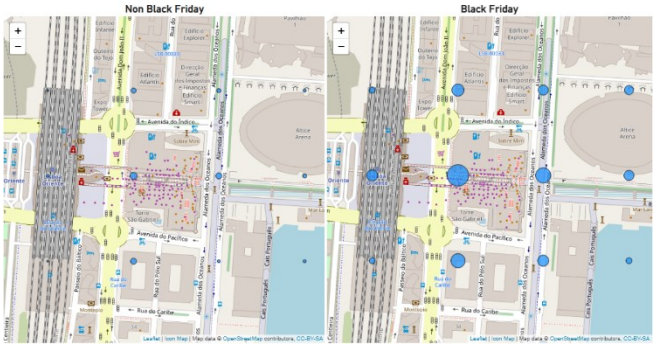

Fig 14 – Effect of Black Friday in Vasco da Gama Mall

V. CONCLUSIONS

With this study we were able to understand the mobility patterns of tourists in Lisbon.

They tend to frequent the historic downtown and centre area, and explore the coastal areas, which have points of interest.

We verified that after the 20th of each month there is usually a decrease in the presence of tourists in Lisbon.

The precipitation discourages tourists from visiting tourist sites. They tend to stay in the "hotspots" (the centre area and the historical downtown area), visiting museums, shopping malls, or staying in the comfort of their place of stay. When it's sunny, tourists tend to spread out more around the city and visit more areas than they stay in the hotspots (behaviour seen when it's raining).

And finally, international events bring a high number of tourists to the city where they're being held and especially to the surrounding area.

Understanding the geographical distribution of urban tourism is crucial for public policy. Thus, in areas with a large concentration of visitors, local authorities may consider initiatives to enhance the tourist experience, such as developing pedestrian-only lanes or enlarging sidewalks, expanding public places with free Wi-Fi, and situating new tourist information centres, among others. The big picture in real time provided by current developed work allows local authorities to understand this movement, identify dangerous concentration in big events.

We have developed a platform that collects anonymized data from mobile operators. The presence of mobile operators in the market allows for a representation of a city's population (if there are multiple operators in a city). Our approach started with a data cleaning and processing developed in python and then a visualization of the data in maps and dashboards made in PowerBI. This can be replicated in other cities and it's an important tool for city management authorities to understand the concentration and movements of tourists and adjust processes and facilities.

This work allows us to understand tourist movements and their patterns, correlated with weather, nationality and events. Modeling tourist behavior is another important topic.

ACKNOWLEDGMENT

We thank the Lisbon City Council for providing us with the data necessary for this study, namely Mr. António Costa (Lisbon City Council), Mrs. Helena Martins (Lisbon City Council) and Mrs. Paula Melicias (Lisbon City Council). We also thank IPMA for providing us with the data necessary to complement our study.

This work was supported by EEA Grants Blue Growth Programme (Call #5). Project PT-INNOVATION-0045 – Fish2Fork.

REFERENCES

[1] LCG, "Toursim numbers in Portugal | March 2022." https://travelbi.turismodeportugal.pt/turismo-em-portugal/turismo-em-numeros-marco-2022/ (accessed May 13, 2022).

[2] D. Moher, A. Liberati, J. Tetzlaff, and D. G. Altman, "Preferred reporting items for systematic reviews and meta-analyses: the PRISMA statement," *BMJ*, vol. 339, p. b2535, Jul. 2009, doi: 10.1136/bmj.b2535.

[3] M. Fekih, T. Bellemans, Z. Smoreda, P. Bonnel, A. Furno, and S. Galland, "A data-driven approach for origin–destination matrix construction from cellular network signalling data: a case study of Lyon region (France)," *Transportation*, vol. 48, no. 4, pp. 1671–1702, 2021, doi: 10.1007/s11116-020-10108-w.

[4] C. Badii, A. Difino, P. Nesi, I. Paoli, and M. Paolucci, "Classification of users' transportation modalities from mobiles in real operating conditions," *Multimed. Tools Appl.*, vol. 81, no. 1, pp. 115–140, 2022, doi: 10.1007/s11042-021-10993-y.

[5] E. Carter, P. Adam, D. Tsakis, S. Shaw, R. Watson, and P. Ryan, "Enhancing pedestrian mobility in Smart Cities using Big Data," *J. Manag. Anal.*, vol. 7, no. 2, pp. 173–188, 2020, doi: 10.1080/23270012.2020.1741039.

[6] J. Jeong *et al.*, "Mobility Prediction for 5G Core Networks," *IEEE Commun. Stand. Mag.*, vol. 5, no. 1, pp. 56–61, 2021, doi: 10.1109/MCOMSTD.001.2000046.

[7] X. Li *et al.*, "Position prediction system based on spatio-temporal regularity of object mobility," *Inf. Syst.*, vol. 75, pp. 43–55, 2018, doi: 10.1016/j.is.2018.02.004.

[8] S. A. Haidery, H. Ullah, N. Ullah Khan, K. Fatima, S. Shahla Rizvi, and S. J. Kwon, "Role of big data in the development of smart city by analyzing the density of residents in shanghai," *Electron. Switz.*, vol. 9, no. 5, 2020, doi: 10.3390/electronics9050837.

[9] P. Guo, K. Xiao, Z. Ye, and W. Zhu, "Route Optimization via Environment-Aware Deep Network and Reinforcement Learning," *ACM Trans. Intell. Syst. Technol.*, vol. 12, no. 6, 2021, doi: 10.1145/3461645.

[10] C. Li, J. Hu, Z. Dai, Z. Fan, and Z. Wu, "Understanding individual mobility pattern and portrait depiction based on mobile phone data," *ISPRS Int. J. Geo-Inf.*, vol. 9, no. 11, 2020, doi: 10.3390/ijgi9110666.

[11] C. Mizzi *et al.*, "Unraveling pedestrian mobility on a road network using ICTs data during great tourist events," *EPJ Data Sci.*, vol. 7, no. 1, 2018, doi: 10.1140/epjds/s13688-018-0168-2.

[12] P. Keawsomnuk, "A structural equation model of factors relating to smart cities that affect the management of the world heritage site as well as the quality of life of tourists and villagers in Ayutthaya, Thailand," *Humanit. Arts Soc. Sci. Stud.*, vol. 21, no. 1, pp. 35–42, 2021, doi: 10.14456/hasss.2021.4.

[13] A. Cheshmehzangi *et al.*, "A hierarchical study for urban statistical indicators on the prevalence of COVID-19 in Chinese city clusters based on multiple linear regression (MLR) and polynomial best subset regression (PBSR) analysis," *Sci. Rep.*, vol. 12, no. 1, 2022, doi: 10.1038/s41598-022-05859-8.

[14] M. Šauer, J. Vystoupil, M. Novotná, and K. Widawski, "Central European Tourist Flows: Intraregional Patterns and Their Implications," *Morav. Geogr. Rep.*, vol. 29, no. 4, pp. 278–291, 2021, doi: 10.2478/mgr-2021-0020.

[15] X. Lao, X. Deng, H. Gu, J. Yang, H. Yu, and Z. Xu, "Comparing Intercity Mobility Patterns among Different Holidays in China: a Big Data Analysis," *Appl. Spat. Anal. Policy*, 2022, doi: 10.1007/s12061-021-09433-z.

[16] N. X. Leow and J. Krishnaswamy, "Smart cities need environmental consciousness and more social responsibilities as an outcome of COVID-19 – reflections from urban road commuters," *Foresight*, vol. 24, no. 2, pp. 276–296, 2022, doi: 10.1108/FS-02-2021-0035.

[17] U. Türk, J. Östh, K. Kourtit, and P. Nijkamp, "The path of least resistance explaining tourist mobility patterns in destination areas using Airbnb data," *J. Transp. Geogr.*, vol. 94, 2021, doi: 10.1016/j.jtrangeo.2021.103130.

[18] T. G. Martins, N. Lago, E. F. Z. Santana, A. Telea, F. Kon, and H. A. de Souza, "Using bundling to visualize multivariate urban mobility structure patterns in the São Paulo Metropolitan Area," *J. Internet Serv. Appl.*, vol. 12, no. 1, 2021, doi: 10.1186/s13174-021-00136-9.

[19] R. Wirth and J. Hipp, "CRISP-DM: Towards a Standard Process Model for Data Mining," p. 11.

[20] K. Healy, *Data Visualisation: A Practical Introduction*. Princeton University Press, 2018.

[21] "Web Summit: Lisbon hosting the largest tech event in the world - Portugal - Portuguese American Journal." https://portuguese-american-journal.com/web-summit-lisbon-hosting-the-largest-tech-event-in-the-world-portugal/ (accessed May 13, 2022).

Intrusion Detection System in IoT to prevent cyber-attacks in organizations

Susmita Paul

Symbiosis Centre for Information Technology, India

Abstract:

Internet of things (IoT) devices are connected objects which are able to collect and exchange data. IoT offers many opportunities to make day-to-day life more fulfilling but is impacted by many security challenges. IoT is fast gaining traction in a wide range of industries, including health care, automotive and logistics. The Internet of Things (IoT) ecosystem has grown in importance as a method of ensuring the security and stability of both information and connection. This paper is based on the analysis of intrusion Detection Systems that is used in organizations and how they can be improved. An IDS is used to detect and remove malicious packets before it enters the network. It is a technique to detect the attack source when cryptography is broken and it also monitors the system activities or network traffic to detect policy violations.

The objective of this research paper is to do a bibliometric analysis and improve the efficiency and security of organizations and human life. An IoT-based environment is used to enable the integration and realization of smart objects in smart industry, Smart health, smart homes and smart buildings. An Intrusion Detection System (IDS) is a technique to detect malicious activities in an IoT network.

Introduction: Smart environments help to improve the efficiency of an organisation and quality of human life. Over the past few decades, technology has become an integral aspect of the workplace and businesses started relying on technology to conduct work effectively and efficiently. Due to the rapid development, the internet is going to connect the world from anywhere and everywhere and thus a new concept arrives i.e., IOT (Internet of Things) but with this technology also comes the protection of IOT otherwise it can have adverse effects. [1]

With advanced technology in businesses, comes the responsibility to take IoT security more seriously. When an organisation is connected via Internet or Intranet, the most crucial aspect for the organisation to make success is to maintain a stable and secure network security system and hence protection of IoT is important and necessary. So, to detect and monitor any malicious packets or malpractices that are happening in and outside the network, IDS is employed.[2]

An Intrusion Detection System monitors the network traffic and warns the user if any malicious activity is going on the network by giving alerts. An IDS will detect the malicious activity in IoT ensuring the organizations that their IoT devices stay connected without any interruption or cyber threats making it protected from the DOS attacks and the network spoofing that is done by the hackers.

Intrusion Detection in IoT:

Classification of intrusion detection system is explained based on the existing research. Figure 1 shows how IDS systems can be classified based on various classifications that is a) type of intruders b) Type of intrusions c) Detection techniques and d) Type of IDS. Intruders are referred to the one who try to gain unauthorised access to exploit a computer system. The difference between the external and internal intruders is that external intruders are the one who doesn't have access in any form and are completely unauthorized users but internal users are the one who have access only to a few sections but not all of them for example employees of an organisation can be an internal intruder.

Intrusion refers to the act of intruding and it affects the CIA (Confidentiality, Integrity and availability) of the information and the resource. There can be many types of intrusions including active attacks, passive attacks, fraud, DOS/DDOS, malicious attacks and others [3,4,5]. If the information is only eavesdropped but is not modified then that type of attack is known as passive attacks and if the information has gained unauthorised access as well as the information has been destroyed or changed then it is known as active attack. There are various types of passive attack like eavesdropping, location disclosure, traffic analysis and the various types of active attacks are malicious packet dropping, and routing attacks like men-in-the-middle attack, sleep deprivation, spoofing. The various types of frauds can be a situation where an account is compromised, phishing, unauthorised transaction, sniffer attack. If a website or resource is made unavailable by flooding a server with traffic then it is known as DOS attack. If a DOS attack is made using multiple computers and machines then it is known as DDOS attack. If an employer's system executes abnormal or unauthorized actions by a Malicious software then it is known as Malicious attacks or Malware/Botnet attacks. [7]

Matching algorithms are used in signature-based intrusion detection systems (SIDS) to locate a previous incursion. An alarm signal is triggered when an intrusion signature is matched against the signature of a previous intrusion that

exists in the signature database. Though SIDS is the effective approach to detect known attacks [6]. For known attacks, it has a high detection accuracy and a low computing cost, with a very low false alarm rate. However, it is unable to identify unknown attacks, evasive attacks and variants of existing attacks. Only the attacks for which they have been trained can be detected. Anomaly-based intrusion detection system (AIDS) methods might be a viable answer to this problem. A normal model of a computer system's behaviour is produced in AIDS utilising machine learning, statistical based, or knowledge based approaches [8,9,10,11,12]. An anomaly is defined as a significant difference between observed behaviour and the model, which might be regarded as an intrusion. AIDS technique is all about how a malicious behaviour differs from normal user behaviour. It can detect unforeseen and new vulnerabilities and also novel attacks or unknown attacks.

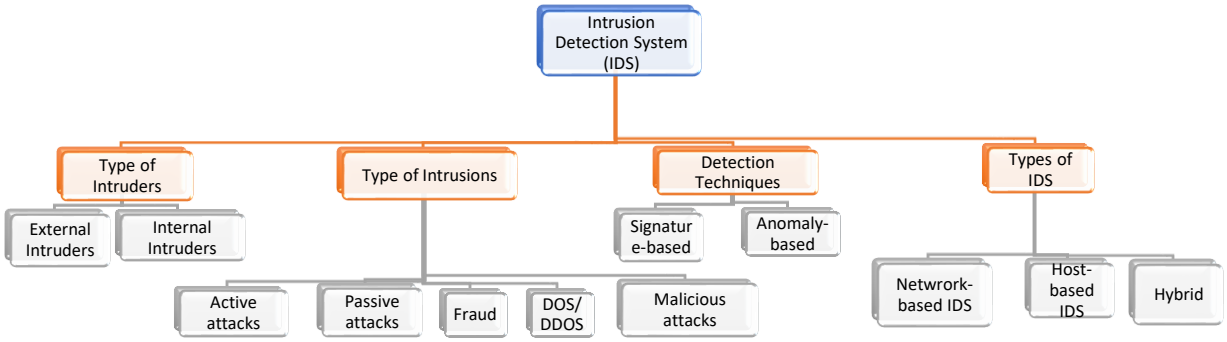

Figure 1: Classification of IDS for IoT

Different types of IDS systems are Host-based, Network based and Hybrid. Host-based IDS (HIDS) monitors the network traffic at the transport layer. It monitors the operating system's audit information for any signs of intrusion on a specific machine, such as mobile devices or servers. The attacks that are skipped by HIDS, can be detected by NIDS i.e., Network based IDS [11,12,13,14,15]. It monitors any form of intrusion in network traffic and application protocol activity between any two machines. The combination of Host-based IDS and Network based IDS is known as Hybrid and it provides in-depth defence.

Literature review:

There are a lot of stakes for organizations of all sizes including big, medium and small for all the data and information it has. Even a small gap in the layered security approach can keep the system vulnerable to malicious attacks. With a mounting number of enterprises that are becoming reliant on Internet of Things, the need for ample security measures is becoming more and more significant. As discussed earlier, there are mainly two types of Intrusion detection system like the anomaly based or the signature based and or as proposed “AS-IDS” model which combines both the approach which is Anomaly-Signature Intrusion Detection System to detect the attacks that takes place in IoT networks.

A review of Intrusion detection systems for IoT based smart environment has been done for improving the efficiency of work. The latest designs of the IoT model’s Intrusion detection systems [2] has been discussed which also gives a brief overview of the IoT architecture, its vulnerabilities and threats and the respective layers of the IoT.

Literature review for this particular topic of IDS on IOT is given to put emphasis on the challenges and up-to-date information. And an analysis has been made to determine the gaps or flaws we found for this particular topic. So, now improvement needs to be done based on the analysis which will also give a future perspective of the topic on how to accept and take the challenging tasks and securities that is based on IOT. After completing full security assessment, organization will be more effective and informed when it comes to vulnerabilities of the IOT systems, including how to mitigate them using IDSs.

Given the rise in cyber-attacks against organizations, we expect cybersecurity to continue to play a key role in the sector. Despite the increased study and attention paid to cybersecurity, there are still gaps in the analysis.

Methodology:

Bibliometric as the name itself talks about statistical analysis of articles, books or/and other publications. Bibliometric analysis is a common research technique for determining the state of the art in a specific subject [13,14]. The approach may be used to describe trends of publishing within a specific time or particular country or specific language or body of literature using statistics and quantitative analysis.

While there are a good number of databases like Scopus, Google Scholar, Web of Science and others to index articles, Scopus was chosen over others since it is said to have the largest citation database which is 'Elsevier's abstract and citation database' and was launched in 2004. First of all, an extensive search was made by including few keywords using Scopus. Then it was excluded using other parameters like years, languages, etc., The keyword list: Scopus (Journals, articles, books, all years, all languages):

Criteria	Explanation
Within 5 Years (YR)	Limited to papers which are within 5 years
English (E)	Language papers which are English language were included.
Open Access (OA)	Open Access Papers only are included
Non-related Subject Area (NSR)	Keywords related to only related Subject Areas

Table 1: Naming Convention of exclusion and inclusion criteria

Articles which were published prior to 5 years were excluded, articles ranging from the year 2016 to 2020 were included which offered only 'Open Access'. Articles that don't follow English language were excluded and only related Subject areas were included. The final keyword list: Scopus (Journals, articles, books, 2016-2021, Open Access, English language, Subject Area -Computer Science, Engineering, etc)

(TITLE-ABS-KEY (intrusion AND detection AND system) AND TITLE-ABS-KEY (IOT) OR TITLE-ABS-KEY (cyber AND attack) OR TITLE-ABS-KEY (cyber-attack) OR TITLE-ABS-KEY (organization) OR TITLE-ABS-KEY (organizations)) AND (LIMIT-TO (OA , "all")) AND (LIMIT-TO (PUBYEAR , 2020) OR LIMIT-TO (PUBYEAR , 2019) OR LIMIT-TO (PUBYEAR , 2018) OR LIMIT-TO (PUBYEAR , 2017) OR LIMIT-TO (PUBYEAR , 2016)) AND (LIMIT-TO (LANGUAGE , "English")) AND (EXCLUDE (SUBJAREA , "MATH") OR EXCLUDE (SUBJAREA , "PHYS") OR EXCLUDE (SUBJAREA , "SOCI") OR EXCLUDE (SUBJAREA , "CHEM") OR EXCLUDE (SUBJAREA , "BIOC") OR EXCLUDE (SUBJAREA , "CENG") OR EXCLUDE (SUBJAREA , "MEDI") OR EXCLUDE (SUBJAREA , "EART") OR EXCLUDE (SUBJAREA , "PSYC") OR EXCLUDE (SUBJAREA , "ARTS"))

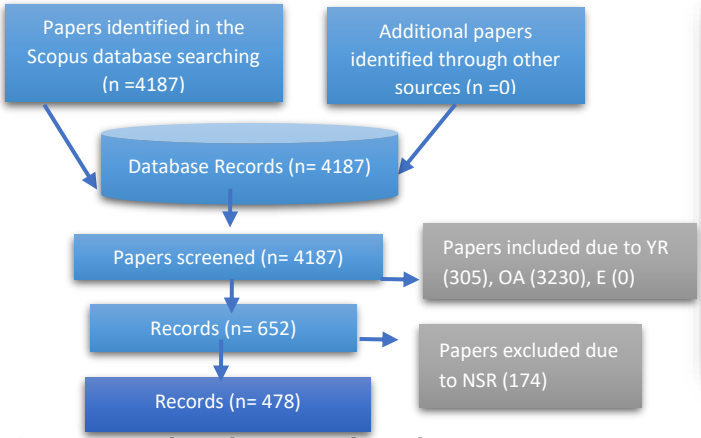

Figure 2: Search Techniques and Results

Search Results: The preliminary search on Scopus having the basic keywords yielded 4,187 document results. Then after making it open access and limiting to only five years publications it gave 652 results. Finally, limiting to English Language and excluding irrelevant subject areas, it yielded 478 results. Figure 2 explains how the search was executed.

Findings:

This section outlines the finding of detection systems upon

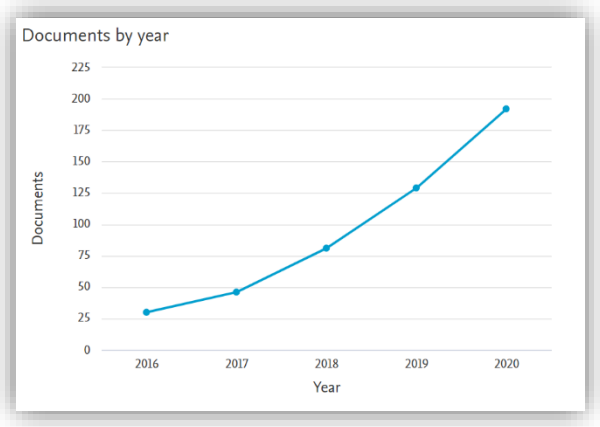

Figure 3: Number of publications year wise

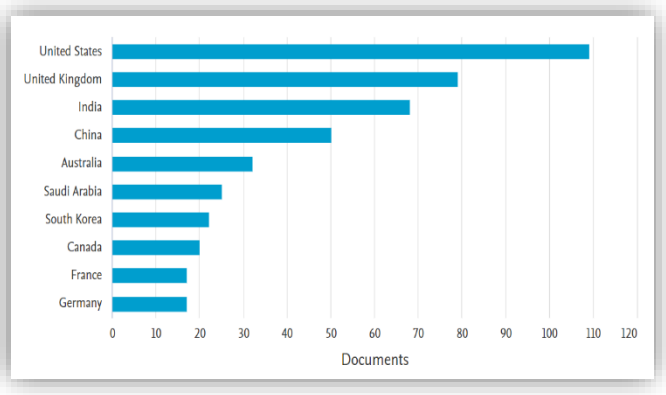

Figure 4: Number of publications Country wise

This section outlines the finding of detection systems upon which the research is done. This section is broken down into many sections which includes number of publications per year, number of publications per country, comparison of document type and productivity of different sources. These results are significant because they combine bibliometric data with publishing rates. Here, the results are discussed and the findings are analysed that was received from the search result section. This finding is important as it helps us to analyse the publishing rates in terms of years, countries and other parameters in an in-depth manner.

Figure 3 shows the number of publications year wise from 2016 to 2020. In 2016, there were only 30 articles and it increased to 192 in the year 2020. The curve rise is increasing almost linear which indicates the publications are increasing except the fact that the increased percentage from 2019 to 2020 is 48.83 percent while previous years have more than 50 percent. The reason may be the affect in publications due to Covid cases.

Figure 4 is comparing the document counts per country or territory and the top ten countries in terms of publications has been shown in the graph. The United States tops the chart having 109 publications followed by the United Kingdom with 79 publications which implies that the United States does most of the research in the Intrusion Detection System of IoT. India is ranked third having 68 active publications in this field. Germany has the least publications in the top ten countries but still has a good number i.e., 17.

This section talks about the categorization of the publications. Table 2 illustrates that major portions that got published are in the form of articles acquiring 61.3 percent of all and followed by Conference Papers which is 33.7% and Review Materials which is 3.8%. Articles which are published in the form of Data Paper, Erratum and Short Survey has only 0.2% which shows research papers were published in the least manner for these three types.

Document Type	No. of Document	No. of Document (%)
Article	293	61.3
Book Chapter	3	0.6
Conference Paper	161	33.7
Data Paper	1	0.2
Erratum	1	0.2
Review	18	3.8
Short Survey	1	0.2

Table 2: Document Type research comparison

Source	Year					
	2016	2017	2018	2019	2020	Total
IEEE Access	1	6	7	20	47	81
Electronics Switzerland	0	1	0	1	18	20
Procedia Computer Science	0	1	4	2	9	16
ACM International Conference Proceeding Series	2	2	5	2	4	15
International Journal Of Innovative Technology And Exploring Engineering	0	0	0	10	0	10
International Journal Of Advanced Computer Science And Applications	0	0	1	3	5	9
Security And Communication Networks	0	1	3	2	3	9
International Journal Of Advanced Trends In Computer Science And Engineering	0	0	0	0	8	8
IEEE Communications Surveys And Tutorials	0	0	2	3	2	7
Future Generation Computer Systems	0	0	1	2	3	6
Future Internet	1	0	1	0	4	6
IEEE Transactions On Smart Grid	0	1	2	3		6
International Journal Of Electrical And Computer Engineering	0	0	1	0	4	5
Proceedings Of The ACM Conference On Computer And Communications Security	1	0	2	2	0	5
Advances In Intelligent Systems And Computing	3	0	0	0	1	4

Table 3: Comparison of sources per year

Table 3 gives a comparative view about productivity among various sources. Productivity refers to the number of publications it had every year or the frequency at which it publishes. It compares the publications of various sources in a year wise manner. This comparison is important as it not only helps the researchers from each source to compare and compete but it also helps them to stay focussed and diligent while doing the research of the detection and prevention systems of the cyber world. Table 3 shows IEEE source gave the major contribution in the number of publications with 81 number of published articles from 2016 to 2020 and is followed by the source, Electronics Switzerland. Top 15 sources in terms of publications have been selected against five consecutive years i.e., 2016 to 2020 and it has been noticed that maximum publications are from IEEE Access having 81 publications followed by Electronics Switzerland (20 publications) and Procedia Computer Science (16 publications).

Analysis:

Analysis technique has been discussed here, where we used VOSviewer tool to analyse the different relationships between the demo graphs, authors, citations and others. Though there are other tools for the network, VOSviewer has been preferred since it gives a standard visualisation for the bibliometric network. The types of visualisation analysis done are as follows:

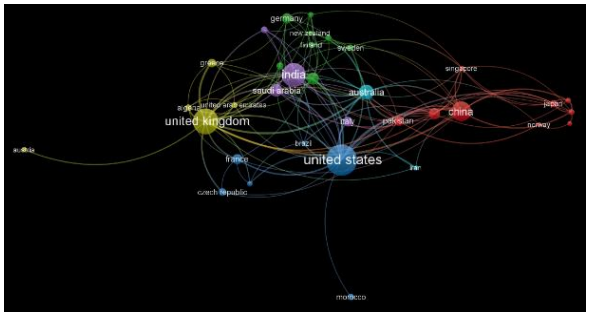

Figure 5: Country – co-authorship clusters

- Types of analysis: Co-authorship
- Unit of analysis: Countries
- Visualisation: Overlay Visualisation

Description: A co-author is any person who has made a significant contribution to a journal article. Here, different colours are used to depict co-authorship that the top countries (in terms of publications) share with other neighbours. Six clusters have been shown where blue colour is the cluster for US with others, Yellow for UK, Purple for India, Red for China, light blue for Australia. In the visualisation it is showing Co-authorship demographic wise and United States holds maximum of it. In the figure 5, the size of the clusters is varied according to the number of publications that a co-author has with respect to other countries, so, we can say for e.g., United States has maximum of co-authors that shares with its neighbouring countries like Australia, Morocco, Czech Republic, Brazil, France and Iran. Similarly, the next largest size is United Kingdom and shares its co-authors with neighbours like Greece, Arab, Austria and others.

- Types of analysis: Bibliographic-coupling
- Unit of analysis: Sources
- Visualisation: Density visualisation

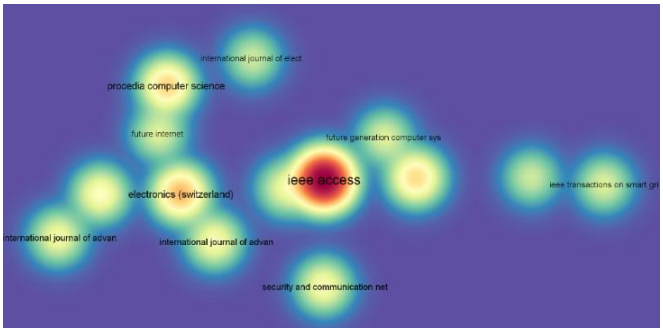

Figure 6: Source clusters

Description: In Bibliographic-coupling, two documents are bibliographically coupled if they both cite one or more documents in common. Heat map has been used here to explain the coupling bond, a heatmap is a diagrammatic representation of data that uses color-coding strategy to represent various values. Here, in the heat map, the deepest and largest maroon colour circle is for the IEEE access. So, it means maximum is from the Source, IEEE Access followed by Electronics Switzerland which means the articles in IEEE Access has more common sources with others.

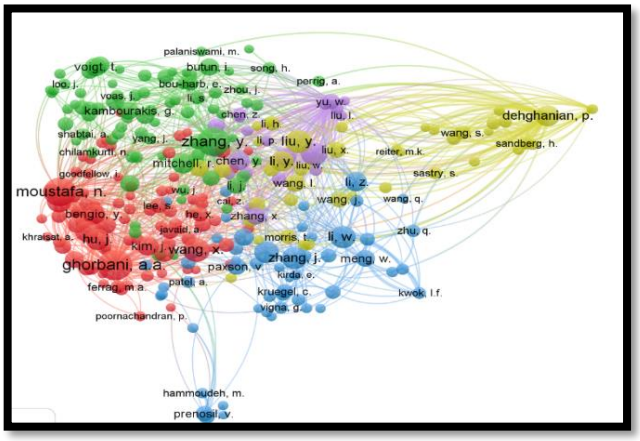

Figure 7: Co-cited author clusters

- Types of analysis: Co-citation
- Unit of analysis: Cited authors
- Visualisation: Network Visualisation

Description: Co-citation is defined as the frequency with which two documents are cited together by other documents. Here, it is inferred that each cited-author cites two or many documents in common. The initial and main source was from dehghanian, p. and is followed by other authors where any two documents are cited by other documents.

Limitations and suggestions:

This paper was limited to the publications based on Scopus database and for a stipulated period of 5 years i.e., 2016 to 2020. We have also limited to English language only with selected Keywords and didn't prefer other languages.

Future Analysis can be made on a more in-depth basis, probably the review can be made particularly on the latest Intrusion detection systems that is used in the industry and the gaps it is overcoming till date. Future reviews can have more analysis on the clusters of sources and suggest on the recovery plans like business continuity and disaster recovery planning, as well as for the prevention of Industry cyber-attacks. Such a narrow emphasis can aid in the synthesis of research findings and the dissemination of quality standards.

Reference:

[1] Otoum, Y. and Nayak, A., 2021. AS-IDS: Anomaly and Signature Based IDS for the Internet of Things. Journal of Network and Systems Management, 29(3).

[2] Elrawy, M., Awad, A. and Hamed, H., 2018. Intrusion detection systems for IoT-based smart environments: a survey. Journal of Cloud Computing, 7(1).

[3] Khraisat, A. and Alazab, A., 2021. A critical review of intrusion detection systems in the internet of things: techniques, deployment strategy, validation strategy, attacks, public datasets and challenges. Cybersecurity, 4(1).

[4] A. Abbasi, J. Wetzels, W. Bokslag, E. Zambon, S. Etalle, 2021. "On emulation-based network intrusion detection systems," in Research in attacks, Intrusions and Defenses: 17th International Symposium, RAID 2014, Gothenburg, Sweden, September 17–19, 2014. Proceedings, A. Stavrou, H. Bos, G. Portokalidis, Cham: Springer International Publishing, 2014, pp. 384–404 lenges.

[5] Okan CAN, Ozgur Koray SAHINGOZ, 2015. A Survey of Intrusion Detection Systems in Wireless Sensor Network, 6th International Conference on Modeling, Simulation, and Applied Optimization (ICMSAO).

[6] Zhang, Y., Li, P. and Wang, X., 2019. Intrusion Detection for IoT Based on Improved Genetic Algorithm and Deep Belief Network. IEEE Access, 7, pp.31711-31722.

[7] Aafer, Y., Du, W. and Yin, H., 2021. DroidAPIMiner: Mining API-Level Features for Robust Malware Detection in Android. [online] Eudl.eu. Available at: <https://eudl.eu/doi/10.1007/978-3-319-04283-1_6> [Accessed 30 December 2021].

[8] Lv, L., Wang, W., Zhang, Z. and Liu, X., 2020. A novel intrusion detection system based on an optimal hybrid kernel extreme learning machine. Knowledge-Based Systems, 195, p.105648.

[9] M. Bhargavi1, M.Nandha Kumar2, N. Venkata Meenakshi3, and N.Lasya, 2019. Intrusion Detection Techniques Used For Internet of Things, International Journal of Applied Engineering Research ISSN 0973-4562 Volume 14, Number 24.

[10] Docplayer.net. 2021. Development of Industrial Intrusion Detection and Monitoring Using Internet of Things P. Gokul Sai Sreeram 1, Chandra Mohan Reddy Sivappagari 2 - PDF Free Download. [online] Available at: <https://docplayer.net/3665575-Development-of-industrial-intrusion-detection-and-monitoring-using-internet-of-things-p-gokul-sai-sreeram-1-chandra-mohan-reddy-sivappagari-2.html> [Accessed 30 December 2021].

[11] Aburomman, A. and Reaz, M., 2017. A survey of intrusion detection systems based on ensemble and hybrid classifiers. Computers & Security, 65, pp.135-152.

[12] Zhang, Y., Li, P. and Wang, X., 2019. Intrusion Detection for IoT Based on Improved Genetic Algorithm and Deep Belief Network. IEEE Access, 7, pp.31711-31722.

[13] Benkhelifa, E., Welsh, T. and Hamouda, W., 2018. A Critical Review of Practices and Challenges in Intrusion Detection Systems for IoT: Toward Universal and Resilient Systems. IEEE Communications Surveys & Tutorials, 20(4), pp.3496-3509.

[14] Iman, A. and Ahmad, T., 2020. Data Reduction for Optimizing Feature Selection in Modeling Intrusion Detection System. International Journal of Intelligent Engineering and Systems, 13(6), pp.199-207.

[15] Mazini, M., Shirazi, B. and Mahdavi, I., 2019. Anomaly network-based intrusion detection system using a reliable hybrid artificial bee colony and AdaBoost algorithms. Journal of King Saud University - Computer and Information Sciences, 31(4), pp.541-5

CONASENSE2022 Keynote Speeches

Rute C. Sofia, Ramjee Prasad, Paulo Rufino

1. INTRODUCTION

The keynote session of CONASENSE2022 counted with four short talks provided by industrial experts from IBM, Eclipse Foundation, Infineon, and Unternehmer TUM.

Felizitas Müller, IBM, introduced the IBM Innovation Studio Munich as an innovation catalyzer, open to external entities.

Florian Küster, UnternehmerTUM, presented the large enterpreneurial hub of Munich, UnternehmerTUM and in particular the new MakerSpace, appealing to developers and startups, as well as entrepreneurs.

Gael Blondelle, Eclipse Foundation, addressed the relevancy of the use of open-source in future services, explaining the trade-offs.

Avik Santra, Infineon, presented an AI-based sensing approach for IoT building applications like lighting/HVAC controls, location-based services, and describe AI architectures for sensor data processing.

This part provides title, short abstract and short biography for the speakers. All presentations are available via the CONASENSE Website.

2. IBM INNOVATION STUDIO MUNICH, FELIZITAS MÜLLER, IBM

Bio: After studying business administration at the University of Applied Sciences in Constance, Felizitas, started her professional career in Strategic Sales at IBM Technology Support Services. In addition to her work at IBM, she completed a Master's degree in Strategic Sales Management at the ESB in Reutlingen. Since 2018, she is working as a project manager within the IBM Sustainability Software Business Unit responsible for software implementation projects. Since 2021, she is leading the "Center for AI" (research center for artificial intelligence between fortiss and IBM) from IBM-side.

3. UnternehmerTUM - We turn visions into value , Florian Küster, UnternehmerTUM MakerSpace

Abstract: Learn how the largest European entrepreneurship center supports start-ups from idea to IPO and how your team can benefit.

Florian is part of the management board at UnternehmerTUM where he is responsible for running the high-tech workshops of MakerSpace. In addition, Florian is Venture Director Robotics/AI at TUM Venture Labs, an initiative of TU Munich that helps transferring research to applicable products and services. Florian holds a M.Sc. and Diplome Grande Ecole in Management from ESCP Europe.

4. The EU platform for IoT and Edge must be open source! , Gaël Blondelle, Eclipse Foundation

Abstract: This talk will cover why Europe needs a widely adopted open source IoT and Edge platform. Of course, interoperability and scalability come to mind, but beyond that, digital sovereignty should also be a strong incentive. And finally, this is also an opportunity to show the EU leadership and to better disseminate our research efforts to industry players.

Gaël Blondelle joined the Eclipse Foundation in 2013 where he is now Managing Director of Eclipse Foundation Europe GmbH and VP, Ecosystem Development, of the Eclipse Foundation. Gaël joined the Eclipse Foundation with the desire to help organizations to work in open source as the best way to implement open innovation and open collaboration. Gaël has been involved in open source for more than 18 years in various roles, including as an entrepreneur, as a business developer, and as a manager of a large European research project aiming to create an open source ecosystem for industrial players.

5. AI based sensing for IoT Building Applications, Avik Santra, Infineon

Abstract - Sensing technologies play an important role in realizing smart, energy-efficient and sustainable buildings. Sensors of different modalities are part of building infrastructures, like lighting, HVAC and surveillance, that are

increasingly becoming connected. Data from such multi-modal IoT sensors can be used to realize new and improved building applications using advanced signal processing and machine learning. In this talk, we will cover topics, such as IoT building applications like lighting/HVAC controls, location-based services, and describe AI architectures for sensor data processing.

Avik Santra received his M.S. in Signal Processing (Hons) from Indian Institute of Science, Bangalore and Ph.D. in Electronics, Electrical and Informatics (summa cum laude) from FAU University of Erlangen. He is currently heading the advanced AI team developing signal processing and machine learning algorithms for industrial and consumer radars and depth sensors at Infineon, Neubiberg. Earlier in his career, he has worked as system engineer for LTE/4G modem at Broadcom Communications, and also has worked as research engineer developing cognitive radars at Airbus. He is co-author of the book titled 'Deep Learning Applications of Short-Range radars', published by Artech House and has filed more than 70 patents and published over 50 papers. He is a Senior Member of IEEE.

CONASENSE2022 Invited Talks – 6G Advanced Visions

Rute C. Sofia, Ramjee Prasad, Paulo Rufino

1. INTRODUCTION

The session of invited talks concerning 6G advanced visions aimed at bringing talks by senior experts in the context of fundamental aspects of 6G communications, or challenges that need to be addressed, when scaling services towards a 6G future.

Kwang-Chen Cheng, University of South Florida, USA (Best presentation award), debated on the use of Machine Learning to assist predictive radio resource use and coordination, alerting for the need to address trade-off aspects in uRLLC.

Jean-Paul Linnartz, Signify, Philips Lighting, debated on the possibility to deduce surrounding context at the network layers, including the PHY layer, and how relevant these aspects become, when considering 6G dense environments, in particular involving lighting infrastructures, where over 100 million digitally cloud-connected light points can be considered.

Fred Harris, University of San Diego, USA, brought a debate on the capabilities of channelizers involving multiple bandwidth and arbitrary frequencies, focusing on the possibility to reduce workload processing in orders of magnitude.

2. MACHINE LEARNING ENABLES RADIO RESOURCE UTILIZATION OF URLLC, KWAN-CHENG CHEN, UNIVERSITY OF SOUTH FLORIDA, USA

Abstract: Proactive open-loop communication in the virtual-cell network architecture emerges as a compelling approach to accomplish minimal end-to-end latency communication. To achieve ultra-reliability, predictive radio resource utilization is required without feedback control mechanism. In this talk, we introduce Machine Learning to facilitate predictive radio resource utilization by smartly taking advantage of delayed information, and effectively accomplish proactive communication. The trade-off between reliability and density of access points is also identified to guide the uRLLC system design.

Kwang-Cheng Chen has been a Professor at the Department of Electrical Engineering, University of South Florida, since 2016. From 1987 to 2016, Dr. Chen worked with SSE, Communications Satellite Corp., IBM Thomas J. Watson Research Center, National Tsing Hua University, HP Labs.,

and National Taiwan University in mobile communications and networks. He visited TU Delft (1998), Aalborg University (2008), Sungkyunkwan University (2013), and Massachusetts Institute of Technology (2012-2013, 2015-2016). He founded a wireless IC design company in 2001, which was acquired by MediaTek Inc. in 2004. He has been actively involving in the organization of various IEEE conferences and serving editorships with a few IEEE journals (most recently as a series editor on Data Science and AI for Communications in the IEEE Communications Magazine), together with various IEEE volunteer services to the IEEE, Communications Society, Vehicular Technology Society, and Signal Processing Society, such as founding the Technical Committee on Social Networks in the IEEE Communications Society. Dr. Chen also has contributed essential technology to various international standards, namely IEEE 802 wireless LANs, Bluetooth, LTE and LTE-A, 5G-NR, and ITU-T FG ML5G. He has authored and co-authored over 300 IEEE publications, 4 books published by Wiley and River (most recently, Artificial Intelligence in Wireless Robotics, 2019), and more than 23 granted US patents. Dr. Chen is an IEEE Fellow and has received several awards including 2011 IEEE COMSOC WTC Recognition Award, 2014 IEEE Jack Neubauer Memorial Award, 2014 IEEE COMSOC AP Outstanding Paper Award. Dr. Chen's current research interests include wireless networks, quantum communications and computing, cybersecurity, artificial intelligence and machine learning, IoT/CPS, and social networks.

3. REACHING OUT TO BILLIONS OF CLIENT DEVICES: CHALLENGES AND OPPORTUNITIES IN VERY DENSE WIRELESS NETWORKS, JEAN-PAUL LINNARTZ, SIGNIFY, PHILIPS LIGHTING

Abstract: To carry the predicted amounts of traffic from more users, more devices, each generating more bit/s than today, future generations of wireless networks need to be very dense (bit/s/m2) with access points at many locations. The (installation of the) infrastructure to support this can become a major cost factor in the economics of connectivity provision. But the value generated by such network goes beyond pure communication.

The physical layer of an advanced communication infrastructure lends itself well to functions, features and services beyond transporting bits. The estimation of the wireless channel response gives side information about the time of flight between the transmitter and receiver but also the excess distance of reflections gives information about objects and human that are in the propagation environment. Similarly, at the network layer, insights about activities in the environment can be deduced.

The use of a variety of radio and optical wavelength to leads to interesting propositions. But the convergence of communication, sensing and positioning not

only happening at the lower layers. At an infrastructure level, the presence of power and a high-speed data connection are critically important. The lighting infrastructure is rapidly expanding. With more than 100 Million of digitally cloud-connected light points, it forms (one of) the largest Internet of Things installations.

Jean-Paul Linnartz (Fellow, IEEE) currently is a Research Fellow with Signify (Philips Lighting) Research, and a Part-time Professor with TU Eindhoven, addressing Personalized Human Centric Lighting and optical wireless communication. His inventions led to more than 75 granted patent families and have been a basis for three ventures. From 1992 to 1995, he was an Assistant Professor with the University of California, Berkeley, CA, USA. In 1994, he was an Associate Professor with TU Delft. From 1988 to 1991, he was an Assistant Professor with the TU Delft. He was Senior Director with Philips Research, Eindhoven, The Netherlands, where he headed Security, Connectivity, and IC Design Research Groups.

4. POLYPHASE CHANNELIZERS IN MODERN COMMUNICATION SYSTEMS, FRED HARRIS, UNIVERSITY OF SAN DIEGO

Abstract: We learn to design filters and how to apply their use in the sampled data domain that satisfy their often-repeated constraint; Linear Time Invariant (LTI)! The body of tools with which we are armed in LTI is remarkable: transfer functions, impulse response, superposition, reciprocity, commutability, and so on. One's intuition and understanding about sampled data filters fail us when we change the playing field to Linear Time Varying (LTV). All our tools vanish! In this presentation we will explain how an LTI filter is changed to an LTV filter and the three reasons we choose to do this. They are to reduce cost, to improve performance, and have fun being creative. We take our audience on a trip through Alice's looking glass where things seem to operate backwards and accomplish what appears to be applied magic. We learn how to form an M-path polyphase analysis filter bank and its dual, an M-path polyphase synthesis filter bank. These are amazing processing engines that perform their processing tasks by using spectral aliasing, caused by a sample rate change, to move spectral bands between baseband and selected center frequencies and then separate these aliases by their distinct phase profiles. Remarkably, they accomplish this with a single prototype filter and an inverse FFT that performs channelization of all the filters in the filter bank. Strangely, the same filter is centered at multiple center frequencies simultaneously. Even more remarkable is the capabilities offered by a cascade of the analysis and synthesis filter banks. How about channelizers with multiple simultaneous bandwidths and arbitrary center frequencies. Would an order of magnitude reduction in processing workload be of interest to you? This presentation is low on math and high in comprehension.

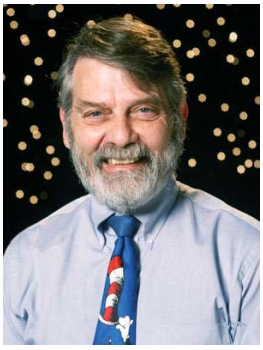

Professor harris is at the University of California San Diego where he teaches and conducts research on Digital Signal Processing and Communication Systems. He holds 40 patents on digital receiver and DSP technology and lectures throughout the world on DSP applications. He consults for organizations requiring high performance, cost effective DSP solutions.

He has written some 285 journal and conference papers, the most well-known being his) 1978 paper "On the use of Windows for Harmonic Analysis with the Discrete Fourier Transform" (9400 citations). He is the author of the book **Multirate Signal Processing for Communication Systems,** coauthor with Bernie Sklar of **Digital Communications** and has contributed to several other DSP books. His special areas include Polyphase Filter Banks, Physical Layer Modem design, Synchronizing Digital Modems and Spectral Estimation

He was the Technical and General Chair respectively of the 1990 and 1991 Asilomar Conference on Signals, Systems, and Computers, was Technical Chair of the 2003 Software Defined Radio Conference, of the WPMC-2006 Wireless Personal Multimedia Conference, of the DSP-2009, DSP-2013 Conferences and of the SDR-WinnComm 2015 Conference. He became a Fellow of the IEEE in 2003, cited for contributions of DSP to communications systems. In 2006 he received the Software Defined Radio Forum's "Industry Achievement Award". He received the DSP-2018 conference's commemorative plaque with the citation: *We wish to recognize and pay tribute to fred harris for his pioneering contributions to digital signal processing algorithmic design and implementation, and his visionary and distinguished service to the Signal Processing Community.*

The spelling of his name with all lower case letters is a source of distress for typists and spell checkers. A child at heart, he collects toy trains, old slide-rules, and gyroscopes.

CONASENSE2022 Invited Talks – 6G Business Models, Use-cases and Sustainability

Rute C. Sofia, Ramjee Prasad, Paulo Rufino

1. INTRODUCTION

The session of invited talks focused on 6G business models, use-cases and design aspects relevant to achieve sustainability.

Milica Pejanović-Djurišić, University of Montenegro, addressed cybersecurity challenges in 6G, taking into consideration the CONASENSE interdisciplinary approach, and the boundaries created in terms of regulation, data privacy, and security policies towards AI, heterogeneous wireless networks, etc.

Hoomayoun Nikookar, Defence Academy, Netherlands addressed green radio communication design for OFDM systems, explaining how such design can be formulated as an optimization problem.

Vladimir Poulkov, University of Sofia, Bulgaria, provided a use-case for the design and implementation of a holographic system.

Martjin Kuipers, Lusíada University/INOV-INESC, Portugal, addressed the need to rethink the 6G business models having as key technological aspect virtualization and as such, to re-think the 6G value-chain.

Per Valter, Aarhus University,

Peter Lindgren, CGC, Aarhus University, closed the session with a presentation on Green Business Models, in particular alerting to the need to integrate novel and more advanced business model security approaches, technologies and understanding. The talk brought the vision to the power of business models combined with 6G and wide-area wireless technologies in bringing societal benefits.

2. CYBERSECURITY IN THE ERA OF NEXT GENERATION WIRELESS NETWORKS, MILICA PEJANOVIĆ-DJURIŠIĆ, UNIVERSITY OF MONTENEGRO

Presentation

Milica Pejanović-Djurišić is full professor in Telecommunications and Wireless Communications at the Faculty of Electrical Engineering, University of Montenegro, founder and director of its Research Centre for ICT. Prof. Pejanović-Djurišić has been cooperating with numerous universities, research centers, international and think tank organizations worldwide as a visiting researcher and lecturer. In her research work she is focused on

various aspects of wireless communications and networks, where she has achieved notable results that were published in several hundred scientific papers in international journals and international conferences, scientific and professional papers in domestic journals and conferences, as well as in several books and other publications.

Abstract: Proactive open-loop communication in the virtual-cell network architecture emerges as a compelling approach to accomplish minimal end-to-end latency communication. To achieve ultra-reliability, predictive radio resource utilization is required without feedback control mechanism. In this talk, we introduce Machine Learning to facilitate predictive radio resource utilization by smartly taking advantage of delayed information, and effectively accomplish proactive communication. The trade-off between reliability and density of access points is also identified to guide the uRLLC system design.

Kwang-Cheng Chen has been a Professor at the Department of Electrical Engineering, University of South Florida, since 2016. From 1987 to 2016, Dr. Chen worked with SSE, Communications Satellite Corp., IBM Thomas J. Watson Research Center, National Tsing Hua University, HP Labs., and National Taiwan University in mobile communications and networks. He visited TU Delft (1998), Aalborg University (2008), Sungkyunkwan University (2013), and Massachusetts Institute of Technology (2012-2013, 2015-2016). He founded a wireless IC design company in 2001, which was acquired by MediaTek Inc. in 2004. He has been actively involving in the organization of various IEEE conferences and serving editorships with a few IEEE journals (most recently as a series editor on Data Science and AI for Communications in the IEEE Communications Magazine), together with various IEEE volunteer services to the IEEE, Communications Society, Vehicular Technology Society, and Signal Processing Society, such as founding the Technical Committee on Social Networks in the IEEE Communications Society. Dr. Chen also has contributed essential technology to various international standards, namely IEEE 802 wireless LANs, Bluetooth, LTE and LTE-A, 5G-NR, and ITU-T FG ML5G. He has authored and co-authored over 300 IEEE publications, 4 books published by Wiley and River (most recently, Artificial Intelligence in Wireless Robotics, 2019), and more than 23 granted US patents. Dr. Chen is an IEEE Fellow and has received several awards including 2011 IEEE COMSOC WTC Recognition Award, 2014 IEEE Jack Neubauer Memorial Award, 2014 IEEE COMSOC AP Outstanding Paper Award. Dr. Chen's current research interests include wireless networks, quantum communications and computing, cybersecurity, artificial intelligence and machine learning, IoT/CPS, and social networks.

3. GREEN OFDM TRANSMISSION: AN OPTIMAL SIGNAL DESIGN APPROACH, HOOMAYOUN NIKOOKAR, DEFENCE ACADEMY, NETHERLANDS

Presentation

Abstract: In this talk a green Binary Phase Shift Keying (BPSK) modulated Orthogonal Frequency Division Multiplexing (OFDM) transmission is addressed by designing an optimal signal for the minimum average transmit power taking into account the characteristic of the transmit antenna. The optimal waveform is obtained by applying the Calculus of Variations and for the best performance in the BPSK data detection. The optimal waveform is compared with the conventional rectangular and linear ramp waveforms. Results show the transmission greenness of the proposed technique in shaping the signal.

Homayoun Nikookar received his Ph.D. in Electrical Engineering from Delft University of Technology in 1995. He is an Associate Professor at the Faculty of Military Sciences of the Netherlands Defence Academy. Dr Nikookar has published 150 papers in the peer reviewed international technical journals and conferences, 15 book chapters and is author of two books: Introduction to Ultra-Wideband for Wireless Communications, Springer, 2009 and Wavelet Radio: Adaptive and Reconfigurable Wireless Systems based on Wavelets , Cambridge University Press, 2013.

4. CHALLENGES IN THE DESIGN OF A HOLOGRAPHIC TELEPRESENCE SYSTEM – THE CURRENT OUTCOMES FROM THE IMPLEMENTATION OF A USE CASE SCENARIO, VLADIMIR POULKOV,TECHNICAL UNIVERSITY OF SOFIA, BULGARIA

Presentation

Abstract: With the emergence of 6G systems, a whole new range of novel use cases, services and key value and performance indicators, come into play. Examples are the remote interactions between human beings that become more and more part of our everyday living. The current methods are becoming obsolete, as new forms of interactions are being developed leading to a true immersion into a distant environment. Based on the current-state-of the art of holographic telepresence systems some general trends for their future development are identified. The talk focuses on the vision for the research and design for human-centered immersive communications and points out some important performance indicators. As an practical example the challenges, current status, and outcomes from the development of a specific use case for an advanced holographic telepresence system in the framework of the “HOLOTWIN” project, funded by the ministry of Science and Education of Bulgaria, will be considered.

Vladimir Poulkov has received the M.Sc. and Ph.D. degrees from the Technical University of Sofia (TUS), Sofia, Bulgaria. He has more than 30 years of teaching, research, and industrial experience in the field of telecommunications. He has successfully managed numerous industrial, engineering, R&D and educational projects. He has been Dean of the Faculty of the Telecommunications at TUS and Vice Chairman of the General Assembly of the European Telecommunications Standardization Institute (ETSI). Currently he is Head of the Tele infrastructure R&D Laboratory at TUS and Chairman of the Cluster for Digital Transformation and Innovation, Bulgaria. He is Fellow of the European Alliance for Innovation; Senior IEEE Member. He has authored many scientific publications and is tutoring BSc, MSc, and PhD courses in the field of Information Transmission Theory and Wireless Access Networks.

5. 6G - AN ECOSYSTEM FOR TECHNOLOGY AND MARKET OPPORTUNITIES (PDF), MARTJIN KUIPERS,UNIVERSITY LUSIADA/ INESC-INOV, PORTUGAL

Presentation

Abstract: According to National Geographic, an ecosystem is a geographic area where plants, animals, and other organisms, as well as weather and landscape, work together to form a bubble of life. 6G is an ecosystem where technologies, networks, operators and users work together to form a global interconnected network of systems. No longer will there be a particular feature, such as reduced latency, increased datarates, etc, that will drive the systems. Instead, the ecosystem will house different creatures at the same time. New technologies can be quickly deployed and new markets can be targetted without huge investments in updating the entire network core. 6G is going to be exciting for academics, businesses and foremost, end-users.

Berend Willem Martijn Kuipers received a B.Sc. from the Rijswijk University of Technology, the Netherlands, in the area of computer science in 1996. In 1999, he received his M.Sc. in the area of telecommunications from the Delft University of Technology in the Netherlands. He received his Ph.D. in the area of telecommunications from Aalborg University, Denmark in 2005. During his Ph.D. he has developed a novel multicarrier access scheme for 4G systems. Currently he is employed by INOV-INESC Inovação in Lisbon, where is involved in the

application of artificial intelligence algorithms for data analysis, such as clustering algorithms, seasonal ARIMA forecasting and machine learning. He has supervised more than 30 M.Sc. students and was involved with courses on telecommunications and computer networks, artificial intelligence and data structures. He has taken part in National and European projects, like Monitor-BT,E-Balance, TRILLION, ROCSAFE, FASTER e PERSONA and has publications in the area of channel modelling, access techniques and IP networking.

He is also professor and coordinator at the bachelor's degree in Computer Science and Engineering at the Lusíada University of Lisbon, where he is responsible for the courses on artificial intelligence, data structures and computer networking.

6. GREEN BUSINESS MODEL 6G SERVICES: A NEW PERSPECTIVE WITH INTERNET OF THINGS CONNECTED GREEN BUSINESS MODELS EMPOWERED WITH ARTIFICIAL INTELLIGENCE, PER VALTER, AARHUS UNIVERSITY

Abstract: In an increasingly more interconnected world, 5G networks have delivered sufficient results on dimensions such as connectivity, speed, latency, and reliability for most corporations' applications and services.

It's time to investigate how 6G Services could create additional value for c corporations and society. This presentation explores the potential value of Green Business Model 6G Services, where Green Business Models are connected with Internet of Things and empowered with Artificial Intelligence.

Per Valter is Associate Professor of innovation and green business development. Where his main research field areas are Innovation, Green Business Development, Digitization of Business Models and Entrepreneurship. He has successfully been founding serval startup companies and grown them to exit's stage and was awarded "Børsen Gazelle" in 2013, 2014, 2019, 2020 for creating and leading one among the fastest growing companies in Denmark, in addition to these business achievements he is a Graduate in Computer Science and holds an Executive MBA - Master in Management of Technology and an MSc in Business and Management Research at Henley University of Reading and a Ph.D. degree in Social Sciences and Business from Aarhus University. He is an experience teacher on bachelor and master level in addition to supervising.

His research interests are Innovation, Green Business Development, Digitization of Business Models and Entrepreneurship.

7. GREEN BUSINESS MODELS AND USE-CASES FOR 6G, PETER LINDGREN, VICE-PRESIDENT CGC, AARHUS UNIVERSITY, DENMARK

Presentation

Abstract: In the last few years businesses have been motivated and pushed by governments and global society on innovating and developing Green Business Models. However, Reconfiguring, designing and developing green business models to become efficient and valuing Green Business Models have shown to be much more complex than expected due to several barriers and challenges called Green Walls. It also includes balancing monetary and non-monetary value formulas of business models. Not just for the single business – but for businesses in their entire value network. Green Business Models and Green business Model Innovation calls therefore for new and more advanced business model security approaches, technologies and understanding. Previous business model innovation practice and systems cannot offer these solutions – but business models combined with 6G and wide-area wireless technologies give hope to business and societies that this finally can be solved.

Peter Lindgren holds a full Professorship in Multi business model and Technology innovation at Aarhus University, Denmark – Business development and technology innovation and is Vice President of CTIF Global Capsule (CGC) www.ctifglobalcapsule.org. He is founder of the Multi Business Model Innovation Approach. He is Director of CTIF Global Capsule/MBIT Research Center at Aarhus University – Business Development and Technology and is member of Research Committee at Aarhus University – BSS. He is cofounder of five start-up businesses amongst others - www.thebeebusiness.com , www.thedigibusiness.com, www.vdmbee.com .

CONASENSE2022 Invited Talks – IoT Cooperation Opportunities Towards Brazil

Rute C. Sofia, Ramjee Prasad, Paulo Rufino

1. INTRODUCTION

In this CONASENSE session, three Brazilian representatives of relevant IoT entities were invited to debate on current cooperation possibilities.

The session started with a talk by Rodolfo Azevedo, President of the Brazilian university UNIVESP, who explained how UNIVESP is addressing remote teaching in large scale, thus bringing a relevant example of a potential 6G use-case (large-scale immersive education environments) to discussion and alerting for challenges that need to be addressed.

Sergio Gaulindo, president of BrassCom, introduced the initiative and efforts being developed towards a large-scale use of IoT.

Paulo Spacca, president of the Brazilian Association of IoT (ABINC), introduced the development of IoT in Brazil, and key areas being addressed.

2. INFORMATION TECHNOLOGY COURSES IN LARGE SCALE TO SUPPLY NATIONAL DEMANDS, RODOLFO AZEVEDO, PRESIDENT OF UNIVESP, BRAZIL

PRESENTATION

Abstract: According to official statistics, Brazil lacks more than 40k new IT professionals every year. From this number, 26k new jobs are created in São Paulo. In this presentation, we will show UNIVESP's approach to provide bachelor's degree to thousands of students around the state through distance learning. Currently, we have 14k computing students, and we plan to reach 20k by the end of 2022, when we will start graduating in large scale. We will also show how we organized the curriculum of 3 computing courses that share a common core and how we have been partnering with companies to bring the students to market.

Bio: Rodolfo Azevedo is President of the São Paulo Virtual University (UNIVESP) since 2019 and full professor at University of Campinas (UNICAMP). His main research interests are in Computer Architecture and Technology for Teaching where he advised more than 40 MsC and PhD students and received 4 best papers in conferences. He was member of the Brazilian Computing Society Council, and Director of the Institute of Computing at Unicamp from 2017 to 2019. He is member of IEEE, ACM and SBC.

3. INTRODUCTION TO BRASSCOM IOT AND EDUCATIONAL INITIATIVES, SERGIO PAULO GAULINDO, PRESIDENT OF BRASSCOM, BRAZIL

Sergio Paulo Gallindo, CEO of Brasscom, Companies' Association of Information and Communication Technology (ICT) and Digital Technologies, since 2014, works in conception and fostering public policy aimed at competitiveness, digital transformation, education, and innovation.

Sergio Paulo is Lawyer and Engineer; Master's in Political and Economic Law by Mackenzie Presbyterian University; M.Sc. in Computer Science by The University of Texas at Austin, under a Fulbright scholarship; Bachelor's in Law by USP, University of São Paulo; Bachelor's in Electronic Engineering by UFRJ, Federal University of Rio de Janeiro; and lecturer of Tax and Digital Economy in the Tax Management MBA at USP/ESALQ.

Member of the Management Committee of ICP-Brasil, under Brazilian Presidency; member of several advisory boards in the Ministry of Science, Technology and Innovation; member of the Advisory Board of the Social Opportunity Institute – IOS; member of the Certification Board of Vanzolini Foundation; former associated with the Harvard Business School Angels of Brazil; former member of The Economic and Social Development Council to the President of Brazil. Country Manager of BT (British Telecom) Brazil from 2009 to 2014 and Vice-President of Nortel Brazil.

4. IOT IN BRAZIL, UNDERSTANDING CHALLENGES AND OPPORTUNITIES, PAULO JOSÉ SPACCAQUERCHE, PRESIDENT OF ABINC (BRAZILIAN ASSOCIATION OF IOT)

Paulo Jose Spacca is currently the President of ABINC, the Brazilian Association of IoT. He has more than 40 years of professional experience working closely with leading technology companies such as IBM and SAP, as well as banks and retail companies. He is responsible for the implementation in Brazil of American companies such as Sybase, Netscape, Peoplesoft, Quest and others. Excellent relationship with the main executives of national and multinational companies, mainly in the Finance, Public Services, Media, and Government sectors. He was also a professor at IBM for the sales courses.

CONASENSE2022 Project Session – Next Generation IoT Flagship Projects

Rute C. Sofia, Ramjee Prasad, Paulo Rufino

1. INTRODUCTION

The CONASENSE2022 project session counted with presentations from 7 European flagship projects that are focusing their research efforts in the application of Edge computing and IoT, towards the European Sustainable Development Goals. Each of the projects brings use-cases applied to different vertical domains, e.g., manufacturing, energy, health, society, logistics, mobility. The aim of the session was to give awareness into the latest European research developments in this context, promoting discussion towards challenges faced by the next (6G) generation of IoT services and applications.

2. ASSIST-IOT, IGNACIO LACALLE UBELA, UNIVERSIDAD POLITECNICA DI VALENCIA

Presentation

Abstract: ASSIST-IoT is designing and developing an innovative reference architecture, envisioned as a decentralized ecosystem, where intelligence is distributed among nodes by implementing AI/ML close to data generation and actuation, and hyperconnecting nodes, in the edge-cloud continuum, over softwarized smart network. This is supported by several pillars: (i) innovative IoT architecture, to adapt to the NGI paradigm, including intelligence, security and privacy by design; (ii) moving from semantic interoperability to semantically-enabled cross-platform, cross-domain data transactions, within decentralized governance; (iii) development and integration of innovative devices, supporting context-aware computing; (iv) introduction of self-* mechanisms, supporting self-awareness and (semi-)autonomous behaviours across IoT deployments, and (v) Tactile Internet support for latency applications, like AR/VR/MR, and human-centric interaction with IoT components. Finally, to validate research results, and developed solutions, and to ensure their wide applicability, extended pilot deployments with strong end-user participation are taking place in: (i) port automation; (ii) smart safety of workers, and (iii) cohesive vehicle monitoring and diagnostics, bringing about domain-agnostic aspect of the approach. In this talk, we will showcase the main relevant aspects of the project vís-a-vís Next Generation IoT features, will outline the demonstrator pilots and will provide information about our Open Call for funding to individual entrepreneurs like you!

Mr. Ignacio Lacalle (male) is a researcher working at the Universitat Politècnica de València (UPV), a public University at the South-East of Spain. Ignacio is a Telecommunications Engineer (2014) from UPV and is currently working on his PhD. The expertise of Ignacio is mainly rooted on Internet of Things field, having participated in 6 research projects related to interoperability, added value services, data processing and manageability, among others. Ignacio has performed various roles in those projects (ranging from Developer to Community Manager and Project Manager). In addition, most of those projects were focused on applying IoT-related innovations, in particular, to the field of maritime ports, one of the preferred verticals of the research group.

3. INTELLIOT: INTELLIGENT IOT ENVIRONMENTS, ARNE BRÖRING, SIEMENS AG

Presentation

Abstract: Traditional IoT setups are cloud-centric and typically focused around a centralized IoT platform to which data is uploaded for further processing. Next generation IoT applications are incorporating technologies such as artificial intelligence, augmented reality, and distributed ledgers to realize semi-autonomous behaviour of vehicles, guidance for human users, and machine-to-machine interactions in a trustworthy manner. Such applications require more dynamic IoT environments, which can operate locally without the necessity to communicate with the Cloud. In this talk, we describe three use cases of next generation IoT applications and highlight associated challenges for future research. Based on this, we present the IntellIoT framework that comprises the required components to address the identified challenges.

Arne Bröring is a senior researcher at Siemens' corporate research labs in Munich (DE) since 2014. Previously, he has worked for the Environmental Systems Research Institute (ESRI) in Zurich (CH), the 52°North initiative (DE), the University of Münster (DE), and received his PhD in 2012 from the University of Twente (NL). His research interests lay in the area of pervasive systems and particularly the internet of things, semantic web technologies, the sensor web, participatory sensing, as well as mobile and location-based services. He has been the Scientific and Technical Coordinator of the project IntellIoT (http://intelliot.eu), as well as BIG IoT, and contributed to numerous other international innovation and research projects. His research has contributed to over 90 publications in refereed journals, conferences, and workshops resulting in an H-Index of 28.

4. iNGENIOUS: Next-Generation IoT Solutions for the Universal Supply Chain , Erin Seder, Nextworks

Presentation

Abstract: iNGENIOUS (Next-GENeration IoT sOlutions for the Universal Supply chain, https://ingenious-iot.eu/web/) aims to build an holistic architecture for the next-generation supply chain by exploiting the wealth of data that the Internet of Things (IoT) can provide. In practice, iNGENIOUS tackles the digitalisation of supply chain management and aims at optimizing the various logistics processes involved, including sourcing, procurement, conversion, production, and management operations.

Relevant use cases start right in the factories, where automated robots increase efficiency by working fully autonomously or by assisting human workers. To innovate logistics, IoT sensors shall monitor the safety-critical parts of land-based transport vehicles, thereby enabling longer maintenance intervals to reduce costs and ensuring reliable detection of defects that could otherwise lead to accidents. By integrating network technologies ranging from local-area wireless networks all the way up to satellites, the project aims to enable comprehensive tracking of assets in shipping containers across land and sea. iNGENIOUS also seeks to develop tools for optimising container loading and unloading in ports, as well as to exploit 5G networks to remotely control vehicles in situations, where humans would be in danger or exposed to adverse environmental conditions.

IoT data is centric in iNGENIOUS, where an interoperability layer, made by the integration of a data virtualization platform with several Distributed Ledger technologies enable the coexistence of heterogeneous Machine-to-Machine IoT platforms on the one hand for data collection and distribution, and AI/ML techniques on the other for data processing and service optimization.

Bio: Dr. Seder graduated with a PhD in Physics from the University of Connecticut in 2013, followed by postdoctoral work at Jefferson National Lab (USA) and CERN (Switzerland). Her recent research activities have been focused in the fields of IoT and AI/ML in Industry 4.0. Dr. Seder has been active in Horizon 2020 projects including 5G-TRANSFORMER, COREALIS, 5G-EVE, EFPF, 5GZORRO, iNGENIOUS, and HEXA-X. She is currently in the R&D division at Nextworks Srl in the role of system and software engineer.

5. TERMINET: NEXT GENERATION SMART INTERCONNECTED IOT', PANAGIOTIS SARIAGIANNIDIS, UNIVERSITY WESTERN MACEDONIA

Presentation

Abstract: The vision of TERMINET is to provide a flexible, open, and decentralised next generation IoT reference architecture based on cutting-edge technologies such as software-defined networking, multiple-access edge computing, and virtualisation for new real-time capable solutions. This goal will be achieved by enabling secure and privacy-preserving IoT services, user-aware solutions, semi-autonomous devices, and self-aware mechanisms, frameworks, and schemes, supported by distributed AI and new intelligent IoT devices within a virtualized edge-platform-cloud environment. TERMINET envisages six realistic, compelling, and complementary use cases in IoT domains such as energy, smart buildings, smart farming, healthcare, and manufacturing.

Prof. Panagiotis Sarigiannidis is the Director of the ITHACA lab (https://ithaca.ece.uowm.gr/), co-founder of the 1st spin-off of the University of Western Macedonia: MetaMind Innovations P.C. (https://metamind.gr), and Associate Professor in the Department of Electrical and Computer Engineering in the University of Western Macedonia, Kozani, Greece. He received the B.Sc. and Ph.D. degrees in computer science from the Aristotle University of Thessaloniki, Thessaloniki, Greece, in 2001 and 2007, respectively. He has published over 250 papers in international journals, conferences and book chapters, including IEEE Communications Surveys and Tutorials, IEEE Transactions on Communications, IEEE Internet of Things, IEEE Transactions on Broadcasting, IEEE Systems Journal, IEEE Wireless Communications Magazine, IEEE Open Journal of the Communications Society, IEEE/OSA Journal of Lightwave Technology, IEEE Transactions on Industrial Informatics, IEEE Access, and Computer Networks. He has been involved in several national, European and international projects. He is currently the project coordinator of three H2020 projects, namely a) H2020-DS-SC7-2017 (DS-07-2017), SPEAR: Secure and PrivatE smArt gRid, b) H2020-LC-SC3-EE-2020-1 (LC-SC3-EC-4-2020), EVIDENT: bEhaVioral Insgihts anD Effective eNergy policy acTions, and c) H2020-ICT-2020-1 (ICT-56-2020), TERMINET: nexT gEneRation sMart INterconnectEd ioT, while he coordinates the Operational Program MARS: sMart fArming with dRoneS (Competitiveness, Entrepreneurship, and Innovation) and the Erasmus+ KA2 ARRANGE-ICT: SmartROOT: Smart faRming innOvatiOn

Training. He also serves as a principal investigator in the H2020-SU-DS-2018 (SU-DS04-2018), SDN-microSENSE: SDN-microgrid reSilient Electrical eNergy SystEm and in three Erasmus+ KA2: a) ARRANGE-ICT: pArtneRship foR AddressiNG mEgatrends in ICT, b) JAUNTY: Joint undergAduate coUrses for smart eNergy managemenT sYstems, and c) STRONG: advanced firST RespONders traininG (Cooperation for Innovation and the Exchange of Good Practices). His research interests include telecommunication networks, internet of things and network security. He is an IEEE member and participates in the Editorial Boards of various journals, including International Journal of Communication Systems and EURASIP Journal on Wireless Communications and Networking.

Anna Triantafyllou was born in Ioannina, Greece. She received the Diploma degree (5 years) from the Dept. of Informatics and Telecommunications Eng., University of Western Macedonia, Greece, in 2017. She received a Graduation Excellence Award from the Technical Chamber of Greece in 2018. She is a Ph.D. student in the Dept of Electrical and Computer Engineering, University of Western Macedonia, Greece. Her main research interests are in the area of internet of things, communication protocols, and LoRaWAN. Up until now, she has published 11 papers in international journals and conferences, including Wireless communications and mobile computing, MDPI Information, Computer Networks and IEEE Open Journal of the Communications Society. Recently she received the award of "Best Communication Systems Paper" in the 9th International Conference on Modern Circuits and Systems Technologies (MOCAST) on Electronics and Communications 2020. Ms Triantafyllou is also a Research Associate in national and European funded research projects in the same University. More specifically, she was involved in the Operational Program DIAS: Drone Innovation in saffron Agriculture Surveillance (Competitiveness, Entrepreneurship, and Innovation). Currently she participates in the following research projects: the H2020-SU-DS-2018 (SU-DS04-2018-2020), SDN-microSENSE: SDN-microgrid reSilient Electrical eNergy SystEm, the H2020-ICT-2018-20 (ICT-56-2020) TERMINET: nexT gEneRation sMart INterconnectEd ioT and the H2020-LC-SC3-2018-2019-2020 (LC-SC3-EC-4-2020) EVIDENT: bEhaVioral Insgihts anD Effective eNergy policy acTions.

6. VEDLIoT - Very Efficient Deep Learning in IoT, Jens Hagemeyer, Bielefeld University

Presentation

Abstract: The VEDLIoT project targets the development of energy-efficient Deep Learning for distributed AIoT applications. A holistic approach is used to optimize algorithms while also dealing with safety and security challenges. The approach is based on a modular and scalable cognitive IoT hardware platform. Using modular microserver technology enables the user to configure the hardware to satisfy a wide range of applications.

VEDLIoT offers a complete design flow for Next-Generation IoT devices required for collaboratively solving complex Deep Learning applications across distributed systems. The methods are tested on various use-cases ranging from Smart Home to Automotive and Industrial IoT appliances.

Jens Hagemeyer is research associate at Bielefeld University, within the group Cognitronics and Sensor Systems, as part of the technical faculty.

His research interests are in the area of heterogeneous and reconfigurable computing, applied to various applications in the area of cloud and edge computing. He is also co-founder of ParaXent GmbH, a spin-off established in 2018 which targets the development and efficient utilization of heterogenous hardware accelerators. With his team, he is continuously involved in several international research projects and acts as coordinator of the H2020 project VEDLIoT, dealing with the integration of IoT and deep learning.

7. IoT-NGIN Project Presentation, Jonathan Klimt, RWTH, Aachen

Presentation

Abstract: This talk shall provide an overview on the ICT-56 IoT-NGIN project.

Jonathan Klimt, M.Sc. has studied Electrical Engineering at the the Technical University Munich (TUM) and the RWTH-Aachen with a focus on computer engineering and embedded systems. He is currently working as a researcher at the Institute for Automation of Complex Power Systems at RWTH-Aachen and is researching on Unikernels, Cloud and High-Performance Computing, Embedded Systems and Programming Languages. In the IoT-NGIN project, he is pushing the use of Unikernels in the cloud and edge-clouds further, enhancing performance and security in the IoT backend landscape.

8. EFPF, USMAN WAJID, INFORMATION CATALYST

Presentation

Abstract: EFPF is an EC H2020 funded innovation project that aims to establish a federated digital platform for connected smart factories. The federated platform developed in the project interlinks different stakeholders of the digital manufacturing domain and enables users to utilise innovative functionalities, experiment with disruptive approaches and develop custom Industry4.0 solutions to maximise connectivity, interoperability and efficiency across the supply chains. At the core of EFPF platform is an interoperability mechanism called 'Data Spine' that provides open interfaces to support the integration of distributed systems and platforms with their toolset and services. Through the Data Spine based connectivity and interoperability, the EFPF platform aims to realise and support a connected and smart ecosystem of the future. To support the ecosystem development, the project has already provided 2.5million Euros as cascade funding to 20 experiments that will validate EFPF solutions in different industrial scenarios or add new functionalities in the EFPF federation. Moreover, the EFPF platform is now open for access and experimentation. For further details, please consult the project website: https://www.efpf.org/ or drop a line to: info@ef-foundation.com

Dr Usman WAJID is a Technical Director at Information Catalyst (ICE), an innovative ICT SME operating in the domains of Software, Data, and Services with specialism in Process Engineering and Data Analytics.

Usman is increasingly interested in the development and promotion of innovative solutions - with modern views on data capabilities in business transformation - bringing together cutting-edge research and innovation from Industry4.0, IoT, Big Data and AI disciplines into user centric solutions. At ICE, he is also responsible for initiating and leading research & innovation projects in diverse industrial sectors such as manufacturing, eHealth, Big Data and Cybersecurity. Usman's successful collaborations with research and industrial partners have resulted in a number of European funded projects (such as EFPF) in the areas of digital manufacturing, ehealth and big data analytics. With proven experience of managing digital transformation projects and solution development life-cycle in multiple domains, Usman actively collaborates with research, industry and standardisation bodies to develop innovation roadmaps and align individual agendas with research and innovation frameworks.

Overview on the EU-IoT Hackathon

Rute C. Sofia

Rute C. Sofia, fortiss GmbH, Munich, Germany. *sofia@fortiss.org*

Abstract

The EU-IoT/EFPF Hackathon was a collaborative event jointly organised by the Cooperation and Support Action EU-IoT and the Horizon 2020 Research and Innovation project EFPF. Full information on the event is available via the Hackathon DevPost platform, https://eu-iot-hackathon.devpost.com/.

The overall operational guidelines and rules of the Hackathon are described in a specific document available via the Hackathon GitLab.

The EU-IoT/EFPF Hackathon has been developed to encourage the Next Generation IoT (NGIoT) community to interact via the development of i) technical projects (based on open-source tooling and tooling suggested by next generation flagship projects); ii) training tools; iii) business ideas based on the specific domain challenges proposed and which are aligned with the CSA EU-IoT scope areas: tactile Internet/Human IoT interfaces; far Edge; near Edge; infrastructure; data spaces.

In the Hackathon EFPF had a dedicated challenge domain focused on manufacturing focused on Manufacturing.

The Hackathon took place from the 27th until the 28th of June 2022, in Munich (Germany) co-located to the IEEE co-sponsored symposium CONASENSE2022. Hybrid support has also been provided to teams in Brazil, via the support of the university UNIVESP.

Contents

1. INTRODUCTION

The EU-IoT/EFPF Hackathon was a collaborative event jointly organised by the Cooperation and Support Action EU-IoT and the Horizon 2020 Research and Innovation project EFPF. Full information on the event is available via the Hackathon DevPost platform, https://eu-iot-hackathon.devpost.com/ and also via the EFPF Deliverable D8.5 "Management and Support for Experimentation on the EFPF Platform". This section provides a summary of the content provided in the EFPF Deliverable D8.5.

The overall operational guidelines and rules of the Hackathon are described in a specific document available via the Hackathon GitLab.

The EU-IoT/EFPF Hackathon has been developed to encourage the Next Generation IoT (NGIoT) community to interact via the development of i) technical projects (based on open-source tooling and tooling suggested by next generation flagship projects); ii) training tools; iii) business ideas based on the specific domain challenges proposed and which are aligned with the Cooperation and Support Action EU-IoT scope areas: tactile Internet/Human IoT interfaces; far Edge; near Edge; infrastructure; data spaces.

In the Hackathon, the project EFPF had a dedicated challenge domain focused on manufacturing focused on Manufacturing.

The Hackathon took place from the 27th until the 28th of June 2022, in Munich (Germany) co-located to the IEEE co-sponsored symposium CONASENSE2022. Hybrid support has also been provided to teams in Brazil, via the support of the university UNIVESP.

The teams developed their projects during the Hackathon and had to pitch their projects on the Hackathon pitching session to be held in Munich, 28th of June. The presentations were prepared to last 10 minutes, based on the proposed templates, available via GitLab.

All winning the projects are uploaded to the Hackathon GitLab repository. The contents of this repository shall be publicly available and shall last beyond the end of the Hackathon.

2. HACKATHON PREPARATION AND COMMUNITY BUILDING

The Hackathon preparation and development started in 2021, as part of a milestone of the CSA EU-IoT[1]. For the Hackathon development, fortiss proposed to jointly organize the Hackathon with the Research and Innovation project EFPF. This joint organization allowed to reach a broader community of developers, given that the CSA EU-IoT oversees and assists the coordination of 6 flagship projects in the context of Edge and IoT. EFPF brought key challenges in this context to the full end-to-end IoT spectrum with specific focus on manufacturing, as illustrated in **Error! Reference source not found.**.

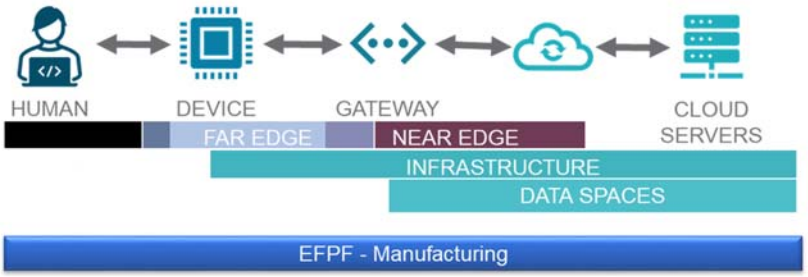

Figure 1: the overall scope of the EU-IoT/EFPF Hackathon.

The co-location to CONASENSE 2022 allowed to bring different experts and keynote speakers to the event, thus increasing the potential for dissemination across the broader European research community.

To build up the community, several actions have been developed since June 2021, as follows:

- First presentation of the Hackathon on IoT Week 2021, in August 2021.
- Regular dissemination via specific channels, to the targeted communities.

[1] https://www.ngiot.eu/eu-iot/

- Direct interaction with different entities, including presentation of the Hackathon and its call for projects in local universities by different partners of the two H2020 projects EFPF and EU-IoT.
- Several hybrid events organized by fortiss to explain the Hackathon to the community being developed.

3. FORMAT

The Hackathon has been co-located to the CONASENSE2022 symposium, starting in the afternoon of the first day of the symposium. The sessions of the Hackathon ran in parallel to the agenda of the symposium. Specific sessions with keynote speakers and project sessions were held jointly, to allow the mentors and participants to attend these sessions if desired. Moreover, several meetups with mentors have been set, given that the participants were in hybrid mode.

The event closed with a final session, where awards to the best paper, best presentation and Hackathon awards have been provided.

3.1. Organizational Structure and Support

The organizational structure of the Hackathon is illustrated in Figure 2. The Hackathon counted with an organizing committee involving EFPF members, EU-IoT members, and teachers of UNIVESP (pole to Brazilian students). This structure was extremely helpful to handle the event in hybrid mode. All the entities and respective members participated in a volunteer way, without any kind of contribution.

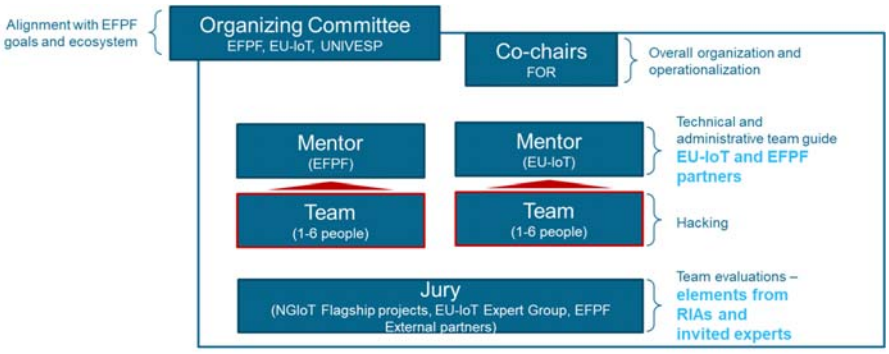

Figure 2: Organizational structure of the EU-IoT/EFPF Hackathon.

3.2. Committees

The Hackathon has been organized by fortiss and had the local support of UnternehmerTUM[2]. It counted with the following technical committees:

- **EU-IoT Committee**: Rute Sofia (fortiss), Lamprini Kolovou (Martel); John Soldatos (Intracom); Mirko Presser (Aarhus University); Brendan Rowan (Bluspecs).
- **EFPF Committee**: Mitula Donga (fortiss), Alexandros Nizamis (ITI-CERTH), Florian Jasche (Fraunhofer FIT), Ingo Martens (Hanse Aerospace); Carlos Coutinho (Caixa Mágica), Usman Wajid (Information Catalyst).
- **UNIVESP/Brazil Committee**: Sergio Galindo, Ricardo Edgard Caceffo.

The Hackathon Committees have been responsible for the overall organization and operationalization of the Hackathon and its different meetings, as well as for the development and maintenance of the different tools. The Hackathon co-chairs moderated moderate the different events, overall dissemination, and were the main contact point for all operational questions and concerns.

3.2.1. Mentors

The Hackathon Mentors, listed in *Table **1***, were volunteer elements from EFPF, EU-IoT and UNIVESP that related with the challenges proposed. The Mentors had the following responsibilities:

- Serve as the primary technical and guidance contact for the team questions and respective project guidance.
- Assist the support of the project artifacts in the Hackathon GitLab account.
- Promote the project in the NGIoT community and in the EFPF community.

Table 1: Hackathon Mentors.

Mentor	Challenge	Type	Affilitation
Florian Jasche	EFPF3: Evaluate the usability of the Data Spine for the creation of composite applications	Business Project	FhG FIT
Alexandros Nizamis	EFPF4: Analyze industrial data coming from EFPF partners and provide insights based on the EFPF analytics tools	Technical Project	CERTH
Sergio Galindo	Any, Brazil	Any	UNIVESP

[2] https://www.unternehmertum.de/

Mentor	Challenge	Type	Affilitation
Ricardo Caceffo	Any, Brazil	Any	UNIVESP
Manel Khelifi	Any	Technical Project	fortiss GmbH
Erkan Karabulut	EFPF1: Semantic matchmaking for the support of environmental monitoring of the shopfloor	Technical Project	fortiss GmbH
Dushyant Dave	EU-IoT 2: far Edge, tinyML	Technical Project	fortiss GmbH
Nikos Vakakis	EFPF4: Analyze industrial data coming from EFPF partners and provide insights based on the EFPF analytics tools	Technical Project	CERTH
Rohit Deshmukh	EFPF3: Evaluate the usability of the Data Spine for the creation of composite applications	Any	FhG FIT
Brendan Rowan	EU-IoT 1: IoT interfaces	Skills Training Project	Bluspecs
Emilie Mathilde Jakobsen	EU-IoT 1: IoT interfaces	Business Project	Aarhus University
John Soldatos	EU-IoT1: interfaces	Skills Training Project	Netsoft-Intrasoft
Victor Banos	Any	Any	Fortiss GmbH
Parwinder Singh	Any	Any	Aarhus University
Cecilia Sosa Arias Peixoto	Any, Brazil	Any	UNIVESP
Dushyant Dave	EU-IoT 2: far Edge, tinyML	Technical Project	fortiss GmbH
Roberto Massi de Oliveira	Any, Brazil	Any	UNIVESP
Higor Souza	Any, Brazil	Any	UNIVESP
Jose Avelino Placca	Any, Brazil	Any	UNIVESP

3.2.2. Jury

The Jury was composed of elements from EFPF and from the Next Generation IoT projects VEDLIoT, IoT-NGIN, TERMINET, IntellIoT, INGENIOUS, ASSIST-IoT, EFPF, and from UNIVESP (Brazil pole). The list of Jury members is provided in ***Table 2.***

Table 2: Jury members.

Name	Affiliation	Projects
Mario Porrmann	University of Osnabrück	VEDLIoT
Jens Hagemeyer	University Bielefeld	VEDLIoT
Josep Escrig	I2CAT	IoT-NGIN
Daniel Calvo	ATOS	IoT-NGIN
Jonathan Klimt	RWTH University of Achen	IoT-NGIN
Ilias Siniosoglou	University of Western Macedonia	TERMINET
Arne Bröring	Siemens AG	IntellIoT
Erin Elizabeth Seder	Nextworks	Ingenious
Ignacio Lacalle Úbeda	UPV	ASSIST-IoT
Carlos Coutinho	CMS	EFPF
Ingo Martens	Hanse Aerospace	EFPF
Alexandros Nizamis	CERTH	EFPF
Usman Wajid	Information Catalyst	EFPF
Higor Amario de Souza	UNIVESP	UNIVESP - Brazil
Ross Campbell	Information Catalyst	EFPF

The jury assessed the projects based on the criteria described in in section 3.4. For this purpose, the evaluation was supported via Google forms.

3.2.3. Teams

The rules of the Hackathon proposed a team to be formed individually or up to 6 persons. The team formation occurred before the Hackathon (due to the pandemic), in May 2022, after the selection of projects.

3.3. Typology of Projects and Pitching Material

The Hackathon, as a tool for experimentation, had the purpose to assist in experimenting and disseminating new business ideas, experiments, and prototypes as first step to best support next generation sustainable IoT solutions.

For this purpose, three types of projects have been considered:

- **Technical projects**: where the focus is on the development of a technical solution to address the challenge. The outcome shall be provided in the form of open-source code to be uploaded to the EU-IoT Hackathon git repository.
- **Training skills projects**: where the focus is on the development of a training tool to be available online which addresses the specific proposed challenge. Outcome can be a Web-based training tool; a Tutorial (e.g., PowerPoint, video), etc.
- **Prototype Business/Design ideas**: where the focus is on the development of a business framework for an IoT solution.

3.4. Evaluation Criteria

The evaluation criteria have been provided via the Hackathon operational rules document. Each member of the jury has been provided with an individual template for the evaluation and provided a grade between 1 (lower value) to 5 (higher value) to each criterium. The final grading was then the average of all jury members.

Technical projects:

- **Novelty:** How novel are the results compared to related work? **20%**
- **Reusability:** How easy is it for non-team members to replicate results? **30%**
- **Usability:** How user-friendly is the developed solution? **30%**
- **Community Impact:** In your opinion, how likely is this solution to be of interest to the community in the future? **20%**

Skills Training projects:

- **Novelty:** How novel is this tool in comparison to others that are similar? **10%**
- **Reusability:** How easy is it for non-team members to replicate results? **30%**
- **Reach:** What is the reach of the tool in terms of community range, e.g., 10 persons, 100 persons? **30%**
- **Resources:** How many trainers does the tool need? Would the training require specific equipment, software, etc.? **10%**
- **Quality:** Quality of developed material (slides, documentation, etc.) in terms of language, graphics, etc. **20%**

Business projects:

- **Value proposition:** Is the description clear? Is the product feasible and targets a real gap? How easily it can be duplicated? Is there a presence of potential substitutes for the product? **20%**
- **Market value:** Is there a genuine need for the product or service? How well

was the target market defined? What is the size and growth of the market? What is the consumers' willingness to pay for the product/service? **20%**

- **Creativity:** Is the problem addressed in a novel and creative way? **10%**
- **Feasibility:** Does the idea/proposal aspire towards clear, realistic, and achievable goals, while thinking big? Can it be implemented effectively? **20%**
- **Quality/Presentation:** Does the proposal engage the audience? Level of graphical quality? Exciting pitch/report? **10%**
- **Sustainability:** Does the proposal consider key EU sustainable goals, e.g., energy efficiency? Does it explain how it could break even or raise additional funding (economic sustainability)? Does it consider the different dimensions of financial and social sustainability in a conscientious manner? **10%**

4. CHALLENGES

The overall Hackathon challenges are provided in Table 3.

Table 3: List of challenges in the Hackathon.

Reference	Title	Description	Tooling
EFPF1	Semantic matchmaking for the support of environmental monitoring of the shopfloor.	Validate and improve the interconnection between TSMatch and the EFPF Data spine.	TSMatch
EFPF2	Evaluate the EFPF SDK in developing digital smart manufacturing applications.	Rely on the EFPF SDK to create new applications.	EFPF SDK
EFPF3	Evaluate the usability of the Data Spine for the creation of composite applications	Test the EFPF Data Spine and its usability, proposing specific improvements.	EFPF Data Spine
EFPF4	Analyse industrial data coming from EFPF partners and provide insights based on the EFPF analytics tools.	Work with open-source Machine Learning Libraries and propose applications for the visualization and analysis of industrial data.	EFPF Visual and Data Analytics Tool and Open-source ML libraries

Reference	Title	Description	Tooling
EU-IoT1	EU-IoT1, IoT Interfaces: Augmented Reality Interfaces based on the Smart Mirror concept	Work with ML open-source solutions for Smart Mirrors, to develop a user-centric interface	MichMich MagicMirror[3]
EU-IoT2	Far Edge: sustainable IoT via TinyML	Develop ML applications for embedded devices	Tensorflow Lite[4], Pytorch[5], Renode[6]., Kenning[7].
EU-IoT3	Near Edge: sustainable MEC applications	Propose novel MEC applications based on the open ETSI MEC API	ETSI MEC API[8]
EU-IoT4	Infrastructure: simulating time-sensitive and deterministic networking IoT applications	Develop novel applications based on ns-3, fortiss deterministic wireless DetNetWiFi framework	Fortiss ns-3 DetNetWiFi framework
EU-IoT5	Data spaces: sustainable, user-centric smart mobility	Play with open data sets and open ML tooling for data analysis	Open mobility data[9] Crawdad datasets[10] Microsoft Geolife[11] Open Nebula

5. COMMUNITY OVERVIEW

5.1. Registered Participants

Figure 3 provides the registrant participation per country. The 141 registrants were well distributed across the globe; 32% were in India, while 12% were in Brazil. We highlight 21% described as “unknown”. In Europe, the countries with a larger

[3] https://github.com/MichMich/MagicMirror
[4] https://www.tensorflow.org/lite
[5] https://pytorch.org/mobile/home/
[6] https://renode.io/
[7] https://antmicro.com/blog/2021/06/kenning-edge-ai-framework/
[8] https://try-mec.etsi.org/
[9] https://openmobilitydata.org
[10] https://crawdad.org/
[11] https://www.microsoft.com/en-us/download/details.aspx?id=52367

database of registrants were Germany, Denmark, Portugal, and Sweden. The type of registrants is provided in Figure 4. Others (42%) comprises registrants that did not enter a profile, or where the profile was somewhat vague, e.g., innovator, ideator, network architectures. 27% of the registrants had a profile of full stack developer, and 13% are profiled as data scientists.

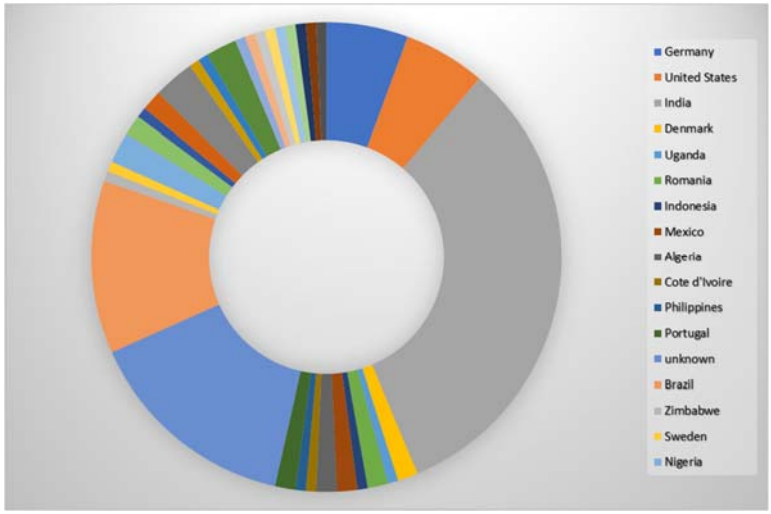

Figure 3: Hackathon Geographic community distribution.

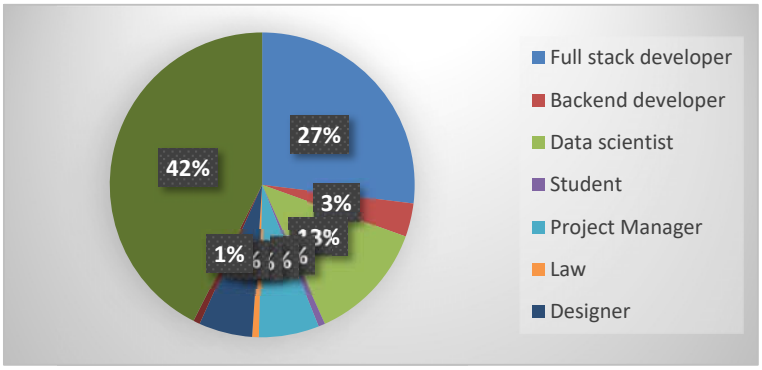

Figure 4: Participant profile.

5.2. Initial Team Formation

Out of the 141 registered participants, 31 participants registered projects having selected specific challenges to address. Out of these, 26 have been considered for team formation. The initial team formation is provided in Table 4 grouped per challenge. After the team number and name of the participant, the table lists whether the attendance is remote or not; if the participant brings a team; type of project; country and affiliation; profile of the participant. As can be seen, most participants were looking for a team.

Table 4: Initial team formation presented per challenge.

Nr	Name	Attendance	Team	Type	Country	Affiliation	Profile
EFPF1: Semantic Matchmaking with TSMatch							
1	Hassannasrallah Berguellah	Remote	Yes	Technical	Algeria		front-end developer
2	Cassio Dias	Remote	Yes	Technical	Brazil	UNIVESP	Student
EFPF SDK							
3	Sudhir Kshirsagar	Remote	No	Technical	CA, USA	University of Illinois at Urbana-Champaign	student
4	Hong Tran	Remote	No	Technical	Texas, USA	Wilmington University	Data Scientist
EFPF Data Spine							
5	Hong Tran	Remote	No	Business ideation	Texas, USA	Wilmington University	Data Scientist
EPF4: Data Analysis							
6	Bianca Gouveia Borges Rodrigues	Remote	No	Technical	Brazil	UNIVESP	Student
7	Hong Tran	Remote	No	Business ideation	Texas, USA	Wilmington University	Data Scientist

Nr	Name	Attendance	Team	Type	Country	Affiliation	Profile
8	Harsh Pandey	Remote	No	Business ideation	India	Vellore Institute of Technology	Data scientist
EU-IoT1: IoT interfaces, smart mirror							
9	Felipe da Silva Braz	Remote	Formed	Skills training	Brazil	UNIVESP	Student
	Ederson de Sordi Vigato	Remote	Formed		Brazil	UNIVESP	Student
	Gabriel Negri	Remote	Formed		Brazil	UNIVESP	Student
	José Angelo de Oliveira	Remote	Formed		Brazil	UNIVESP	Student
10	A. Kaviraj	Remote	Formed	Technical	India	sri vijay vidyalaya	Full-stack developer
	Sanijth Vishal S	Remote	Formed		India	sri vijay vidyalaya	Full-stack developer
	Narendra J	Remote	Formed		India	sri vijay vidyalaya	Full-stack developer
11	Marcelo with Alexander	Remote	Formed	Technical			
	Alexander Farias Molla Andrade	Remote	Formed		Brazil		
12	LOGESH KRISHNA R	Remote	No	Technical	India	Dr.Mahalingam College of Engineering and Technology	Data scientist
13	Nuno Edgar Nunes Fernandes	Remote	No	Business ideation	Portugal		Product Manager
14	Shahbaz Siddiqui	Remote	Formed	Business ideation	Pakhistan		
	Saif ul Islam		Formed		Pakhistan		

Nr	Name	Attendance	Team	Type	Country	Affiliation	Profile
15	Marceo Morales	Remote (Brazil)	No	Skills training	Brasil	UNIVESP	Student
16	Emerson Gomes Marques	Remote (Brazil)	No	Business ideation	Brazil	UNIVESP	Student
17	Shamaine M.		No	Technical			
	Shamaine M.		No	skills training			
EU-IoT2: Near Edge, TinyML							
18	Chongyu Zhang	Local (TUM)	Formed	Technical	Germany	TUM	Student
19	Warp Smith	Remote	No	Technical	IL, USA		
20	Paulo Furlan	Remote	No	Technical	Brazil	UNIVESP	Student
21	Ravinderdeep Singh	Remote	No	Technical	India	steppingstones sr. sec. school	Idea make, inventors, project presentation, project prototype, paper presentation
EU-IoT3: Infrastructure, ns-3 deterministic framework							
22	Muhammed S. Baldeh	Remote	No	Technical	Gambia		
EU-IoT5: Data Spaces, analysing mobility data							
23	Abhishek Gupta	Remote	No	Skills training			
24	Rohit Bazinga	Remote	No	Technical	UK		

Nr	Name	Attendance	Team	Type	Country	Affiliation	Profile
25	Bruno Lowczy	Remote	No	Business ideation	Brazil	UNIVESP	Student
26	Ishmael Ebiasah	Remote	No	Technical	Germany	University of Siegen	Designer

5.3. Final Team Formation

Each of the candidates selected has then been directly contacted several times, to assist in the team formation. The candidates were also in contact with potential mentors. The final list of teams is provided in Table 5. All of the participants confirmed their intention to participate in the Hackathon remotely or in presence. Each team has been assigned with 1 mentor and the teams in Brazil had an additional local mentor provided by partner FOR, to ensure a better technical support. The organizing team and mentors have then interacted until the Hackathon as needed.

Table 5: Final team formation.

Nr.	Name	Attendance	Team	Type	Country	Affiliation	Profile	Mentor 1	Mentor 2
EFPF1: Semantic Matchmaking with TSMatch									
1	Paulo Roberto Rodrigues Furlan	Remote	Formed	Technical	Brazil	UNIVESP	Student	Roberto Massi de Oliveira, UNIVESP	Erkan Karabulut, FOR
	Bianca Gouveia Borges Rodrigues	Remote	Formed		Brazil	UNIVESP	Student		
	Emerson Gomes Marques	Remote	Formed		Brazil	UNIVESP	Student		
EFPF2: EFPF SDK									

Nr.	Name	Attendance	Team	Type	Country	Affiliation	Profile	Mentor 1	Mentor 2
2	Sudhir Kshirsagar	Remote	No	Technical	CA, USA	University of Illinois at Urbana-Champaign	student	Miguel Tavares, CMS	
EPF4: Data Analysis									
3	Harsh Pandey	Remote	No	Business ideation	India	Vellore Institute of Technology	Data scientist	Nikos Vakakis, CERTH	Alexandros Nizamis, CERTH
EU-IoT1: IoT interfaces, smart mirror									
4	Felipe da Silva Braz	Remote	Formed	Skills training	Brazil	UNIVESP	Student	Higor Amaro de Souza, UNIVESP	Mitula Donga, FOR
	Gabriel Negri	Remote	Formed		Brazil	UNIVESP	Student		
	José Angelo de Oliveira	Remote	Formed		Brazil	UNIVESP	Student		
	Cassio Dias	Remote	Formed		Brazil	UNIVESP	Student		
5	Marcelo Moraes	Remote	Formed	Skills Training	Brazil	UNIVESP	Student	Cecilia Sousa Peixoto, UNIVESP	
	Alexander Farias Molla Andrade	Remote	Formed		Brazil	UNIVESP	Student		

Nr.	Name	Attendance	Team	Type	Country	Affiliation	Profile	Mentor 1	Mentor 2
6	Saif ul Islam	Remote	Formed	Business ideation				Emilie Jakobson, Aarhus University	
7	Nuno Edgar Nunes Fermandes	Remote		Business ideation			Product manager	Brenda n Rowan, Bluspecs	
8	Kaviraj Logesh	Remote	Formed	Technical	India	sri vijay vidyalaya	Full-stack developer	Parwinder Singh, Aarhus University	
	Sanijth Vishal S	Remote	Formed		India	sri vijay vidyalaya	Full-stack developer		
	Narendra J	Remote	Formed		India	sri vijay vidyalaya	Full-stack developer		
9	Logesh Khrishna R.	Remote	No	Technical	India	Dr. Mahalingam College of Engineering and Technology	Data scientist	Mitula Donga, FOR	
EU-IoT2: Far Edge, TinyML									
10	Chongyu Zhang	In person	Formed	Technical	Germany	TUM	Student	Dushyant Dave, FOR	

Nr.	Name	Attendance	Team	Type	Country	Affiliation	Profile	Mentor 1	Mentor 2
11	Warp Smith	Remote	No	Technical	IL, USA			Jon Soldatos, Netsoft - Intrasoft	
12	Ravinderdeep Singh	Remote	No	Technical	India	steppingstones sr. sec. school	Idea maker, inventors, project presentation, project prototype, paper presentation	Victor Banos, FOR	
EU-IoT5: Data Spaces, analysing mobility data									
13	Bruno Lowczy	Remote	No	Business ideaiton	Brasil	UNIVESP	Student	Jose Placa, UNIVESP	Victor Banos, FOR

6. HACKATHON WINNING PROJECTS AND AWARDS

The three winning projects, available via the Hackathon GitLab, were as follows:

1. **Sustainable Irrigation, skills training project**. Team 4, Cassio Dias, Felipe da Silva Braz, Gabriel Negri, Jose Angelo de Oliveira, UNIVESP, Brazil.

- Anomaly Detection. Team 2: Sudhir Kshirsagar, University of Illinois at Urbana-Champaign, USA

3. Green Backup. Team 3: Bruno Lowczy, UNIVESP, Brazil

The list of awards that has been provided is as follows:

- **First Team Awards:**
  - UnternehmerTUM TUM Award - Entrepreneurship and Incubation for 1 year, valued in 10000 Euros.
  - EFPF Challenges Award - 1st prize – 1 Google Pixel 6
- **Second team Awards:**
  - IoT Forum voucher for 1 person, IoT Week 2023, provided via the IoT Forum (Aarhus University)
  - EFPF Challenges Award, 2nd prize - Google Next HUB 2nd generation smart display and Google Chromecast Stream player, and 2 Google Nest Audio Smart Speakers
- **Third team:**
  - EFPF Challenges Award - 3rd prize, Arduino Kit Explore
  - IoT Kit (English) Education and a set of 40 sensors for Arduino projects, plus Arduino® Sensor Kit - Base with Shield and 10 Grove Sensors, Arduino® Sensor Kit - Base with Shield and 10 Grove Sensors

All teams have also been provided with the following IoT kits, sponsored by **Infineon**:

- Infineon Kit I(PSoC™ 62S2 Wi-Fi BT Pioneer Kit (CY8CKIT-062S2-43012) and IoT Sense Expansion Kit. CY8CKIT-062S2-43012 and 10x CY8CKIT-028-SENSE. The PSoC™ 62S2 Wi-Fi BT Pioneer Kit (CY8CKIT-062S2-43012) is a low-cost hardware platform that enables design and debug of the PSoC™ 62 MCU and the Murata 1LV Module (CYW43012 Wi-Fi + Bluetooth Combo Chip). The IoT sense expansion kit (Y8CKIT-028-SENSE) is a low-cost Arduino™ UNO compatible shield board that can be used to easily interface a variety of sensors with the PSoC™ 6 MCU platform, specifically targeted for audio and machine learning applications.
- Infineon Kit II CY8CPROTO-062-4343W. PSoC™ 6 Wi-Fi BT Prototyping Kit (CY8CPROTO-062-4343W) is a low-cost hardware platform that enables design and debug of PSoC™ 6 MCUs. It comes with a CY8CMOD-062-4343W module, industry-leading CAPSENSE™ for touch buttons and slider, on-board debugger/programmer with KitProg3, microSD card interface, 512-Mb Quad-SPI NOR flash, PDM microphone,

and a thermistor. It also includes a Murata LBEE5KL1DX module, based on the CYW4343W combo device.

7. HACKATHON HIGHLIGHTS

Figure 5: Hackathon mentors during the project development.

Figure 6: Hackathon mentors in Munich and remotely.

Figure 7: TSMatch demonstration at the fortiss IIoT Lab, during the Hackathon.

Figure 8: EFPF partners, Hackathon ceremony.

Figure 9: Hackathon awards.

Author Biographies

Rute C. Sofia (PhD 2004) is the Industrial IoT Head at fortiss - research institute of the Free State of Bavaria for software intensive services and systems in Munich, Germany. She is also an Invited Associate Professor of University Lusófona de Humanidades e Tecnologias, and an Associate Researcher at ISTAR, Instituto Universitário de Lisboa. Rute's research background has been developed on industrial and on academic context, and she has co-founded COPELABS (2012-2019, Lisbon, Portugal), research unit which she also steered between 2013-2017. and where she was a Senior Researcher until 2019. She has co-founded Senception Lda (2013), a start-up focused on personal communication platforms. Her current research interests are: network architectures and protocols; IoT; edge computing; in-network computation; network mining. Rute holds over 60 peer-reviewed publications in her fields of expertise, and 9 patents.

She is an ACM Senior member and an IEEE Senior Member, and an ACM Europe Councillor. She is also an N2Women Awards Co-chair. Before COPELABS/ULHT,

she was a senior researcher at INESC TEC (07-10, Porto, Portugal), where she steered the "Internet Architectures and Networking" area of UTM, team dedicated to wireless/cellular networking architectures and to user-centric networking paradigms. She was (04-07, Munich, Germany) a senior research scientist in Siemens AG and Nokia-Siemens Networks GmbH, focusing on aspects such as: fixed-mobile convergence; carrier-grade Ethernet; QoS; IPv6 interoperability. Rute holds a BEng in Informatics Engineering by Universidade de Coimbra (1995); M.Sc. (1999) and Ph.D. (2004) in Informatics by Universidade de Lisboa. During her PhD studies, she was a visiting scholar (2000-2003) at Northwestern University (ICAIR) and at University of Pennsylvania

Ramjee Prasad, Fellow IEEE, IET, IETE, and WWRF, is a Professor of Future Technologies for Business Ecosystem Innovation (FT4BI) in the Department of Business Development and Technology Aarhus University, Herning, Denmark. He is the Founder President of the CTIF Global Capsule (CGC). He is also the Founder Chairman of the Global ICT Standardization Forum for India, established in 2009. He has been honoured by the University of Rome "Tor Vergata", Italy as a Distinguished Professor of the Department of Clinical Sciences and Translational Medicine on March 15, 2016. He is an Honorary Professor of the University of Cape Town, South Africa, and the University of KwaZulu-Natal, South Africa. He has received the Ridderkorset of Dannebrogordenen (Knight of the Dannebrog) in 2010 from the Danish Queen for the internationalization of top-class telecommunication research and education. He has received several international awards such as IEEE Communications Society Wireless Communications Technical Committee Recognition Award in 2003 for making a contribution in the field of "Personal, Wireless and Mobile Systems and Networks", Telenor's Research Award in 2005 for impressive merits, both academic and organizational within the field of wireless and personal communication, 2014 IEEE AESS Outstanding Organizational Leadership Award for: "Organizational Leadership in developing and globalizing the CTIF (Center for TeleInFrastruktur) Research Network", and so on. He has been the Project Coordinator of several EC projects, namely, MAGNET, MAGNET Beyond, eWALL. He has published more than 50 books, 1000 plus journal and conference publications, more than 15 patents, over 140 Ph.D. Graduates and a larger number of Masters (over 250). Several of his students are today worldwide telecommunication leaders themselves.

Paulo S. Rufino Henrique holds more than 20 years of experience working in telecommunications. His career began as a field engineer at UNISYS in Brazil, where he was born. There, Paulo worked for almost nine years in the Service Operations, repairing and installing corporative servers and networks before joining British Telecom (BT) Brazil. Paulo worked five years at BT Brazil managing MPLS networks, satellites (V-SAT), IP-Telephony for Tier 1 network operations. He became the Global Service Operations Manager during that period overseeing BT operations in EMEA, Americas, India, South Korea, South African, and China. After a successful career in Brazil, Paulo got transferred to the BT headquarters in London, where he worked for six and a half years as a service manager for Consumers Broadband in the UK and IPTV Ops manager for BT TV Sports channel. Additionally, during his tenure as IPTV Ops manager for BT, Paulo also participated in the BT project of launching the first UHD (4K) TV channel in the UK. He then joined Vodafone UK as a Quality Manager for Consumers Broadband Services and OTT platforms, and he worked in that capacity for almost two years. During his stay in London, Paulo completed a Post-graduation Degree at Brunel London University. His thesis was entitled 'TV Everywhere and the Streaming of UHD TV over 5G Networks & Performance Analysis'. Presently, Paulo Henrique holds the Head of Delivery and Operations position at Spideo, Paris, France. He is also a Ph.D. candidate under Professor Ramjee Prasad's supervision at Global CTIF Capsule, Department of Business, Aarhus University, Denmark. His research field is 6G Networks - Performance Analysis for Mobile Multimedia Services for the Future Wireless Technologies.

CONASENSE2022 Acknowledgements

Rute C. Sofia, Ramjee Prasad, Paulo Rufino

1. INTRODUCTION

The CONASENSE2022 symposium success resulted from the involvement of over 50 experts, and over 20 European entities. We would like to thank all of the individuals involved; all of the sponsors, promotional partners, projects that have supported the development of the symposium and also of the co-located Hackathon.

We thank also the sponsors of the awards for the symposium, and for the Hackathon.

2. CONASENSE2022 SYMPOSIUM COMMITTEES

2.1. General Chairs

Rute C. Sofia, fortiss GmbH, Munich, Germany

Ramjee Prasad, CGC, Aarhus University, Denmark

2.2. Publicity Chair and Treasurer:

Paulo Rufino, CGC, Aarhus University, Denmark

2.3. Student Forum Chairs:

Ernestina Cianca, University of Rome, Italy

Manel Khelifi, fortiss GmbH, Munich, Germany

2.4. EU-IoT/EFPF Hackathon Chairs

Mitula Donga, fortiss GmbH, Munich, Germany

Rute C. Sofia, fortiss GmbH, Munich, Germany

2.5. Technical Programme Commitee

- Albena Mihovksa, CGC, Aarhus University, Denmark (Chair)
- Ernestina Cianca, University of Rome, Italy
- Tomaso de Cola, DLR, Germany
- Eduardo Cerqueira, UFPA, Brazil
- Augusto Casaca, INESC-ID, Portugal
- Elefteris Mamathas, Democritus University, Greece
- Henning Schulzrinne, Columbia University, USA
- Anand Prasad, Deloitte, Japan
- Valeria Loscri, INRIA, France
- Eirini Eleni Tsiropoulo, University of New Mexico, USA
- Diego Lopez, Telefonica, Spain
- Jonathan Fürst, NEC, Germany
- Simone Morosi, University of Florence, Italy
- Pedro Sebastião, ISCTE-IUL, Portugal
- Xiaoming Fu, University of Göttingen, Germany
- Maria Papadopouli, FORTH, Greece
- John Soldatos, Intrasoft, Luxembourg
- Jorge Sá Silva, University of Coimbra, Portugal
- Vassilis Tsaoussidis, Democritus University, Greece
- Artur Hecker, Huawei, Germany
- Marica Amadeo, University Mediterranea of Reggio Calabria, Italy
- Laura Feeney, Uppsala University, Sweden
- Ignacio Lacalle, Universitat Politecnica de Valencia, Spain
- Dianne Medeiros, Universidade Federal Fluminense, Brazil
- Evsen Yanmaz, Ozyegin University, Turkey
- Huiling Zhu, University of Kent, United Kingdom
- Jose Sallent, Universitat Politecnica de Madrid
- Anna Triantafyllou, University of Western Macedonia, Greece
- David Jimenez, Universidad Politecnica de Madrid, Spain
- Carlos Raniery Paula Dos Santos, Federal University of Santa Maria, Brazil
- Arne Bröring, Siemens AG, Germany

3. EU-IOT HACKATHON COMMITTEES

Organizers: fortiss GmbH (Mitula Donga, Rute C. Sofia); UnternhemerTUM Makerspace GmbH (Florian Küster)

Technical Committees :
EU-IoT Committee: Rute Sofia (fortiss), Lamprini Kolovou (Martel); John Soldatos (Intracom); Mirko Presser (Aarhus University); Brendan Rowan (Bluspecs)

EFPF Committee: Mitula Donga (fortiss), Alexandros Nizami (ITI-CERTH), Florian Jasche (Fraunhofer FIT), Ingo Martens (Hanse Aerospace); Carlos Coutinho (Caixa Mágica), Usman Wajid (Information Catalyst)

UNIVESP Committee (Brazil pole): Ricardo Edgard Caceffo (UNIVESP); Rodolfo Jardim de Azevedo (UNIVESP); Higor Amario de Souza (UNIVESP)

4. EU-IOT/EFPF HACKATHON MENTORS

- Mitula Donga, fortiss GmbH, Germany
- Emilie Mathilde Jakobsen, Aarhus University , Denmark
- Brendan Rowan, BluSpecs, Spain
- Miguel Tavares, Caixa Magica, Portugal
- Florian Jasche, Fraunhofer FIT, Germany
- Alexandros Nizamis, CERT-ITI, Greece
- Sergio Galindo, UNIVESP, Brazil
- Ricardo Caceffo, UNIVESP, Brazil
- Manel Khelifi, fortiss, GmbH, Germany
- Erkan Karabulut, fortiss GmbH, Germany
- Dushyant Dave, fortiss GmbH, Germany
- Nikos Vakakis, CERT-ITI, Greece
- Rohit Deshmukh, Fraunhofer FIT, Germany
- John Soldatos, Netsoft-Intrasoft, Luxembourg
- Victor Banos, fortiss GmbH, Germany
- Parwinder Singh, Aarhus University
- Cecilia Sosa Arias Peixoto, UNIVESP, Brazil
- Roberto Massi de Oliveira, UNIVESP Brazil
- Higor Souza, UNIVESP, Brazil

- Jose Avelino Placca, UNIVESP, Brazil

5. EU-IoT/EFPF Hackathon Jury

- Mario Porrmann, University of Osnabrück, Germany
- Jens Hagemeyer, University of Bielefeld, Germany
- Josep Escrig, i2CAT, Spain
- Daniel Calvo, ATOS, Spain
- Jonathan Klimt, RWTH University of Aachen, Germany
- Ilias Siniosoglou, University of Western Macedonia, Greece
- Arne Bröring, Siemens AG, Germany
- Erin Elizabeth Seder, Nextworks, Italy
- Ignacio Lacalle Úbeda, Universidad Politecnica de Valencia, Spain
- Carlos Coutinho, Caixa Magica Software, Portugal
- Ingo Martens, Hanse Aerospace
- Alexander Schneider, Fraunhofer FIT, Germany
- Alexandros Nizamis, CERTH-ITI, Greece
- Usman Wajid, Information Catalyst, United Kingdom
- Higor Amario de Souza, UNIVESP, Brazil
- Roberto Massi de Oliveira, UNIVESP, Brazil
- Victoria Alejandra Salazar Herrera, UNIVESP, Brazil
- Ross Campbell, Information Catalyst, United Kingdom

6. CONASENSE2022 Symposium Promoters

- Fortiss GmbH
- Unternehmer TUM
- CGC, Aarhus University
- Martel Innovate
- Bluspecs
- Netcompany-Intrasoft
- Caixa Mágica Software
- Fraunhofer FIT
- Center for Research and Technology (CERTH)-ITI
- Virtual University of the State of São Paulo, UNIVESP
- Horizon 2020 IntellIoT

- Horizon 2020 TERMINET
- Horizon 2020 VEDLIoT
- Horizon 2020 inGenious
- Horizon 2020 IoT-NGIN
- Horizon 2020 ASSIST-IoT
- Horizon 2020 EFPF

7. CONASENSESYMPOSIUM SPONSORS

- Unternehmer TUM Makerspace – GOLD
- Cooperation and Support Action EU-IOT (Horizon 2020 Program of the European Commission Grant Agreement number 956671) - GOLD
- Horizon 2020 EFPF (Horizon 2020 Program of the European Commission Grant Agreement number 825075) - GOLD
- IBM – GOLD
- Infineon - SILVER
- IoT Forum - Bronze